İSTANBUL TECHNICAL UNIVERSITY ★ INSTITUTE OF SCIENCE AND TECHNOLOGY

PREPARATION AND CHARACTERIZATION OF POLYURETHANE MICRO AND NANOCOMPOSITES

Ph.D. Thesis by

M. Özgür SEYDİBEYOĞLU, M.Sc.

(706012005)

Date of submission : 25 April 2007

Date of defence examination: 26 June 2007

Supervisor (Chairman): Prof. Dr. F. Seniha GÜNER

Members of the Examining Committee Prof.Dr. Nurfer GÜNGÖR (İTÜ.)

Prof.Dr. Lütfi ÖVEÇOĞLU (İTÜ.)

Prof. Dr. O. Sermet KABASAKAL (OGÜ.)

Assoc. Prof.Dr. Yusuf MENCELOĞLU (SÜ.)

JUNE 2007

İSTANBUL TEKNİK ÜNİVERSİTESİ ★ FEN BİLİMLERİ ENSTİTÜSÜ

POLİÜRETAN MİKRO VE NANOKOMPOZİTLERİNİN HAZIRLANMASI VE KARAKTERİZASYONU

DOKTORA TEZİ

Y. Müh. M. Özgür SEYDİBEYOĞLU

Tezin Enstitüye Verildiği Tarih : 25 Nisan 2007
Tezin Savunulduğu Tarih : 26 Haziran 2007

Tez Danışmanı :	**Prof.Dr. F. Seniha GÜNER**
Diğer Jüri Üyeleri	**Prof.Dr. Nurfer GÜNGÖR (İ.T.Ü.)**
	Prof.Dr. Lütfi ÖVEÇOĞLU (İ.T.Ü.)
	Prof.Dr. Osman Sermet KABASAKAL (İ.T.Ü.)
	Doç.Dr. Yusuf MENCELOĞLU (S.Ü.)

HAZİRAN 2007

ACKNOWLEDGEMENTS

I would like to express my deep thanks and my kind respect to my thesis supervisor Prof. Dr. F. Seniha Güner for her excellent guidance, motivation, encouragement and valuable comments to progress during this study. She has been a role model for me how to be a good supervisor and to be a very kind person.

I would like to thank to Prof. Dr. Nurfer Güngör for her expertise in clay science and help for this study. I would like to thank Dr. Sevim İşçi for her help in exploiting the mysteries of clay minerals and doing the experiments in the laboratory together. I would like to express my sincere thanks to Prof. Dr. Ö.Işık Ece for his guidance in the clay research and supplying the precious clay hectorite.

I would like to thank to Prof. Dr. Sezai Saraç for supplying the carbon fiber and for enabling the novel research on polyurethane-carbon fiber composite materials. I want to thank to Koray Yılmaz for his help in preparing the polyurethane-carbon fiber composites.

I would like to thank indeed to our previous Rector, Prof. Dr. Gülsün Sağlamer giving me the opportunity to conduct my Ph.D in a very sophisticated medium in Turkey by arranging the Advanced Technologies in Engineering Programme in Istanbul Technical University. I would like to thank to Prof. Dr. Mustafa Ürgen and Prof. Dr. M.Lütfi Öveçoğlu for their efforts in this programme and being big brothers for us in order to solve our problems during this thorough study. I want to thank to Prof. Dr. Birgül Ersolmaz and Prof. Dr. Ayşe Şenatalar for sharing their knowledge and expertise in membrane science.

I want to thank to Prof. Dr. Kristiina Oksman being excellent supervisor in the polyurethane-cellulose research and helping me to get the Norwegian Government Scholarship and letting me to work in her laboratories in NTNU (Norwegian University of Science and Technology). I wish to thank to each person in the lab group in NTNU, Dr. Magnus Bengtsson, Dr. Linnea Petersson, Dr. Ingvild Kvien, Dr. Daniel Bondeson ve Dr. Marie Le Bailiff, everyone helping me in various parts of the preparation of polyurethane-cellulose nanocomposites.

I would like to thank to Assc. Prof. Dr. Seyhun Solakoğlu from Çapa Medical Faculty of Istanbul University for conducting our TEM observations.

I would like to thank to our laboratory group, Burcu Mutlu, Ebru Uzun and Tuna Çalış for their valuable friendship in the laboratory and making the laboratory much more fun place and their help in my experiments. I would like to express deep thanks to Işık Yavuz and Esra Engin for their help during my thermal analysis and X-ray analysis experiments.

I wish to thank to Yasin Tükek and Flokser Tekstil Co. for supplying the raw materials during this study enabling the production of the nanotechnology for an industrial product. I would like to thank to my dear friend Başar Yıldız from Flokser Co and from our research group for his help and invaluable friendship during this study.

And final thanks to my father and mother who have been so much helpful and patient during my entire education life and especially during this thesis study. They have been always very supportive in the completion of this thorough work. Thanks for my dear cat, Yelda Türkan for her sincere support.

TABLE OF CONTENTS

ABBREVIATIONS

PU	: Polyurethane
HEC	: Hectorite
MMT	: Montmorillonite
Lap	: Laponite
CEC	: Cation Exchange Capacity
PAN	: Polyacrylonitrile
MDI	: Diphenylmethane diisocyanate
DMF	: Dimethylformamide
DTABr	: Dodecyltrimethylammoniumbromide
HDTABr	: Hexadecyltrimethylammoniumbromide
SDS	: Sodiumdodecylsulfate
ALS	: Ammoniumlaurylsulfate
SDS	: Sodiumdodecylsulfate
SEM	: Scanning Electron Microscope
TEM	: Transmission Electron Microscope
FTIR	: Fourier Transform Infrared Spectroscopy
DMA	: Dynamic Mechanical Analysis
TGA	: Thermal Gravimetric Analysis

LIST OF TABLES

LIST OF FIGURES

Page No

Page No

Page No

PREPARATION AND CHARACTERIZATION OF POLYURETHANE MICRO AND NANOCOMPOSITES

SUMMARY

The use of polymeric materials increases everyday finding new application with novel polymers and replacing the metallic and ceramic materials at the same time. Polymers are very important materials exhibiting various properties and having a very large property range enabling to be used for many different applications. There is an intense research done on polymers making the polymers more attractive materials.

The properties of the polymers can be adjusted by many different ways. The most commonly used two methods are chemical route during the synthesis of the polymer and the materials route making polymer composites. The chemical route is not in the scope of this thesis study. Materials modifications form the basis of this thesis.

In this thesis study, polyurethane has been used as the matrix polymer. Polyurethane has been chosen due to the various applications in large quantities such as biomedical, automotive, construction and adhesives. To improve the polyurethane, different kinds of composite materials have been prepared.

This study focuses mainly on three different kinds of composite materials. The first group consists of polyurethane-clay nanocomposites. The second group consists of the polyurethane-cellulose micro and nanocomposites. And the third group consists of polyurethane-carbon fiber micro composites.

In the first group, polyurethane-clay nanocomposite has been studied in detail. The natural clay, hectorite has been incorporated in the polyurethane matrix for the first time in the literature. The properties of the nanocomposites prepared with the hectorite and the montmorillonite from Turkish natural resources have been compared. The successful exfoliated structures of polyurethane hectorite and polyurethane montmorillonite have been obtained without organic modifiers. Detailed investigations of the hectorite and montmorillonite have been performed. As a comparison, the synthetic form of the hectorite, laponite has been incorporated in the polyurethane matrix as well. The three nanocomposite materials have been compared. As a final step in the polyurethane-clay nanocomposites, the effect of silane coupling on the hectorite clay has been studied.

The second group in this thesis study consists of the polyurethane and the cellulosic reinforcements. The cellulosic reinforcements are lightweight, bio-resourced and cheap materials. The polyurethane has been reinforced with micron sized cellulose fibers and

nanosize cellulose fibrils. The difference of the micron size and the nano size reinforcement has been exploited in this study demonstrating the importance of reinforcement at the nanoscale.

The third group consists of the polyurethane carbon fiber composites. This group composite material has been prepared in order to understand the difference between the micron sized and nanosized reinforcements and to see the difference between the other reinforceing phases.

POLİÜRETAN MİKRO VE NANOKOMPOZİTLERİNİN HAZIRLANMASI VE KARAKTERİZE EDİLMESİ

ÖZET

Polimerik malzemelerin kullanımı her geçen gün artmaktadır. Sürekli iyileşen özellikleriyle metalik ve seramik malzemelerin yerini almaya başlamıştır. Polimerik malzemelerin özelliklerindeki çeşitlilik kullanım alanlarını arttırmaktadır. Polimerik malzemeler üzerine bilim dünyasında ve endüstride çok yoğun araştırmalar devam etmektedir.

Polimerik malzemelerin özellikleri iki ana yöntem ile değiştirilebilir. Birincisi monomerleri değiştirerek polimerin özelliklerini değiştirmektedir. Diğeri polimerik malzemelere çeşitli katkı maddeleri, güçlendirici fazlar eklenerek kompozit malzeme hazırlama yöntemidir. Bu tez kompozit malzeme hazırlanarak polimerin özelliklerini değiştirme konusunda yapılan çalışmaları kapsar.

Bu çalışmada biyomedikal, otomotiv, yapı ve yapıştırıcı gibi uygulama alanları olan poliüretan, polimer matris olarak seçilmiştir. Poliüretanın özelliklerini iyileştirebilmek için çeşitli kompozit malzemeler hazırlanmıştır.

Bu çalışmada üç ayrı poliüretan kompozitleri üzerine çalışmalar yapılmıştır. Birinci grup olan poliüretan-kil nanokompozitleri bu tez kapsamında en yoğun çalışma yapılan gruptur. İkinci grup poliüretan-selüloz mikro ve nanokompozitleridir. Üçüncü grup ise, son yıllarda kullanımı yaygınlaşmaya başlayan karbon fiberler ile hazırlanmış olan poliüretan-karbon fiber kompozitleridir.

İlk çalışma grubunda poliüretan-kil nanokompozitleri çok detaylı incelenmiştir. Türkiye'nin yerli kaynaklarından elde edilen iki farklı doğal kille ve sentetik kille çalışmalar yapılmıştır. Doğal kil olarak montmorillonit ve hektorit, sentetik kil olarak hektorit yapısındaki Laponite RD kullanılmıştır. Çalışmada başarılı delamine kil nano kompozitleri elde edilebilmiştir. Son aşamada ise killer silanla kaplanarak nanokompozitlerdeki etkisi incelenmiştir.

İkinci grup çalışmada poliüretan selülozik malzeme ile güçlendirilmiştir. Selülozik malzemeler hafif olmaları, doğal kaynaklı olmaları ve ucuz olmaları bakımından büyük önem arz etmektedir. Poliüretan hem mikron boyutunda hem de nano boyutta selüloz ile güçlendirilmiştir. Çalışmadan elde edilen sonuçlar incelendiğinde, nano boyutta güçlendirmenin malzemenin özellikleri üzerinde çok etkili olduğu sonucuna varılmıştır.

Üçüncü grup çalışmada poliüretan karbon fiber malzemesiyle güçlendirilmiştir. Bu çalışmadaki malzemeler mikro ve nano boyuttaki güçlendirmelerin farkını anlamak için yapılmıştır ve diğer güçlendirici malzemelerle karşılaştırması yapılmıştır.

1. INTRODUCTION

The use of polymers is increasing very rapidly and in this century it will be the most used kind of material [1]. The properties of the polymers can be tailored with many different methods. In one method, certain reinforcing materials are used to make composite materials. It has been used since 1950. In the last quarter of 20^{th} century, the composite materials have been used widely in daily life applications. In the following century, the reinforcement of the polymers will be on the nano scale and this century will be named as nano century [2].

Today there are mainly 4 different kinds of materials [3]. These are metallic, ceramic, polymeric and composites made up of the mixes of minimum 2 components of above materials. The composite material is formed by combining at least two different materials in different phases [4]. The bone in our body and the trees in our lives are examples of composite materials [4]. The properties of the materials and their combination have been summarized in Figure 1.1 [4].

Among the composite materials, the polymeric composite materials family is the most common composite material. Polymers being light weight, flexible and easy to shape have numerous applications. The lower mechanical properties compared with metallic and ceramic materials can be increased with different reinforcing additives in the form of composite materials [5].

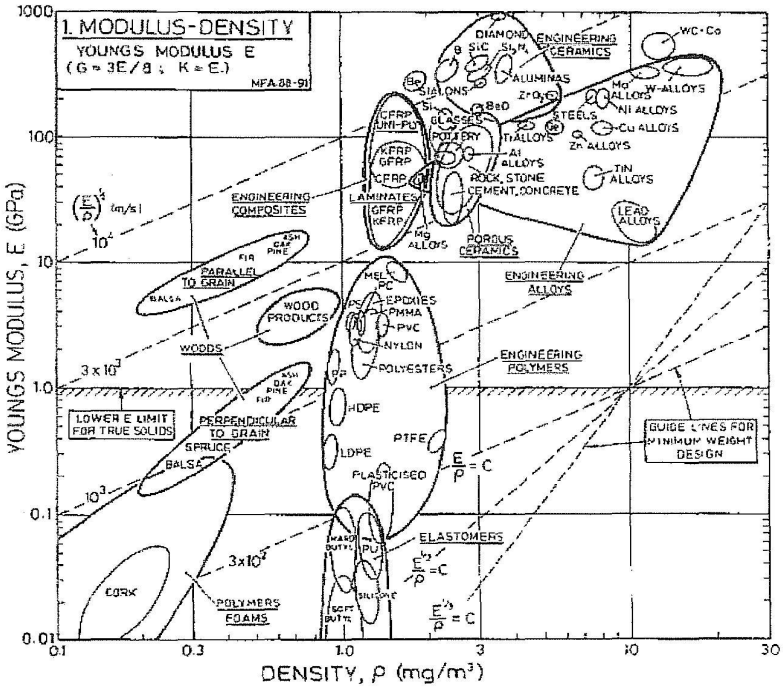

Figure 1.1: Different types of materials combined

The types of conventional composite materials are shown in Figure 1.2 [6];

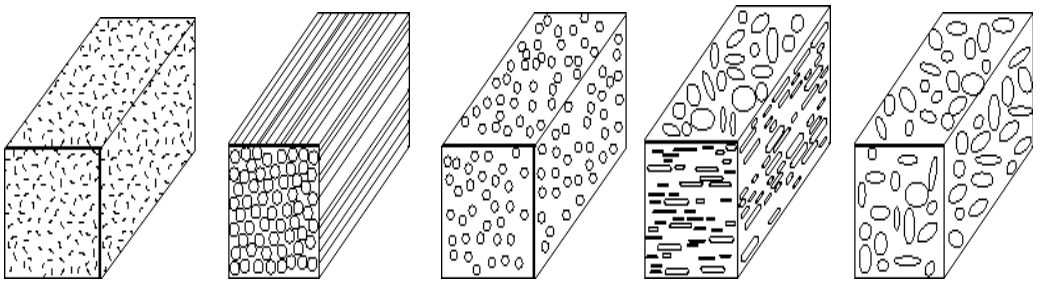

Random fiber Long fiber Particulate Flake Filler

Figure 1.2: Different types of composite materials

The new generation composites will be the nano scale reinforcements. There are many different approaches to nanocomposites. The major nanocomposites can be listed as follows:

a. polymer-clay nanocomposites
b. polymer-carbon nanocomposites
c. polymer-cellulose nanocomposites
d. polymer-inorganic sol-gel nanocomposites
e. polymer-nanometal nanocomposites

In this study polyurethane has been used as the matrix polymer. The polyurethane clay and polyurethane cellulose nanocomposites have been prepared and compared. The polyurethane has been reinforced with micron sized cellulose as well to demonstrate the significance of the nanosize reinforcement. As a final comparison, the polymer has been reinforced with micron sized carbon fibers.

1.1. Polyurethane

Polyurethanes are excellent materials in terms of high tensile strength, abrasion resistance, weather resistance, low temperature resistance and having a wide range of rigidity [7] enabling to be used in many applications such as biomedical, coatings, foams, adhesives, thermoplastic elastomers and composites [8].

Polyurethanes are generally synthesized in 2 steps. In the first step diols, compounds having two hydroxyl compounds and isocyanates are reacted to form the prepolymer and in the second step the polymer is finally chain extended with diamines or diols. The schematic synthesis is given in the Figure 1.3 [9].

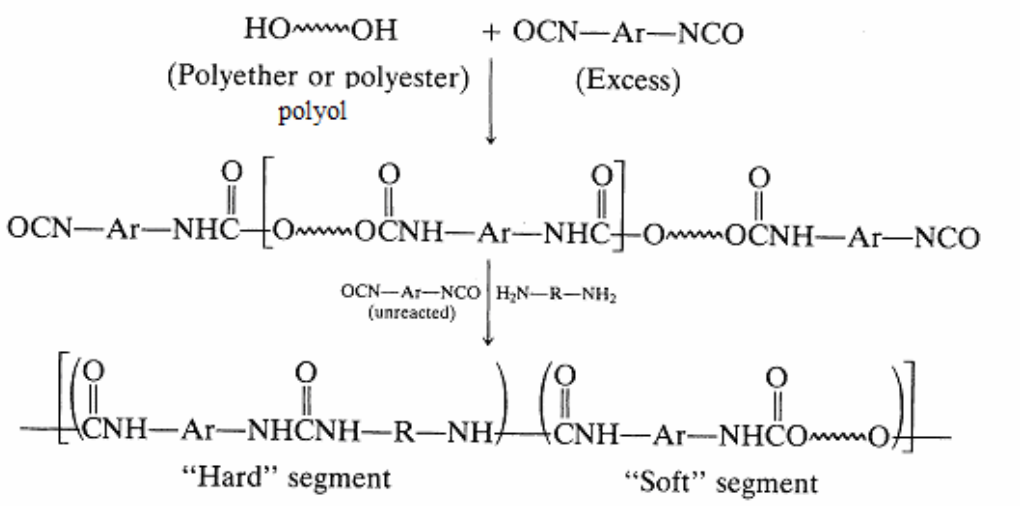

Figure 1.3: Schematic diagram for polyurethane synthesis

Also in some studies the polyurethane is produced without chain extenders. At this time, the isocyanates are reacted with polyols with stoichiometric ratios, not excess [10].

The isocyanates and polyols are varied depending on the application of the polyurethane [11, 12]. The source of polyol can be natural as well [10].

The wide range of polyols and isocyanates give this material many possibilities to be produced in a very broad range of properties resulting in various applications of this material. This two part structure composed of hard segment and soft segment makes the polymer [AB] type copolymer structure. This copolymer structure enables this polymer to be used in many different applications. The hard segment supplies the high mechanical properties and the soft segment gives the polyurethane its flexibility [13]. The properties of the polyurethane are adjusted with the ratio of this hard segment to soft segment and the types of the reactants used in the synthesis.

The new improvements in the polymer technologies help to improve the properties of the polyurethane as well. The formation of composites and nanocomposites with polyurethanes is very important and forms the basis of this study. There are studies on polyurethane glass fiber composites to increase the mechanical properties [14]. Polyurethane-clay nanocomposites have been prepared with the clay, montmorillonite previously to increase the mechanical properties and thermal resistance [15]. There are few studies on polyurethane-cellulose composites [16]. Cellulose being a bioresource

and abundant is a very important material family. Carbon fiber being the strongest material specifically has been recently used to increase the mechanical properties of polyurethane which is an also very new type of material [17]. This is a very important material in terms of the various kinds of applications of polyurethane and carbon fibers.

The next three parts will describe the materials used in the polyurethane composites of this study. The first one will be the polymer-clay part which is the most important part of this study, the second part will be a brief introduction to cellulosic materials and the third part will be the carbon fiber part.

1.2. Polymer-Clay Nanocomposites

The most important class of the nanocomposites is the clay nanocomposites which have been worked on by many scientists [18]. The clays are very interesting class of materials. The interesting point is that the layered silicate morphology disintegrates in the polymer matrix each layer being 1 nm thick and 100-200 nm long and wide sheets being formed. The general structure of the clay is given in Figure 1.4 [18].

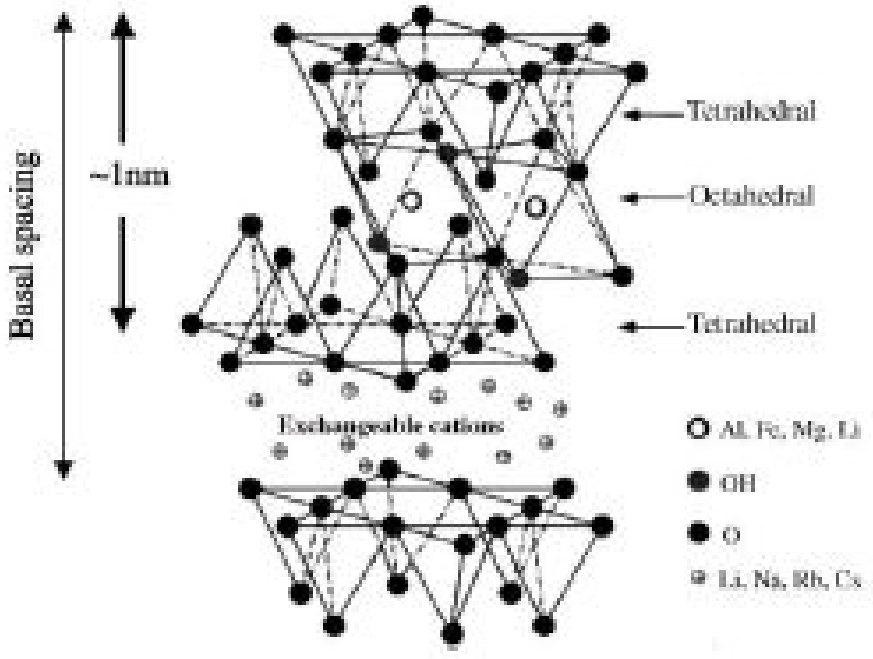

Figure 1.4: The crystal structure of the clay mineral, MMT and HEC

The general chemical structures of three main clays have been summarized in Table 1.1.

Table 1.1: Different types of clays from the smectite family

Type of Clay	Chemical Formula	Cation Exchange Capacity (meq/100g)	Particle Length (nm)
Montmorillonite	$M_x(Al_{4-x}Mg_x)Si_8O_{20}(OH)_4$	110	100-150
Hectorite	$M_x(Mg_{6-x}Li_x)Si_8O_{20}(OH)_4$	120	200-300
Saponite	$M_xMg_6(Si_{8-x}Al_x)Si_8O_{20}(OH)_4$	86.6	50-60

The polymer clay nano composites have many advantages over conventional composite materials [19]. Higher strength, increased thermal stability, gas barrier properties, flame retardancy, increased biodegradation rate, no change in optical properties are the major advantages of nano composites. Also when the tensile strength increases, the toughness does not decrease like in conventional composite materials [20]. The well dispersed nano fillers do not create stress concentrations as in micron composites [21].

The morphologies of polymer clay nano composites are shown in Figure 1.5. For optimum clay composites C and D morphologies are preferred making the composite material better [22].

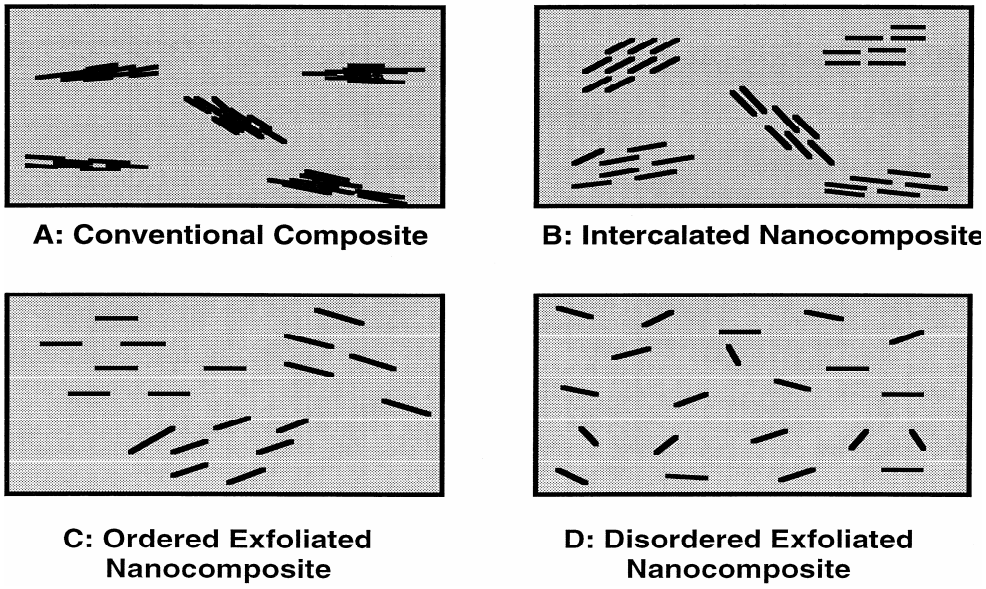

Figure 1.5: Different types of polymer-clay nanocomposites

The dispersion of the clay can be evaluated using X-ray. In exfoliated polymer-clay composites, the peaks of the clay disappear as a result of exfoliation [23]. This is illustrated in the Figure 1.6 [22].

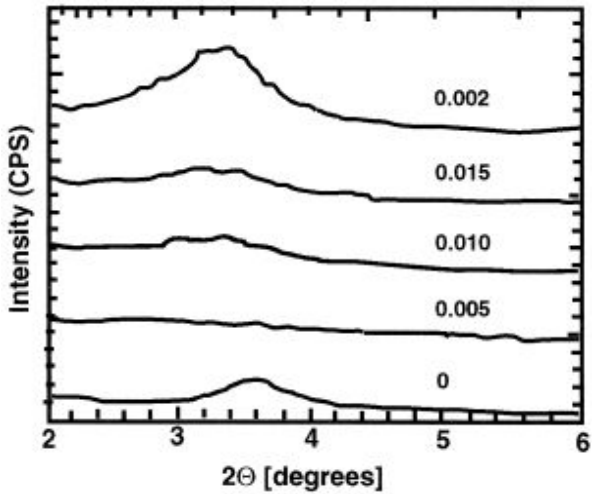

Figure 1.6: The X-Ray pattern of the clay and the polymer-clay nanocomposite

Previously in polyurethane-clay nanocomposites research, the montmorillonite especially the organically modified montmorillonite has been used [13]. They have used the clays in different polyurethanes with different techniques for different applications [23-25]. They have improved the mechanical properties, toughness and gas permeability properties of the polyurethanes significantly. They have mainly used the organically modified clays and/or synthetic clays.

In this study, hectorite clay was used. Research on hectorite (HEC) is limited when compared with montmorillonite. PU-HEC nanocomposite is very novel being studied first time in this study.

In some polymers it has been observed that hectorite improves the mechanical properties of the matrix polymer than the montmorillonite clay [26-28]. The ion exchange capacity of the hectorite we have used is higher than the montmorillonite used in our laboratory.

In one of the reference [29] the chemical composition of a hectorite clay was given as follows. The hectorite has Li_2O and high percentage of MgO which make the hectorite unique in terms of properties and applications.

Table 1.2: The chemical composition of the hectorite taken from literature

Mineral Formula	Content (%)
SiO_2	53.68
Al_2O_3	0.60
MgO	25.34
CaO	0.52
Li_2O	1.12
Na_2O	3.00
K_2O	0.07
Cl^-	0.31
Ignition Loss	15.36

In the previous studies, polyurethane has been reinforced with montmorillonite (MMT) as the nanoclay. In this study, the PU-MMT nanocomposites have been prepared in order to compare the properties of the PU-HEC and PU-MMT nanocomposites and to understand the effect of the hectorite clay.

Laponite, which is the synthetic hectorite clay sold commercially, was used to compare the properties of the nanocomposite prepared with the natural hectorite and synthetic hectorite. Laponite has similar structure with hectorite both structurally and chemically. Laponite is a 2: 1 layered hydrous magnesium lithium silicate consisting of two tetrahedral silica sheets sandwiching a central octahedral magnesia sheet, with the formula reported as $Na^{+0.7}[(Si_8Mg_{5.5}Li_{0.3})\ O_{20}(OH)_4]^{-0.7}$ [30]. The analysis of laponite is given in Table 1.3.

Table 1.3: Chemical analysis of laponite (given by the manufacturer)

Mineral Formula	Content (%)
SiO_2	59.5
MgO	27.5
Li_2O	0.8
Na_2O	2.8
Ignition Loss	9.4

Laponite is a relatively uniform disc-shaped synthetic clay 25 nm in diameter and 1 nm thick, as claimed by the manufacturer with a shape given inthe Figure 1.7.

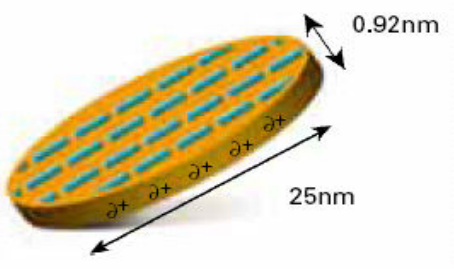

Figure 1.7: The shape and dimensions of each laponite plate

1.3. Silane Coating of Hectorite for Polyurethane Nanocomposites

Silane coupling agents have been used for different inorganic materials to be used in polymer matrices as reinforcing materials [31-33]. The silane coupling agents change the surface chemistry of the reinforcing material enabling the inorganic material disperse better, prevent aggregation and form bridge between the inorganic and the polymer phase [34].

In addition to the properties of the silane coating mentioned above, the silanes modify the clays like the organically modifiers, ammonium salts [35]. Moreover the silane coating can be done on the organoclays in order to enhance the strengthening effect of the clays in polymers [36].

In our investigations, we have obtained exfoliated structure with polyurethane and hectorite clay due to their hydrophilic natures. The aim of using silane coupling agent was to increase the strength of the interfacial region between the clay and the polymer matrix.

The general mechanism of the silane coating was given as follows;

$R\text{-}Si(OCH_3)_3 + 3H_2O \longrightarrow R\text{-}Si(OH)_3$ Hydrolysis

$R\text{-}Si(OH)_3 + R\text{-}Si(OH)_3 + \ldots \longrightarrow R\text{-}Si(OH)_2\text{-}O\text{-}Si\text{-}(R)(OH)\text{-} \ldots$ Condensation

There are two steps in the preparation of the silane grafting to the inorganic phase. In the first step, the silane is hydrolyzed with either water or any other solvent. In the second step, the condensation of the silane occurs and this binds the silane to the inorganic phase [37]. When the silane grafted inorganic material is combined with the polymer phase, the Figure 1.8 is generally obtained. Covalently bonded materials have been obtained [37].

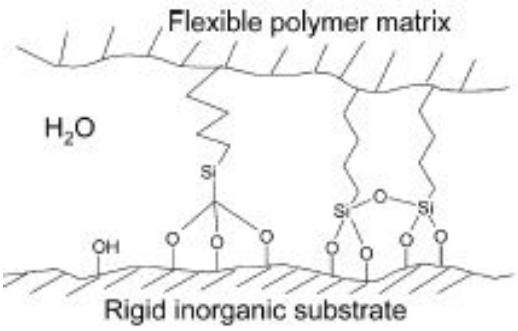

Figure 1.8: Silane coupling between the polymer and inorganic phase

Three different silane coupling agents have been used, namely 3-aminopropyltriethoxysilane, glycidoxypropyltrimethoxysilane and gamma-methacryloxypropyltrimethoxysilane. These were chosen as they have been used in different clays which have produced good results. The structures of these silanes have been given in the Figures 1.9, 1.10 and 1.11 [38-40].

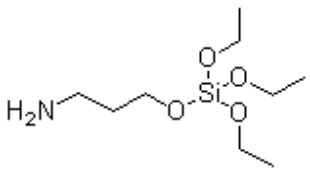

Figure 1.9: The chemical structure of 3-aminopropyltriethoxysilane

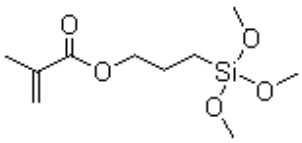

Figure 1.10: The chemical structure of gamma-methacryloxypropyltrimethoxysilane

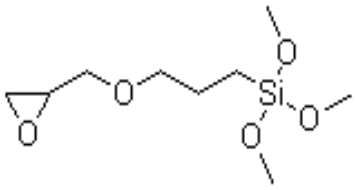

Figure 1.11: The chemical structure of glycidoxypropyltrimethoxysilane

1.4. Polyurethane-Cellulose Composites

Polyurethane is reinforced with cellulose fibers and cellulose fibrils. The composites have been prepared both at the micron scale and the nano scale. Brief information about cellulose is given below. Further information can be found in the literature.

Cellulose is one of the main parts of many plants. It is a linear condensation polymer formed with D-anhydroglucopyranose units and β-1,4-glycosidic bonds [41]. The Haworth projection formula of cellulose is given in Figure 1.12 [42].

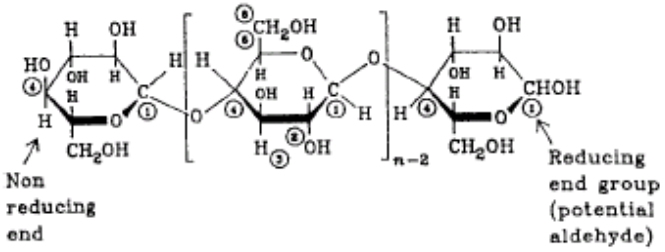

Figure 1.12: The haworth projection formula of cellulose

In all species, the primary cell wall of the cellulose has a dynamic structure. The cell wall of the cellulose is a composite material consisting microfibrils in a matrix of hemicellulose and lignin [43].

The physical and chemical properties of the cellulose are determined with this molecular structure. There are different types of cellulose materials resulting in the formation of different type natural fibers with various mechanical properties [41].

Wood is one of the major sources for the cellulose. Hardwood cellulose is one kind of the wood cellulosic materials. Wood-polymer composites have been studied by different researchers [44-46]. With improvements in the polymers and new improvements in the nanotechnology, people have been working on nanosize cellulose reinforced polymers [47-49]. Obtaining cellulose whiskers with sulfuric acid treatment has been one route [50] whereas newly homogenization of the cellulose into microfibrils was very recently worked [49]. The application of homogenization of cellulose to be used in polyurethanes was demonstrated for the first time during this study.

In this study, both micron sized cellulose and nano sized cellulose were used. The main outcome of the research was the emphasis of the nano reinforcement resulting much better improvements in the mechanical properties than the micron sized fiber reinforcement.

1.5. PU-Carbon Fiber Composites

Carbon fibers are very important materials in the composite industry with highly increasing demand to be used in many different applications. The Figure 1.13 shows the potential of carbon fiber usage in the coming near future [51]. The carbon fiber reinforced polymers will be used in many different applications including structural applications.

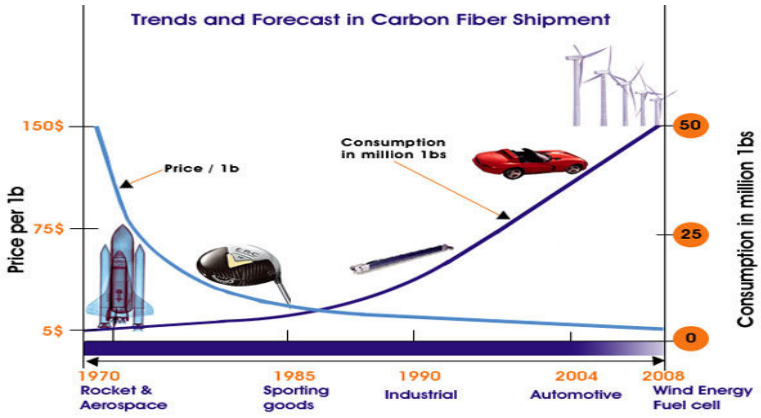

Figure 1.13: The graph of the carbon fiber demand vs. the price of carbon fiber in the time interval 1970-2008.

The major important property of the carbon fiber is the specific strength obtained by the mechanical strength/density of the material. The carbon fiber has 15 times higher specific strength than steel and 1.5 times higher than Kevlar [52]. The high mechanical strength of carbon fibers is related with the hexagonal lattice in other words, the graphene layer. The graphene layer has the shortest covalent bond in a plane. This makes the carbon fibers having the highest elastic modulus in the nature [53].

There are 4 different types of carbon fibers [52]. The source of carbon fiber determines the carbon fiber type. The PAN (polyacrynotrile) based carbon fiber is the most commonly used carbon fiber. The first carbon fiber was obtained form cellulose precursor. The third type is the pitch based carbon fiber and the fourth one is obtained with vapor grown carbon fibers [52].

In this study 7 micron thick PAN based carbon fibers have been used. The major aim of this study was to compare the results of the carbon fiber reinforced polyurethane with the results of the polyurethane nanocomposites prepared with clays and cellulose.

2. EXPERIMENTAL

This study has three main parts, the polyurethane-clay nanocomposites, polyurethane-cellulose nanocomposites and polyurethane carbon fiber composites. The clay and carbon composites were prepared in a similar way whereas cellulose composites were prepared with a different method.

2.1. Materials

There are mainly 4 different materials used in this research. The polymer matrix was polyurethane (PU). The reinforcing phases were clay, cellulose and carbon fiber. The polyurethane was taken from Flokser Co. (Istanbul, Turkey) with a weight average molecular weight of 30,000 Dalton. The polyurethane has a commercial code of TS-161. The solid content of PU was 35 wt % in PU-dimethylformamide (DMF) solution. It was the ester product of polyester polyol and diphenylmethanediisocyanate (MDI). The chain extender was 1,4-butanediol.

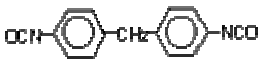

Figure 2.1: The chemical structure of MDI

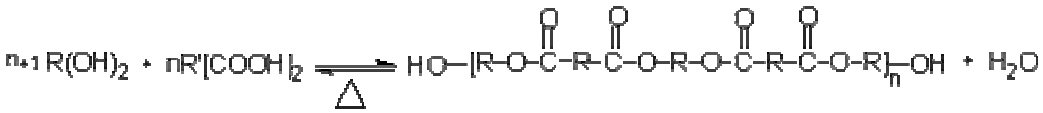

Figure 2.2: The synthesis and chemical structure of polyester polyol

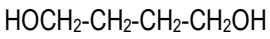

Figure 2.3: The chemical structure of 1,4-Butanediol

Two types of natural clays, hectorite and montmorillonite and synthetic clay were used. The clays were taken from Bigadiç, Balıkesir region of Turkey. The clays were used without purification. Both of the clays were delaminated with the solvent dimethylformamide (DMF).

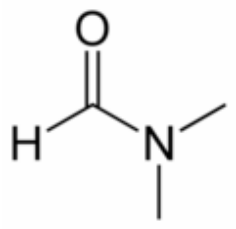

Figure 2.4: The chemical structure of DMF

The hectorite clay was further treated with organic modifiers to delaminate the structure of the clay and to obtain organo-clay. The organic modifiers used to obtain organoclay were Dodecyltrimethylammoniumbromide (DTABr), Hexadecyltrimethylammoniumbro mide (HDTABr), Sodiumdodecylsulfate (SDS), Ammoniumlaurylsulfate (ALS). The chemical formulas of the surfactants are given below.

Dodecyltrimethylammoniumbromide: $CH_3(CH_2)_{11}N(CH_3)_3Br$
Hexadecyltrimethylammoniumbromide: $CH_3(CH_2)_{15}N(Br)(CH_3)_3$
Sodiumdodecylsulfate: $CH_3(CH_2)_{11}OSO_3Na$
Ammoniumlaurylsulfate: $CH_3(CH_2)_{11}OSO_3NH_4$

The synthetic clay, laponite was taken from Southern Clay as a comparison to natural clay. The laponite has the similar chemical structure with the hectorite. The product is sold in the market.

Furthermore the hectorite was silane grafted with three different silanes in order to improve the properties of the nanocomposites. The silane coatings used were 3-aminopropyltriethoxysilane, glycidoxypropyltrimethoxysilane and gamma-methacryloxypropyltrimethoxysilane.

In the second part of the study cellulose was used as reinforcing phase. The cellulose was used at the micron level (approximately 15 micronmeter thickness) and nanosize (approximately 50-100 nanometer thickness) level. The cellulose was hardwood cellulose and it was taken from, Rayonier, USA with the trade name Terracel ^{TM}. The microfibrillated nanosize cellulose was prepared from this micron-meter cellulose material in the laboratory during this Ph.D study.

In the third part, carbon fiber was used for reinforcement. The carbon fiber was polyacrylonitrile based carbon fiber. The carbon fiber was taken from SGL Carbon Group, SGL SIGRAFIL C 320 B, high strength and high modulus of elasticity coupled with high electrical conductivity carbon fibers. The fiber thickness was 7 micron-meter.

2.2. Material Preparation

2.2.1. Preparation of clay

Clays were obtained in the form of large rocky form. They were crushed to small particles in the laboratory conditions. The crushed particles were reduced to fine particles using vibratory disc milling. In this disc milling, the particles were dispersed between metal rings and huge force is generated to rotate these rings enclosed in a metal container. While turning for 20 seconds with 1000 rpm, the clay particles were crushed to smaller particles. The schematic operation of the disc milling machine is shown in the Figure 2.5.

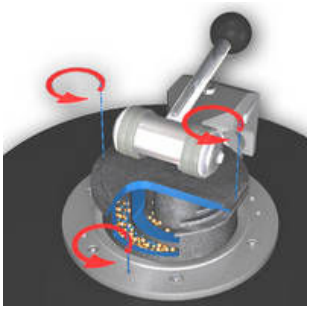

Figure 2.5: The disc milling device

After the disc milling operation, further milling was done with ball milling device. Three different ball milling times (5 hours, 10 hours and 16 hours) were used to determine the best milling time for the clay.

2.2.2. Preparation of organoclay

HEC powder was mixed with deionized water for 24 hours (2 wt % HEC stock dispersion) at room temperature. 20 mM DTABr stock solution was prepared by dissolving DTABr in water. Then, 10 mL DTABr stock solution and 10 mL 2 wt % HEC stock dispersion were mixed together to obtain 4 wt % HEC in 10 mM DTABr surfactant. Then, thix mixture was shaken for 24 hours. HDABr were added to the 4 wt % montmorillonite in the concentration range of $5 * 10^{-5} – 10 * 10^{-2}$ mol/L.

2.2.3. Silane coating of hectorite

The silane was mixed with ethyl alcohol (1 gram per 100 ml) to prepare a solution to coat the hectorite. The hectorite was added to this solution and the final mixture was stirred for 30 minutes. The final hectorite was dried in an oven at 100 ^{0}C for 5 hours to evaporate the ethyl alcohol completely.

2.2.4. Cellulose microfibril preparation and cellulose mat preparation

The cellulose fibers were taken in the form of pellets from the Terracel. The fibers were separated in water solution and waiting for 4 days to be sure of good dispersion of the cellulose fibers. Different cellulose concentrations were tested for the homogenization process (0.025, 0.05, 0.1 and 0.2). Different pressures (250 and 500 bar) were tested. The homogenizer applies 500 bar pressure fibrillating the cellulose fibers to nanosize fibrils. This fibrillated cellulose was used in experimental study.

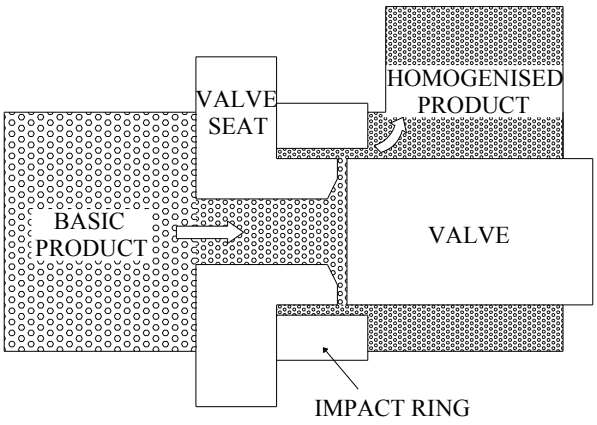

Figure 2.6: The schematic view of the homogenizer

The fiber mats used in composite preparation were prepared from two different materials, cellulose fibers and cellulose microfibrils. The mat formation of these two materials was similar. The cellulose-water slurry was filtrated and the retentate being cellulose on the filter forms a mat structure due to the strong hydrogen bonds of cellulose. The mats were like films with variables thicknesses. The thickness of the mat can be adjusted with varying the slurry volume. The thickness variation results in composite materials having different weight percentages of cellulose in the polyurethane matrix. The thickness of the mats varied between 50-250 micronmeter.

2.2.5. Preparation of composites

The composite samples were prepared with two different methods. The polyurethane-clay and polyurethane-carbon fiber composites were prepared by solvent casting method. The polyurethane–cellulose composites were prepared by film stacking method.

2.2.5.1. Preparation of polyurethane-clay nanocomposite

PU-hectorite nanocomposites were prepared by solvent casting method. The final optimum preparation technique is listed below.

a. Preparation of DMF-clay dispersion in ultrasonic bath at room temperature for 15 minutes

b. addition of PU-DMF solution to DMF-clay solution
c. stirring the final solution for 4.5 hours with magnetic stirrer
d. waiting for 1 day to avoid bubbles
e. using solvent casting knife to obtain nanocomposite films.

The important points for film preparation are given below.

1. The knife at 1000 micron thickness, obtaining 100 micron-meter final thickness of polyurethane films
2. Casting on a special silicon coated paper,
3. Evaporation of solvent at 150 ^{0}C for 10 minutes

The compositions shown in Table 2.1 and Table 2.2 were prepared.

Table 2.1: Different compositions of PU-clay nanocomposites

Sample code	Polyurethane (wt %)	Hectorite (wt %)	MMT (wt %)	Lap (wt %)
PU	100	-	-	-
PUH1	99	1	-	-
PUH3	97	3	-	-
PUH5	95	5	-	-
PUH7	93	7	-	-
PUH10	90	10	-	-
PUH15	85	15	-	-
PUMMT3	97	-	3	-
PUMMT5	95	-	5	-
PUMMT7	93	-	7	-
PUL1	99	-	-	1
PUL3	97	-	-	3
PUL5	95	-	-	5

Table 2.2: Different compositions of PU-silane coated clay nanocomposites

Sample code	Polyurethane (wt %)	Silane A Grafted HEC (wt %)	Silane B Grafted HEC (wt%)	Silane C Grafted HEC (wt %)
PU	100	-	-	-
PUA7	93	7	-	-
PUB7	93	-	7	-
PUC7	93	-	-	7
PUA1	99	1		
PUA3	97	3		
PUA5	95	5		
PUA10	90	10		

Silane A: 3-Aminopropyltriethoxysilane

Silane B: Gamma-methacryloxypropyltrimethoxysilane

Silane C: Glycidoxypropyltrimethoxysilane

2.2.5.2. Preparation of polyurethane-cellulose micro and nanocomposite

The composite materials were prepared using film-stacking method (see Fig 2.7). In this method the PU films and the cellulose mats were stacked and compression moulded (Fontijne Grotnes B.V., Vlaardingen, the Netherlands). Varying temperature (T) (150-200 ^{0}C), pressure (F) (100-200 bar) and stacking duration (1-4 minutes) were tested to find the optimum composite properties.

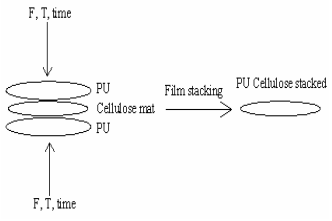

Figure 2.7: Schematic picture of film stacking method

The compositions shown in Table 2.3 were prepared.

Table 2.3: The compositions of prepared materialsof PU-cellulose composites

Sample code	Polyurethane (wt %)	Cellulose fibers (wt %)	Cellulose microfibrils (wt %)
PU	100	-	-
PU-CF1	91.5	8.5	-
PU-CF2	81.3	18.7	-
PU-CNF1	92.5	-	7.5
PU-CNF2	83.5	-	16.5

2.2.5.3. Preparation of Polyurethane-Carbon Fiber Composite

Polyurethane-carbon fiber composites were prepared with solvent casting method. The procedure was the same as the preparation of clay nanocomposites except the stirring time. Samples were stirred for overnight. The steps of film preparation are given below.

a. Addition of carbon fiber to polyurethane-DMF solution
b. Stirring the solution for overnight
c. Waiting for 1 day to avoid bubbles
d. Using solvent casting knife to obtain composite films. This stage was achieved in 4 steps.
    i. The knife at 1000 micron thickness, obtaining 100 micron final PU film thickness
    ii. Casting on a special silicon coated paper
    iii. Evaporation of solvent at 150 ^{0}C for 10 minutes
    iv. Removing the film from the silicon coated release paper

Table 2.4: The compositions of PU-carbon fiber microcomposites

Sample Codes	Polyurethane Content (wt %)	Carbon Fiber Content (wt %)
PU	100	-
PUCar05	99,5	0,5
PUCar1	99	1
PUCar2	98	2
PUCar3	97	3

2.3. Characterization

2.3.1. Particle Size Analysis

Malvern Mastersizer 2000 was used to determine the particle size of the clay. In this instrument, the measurement is done with laser beam. The particles were dispersed in the water tank of the machine. The laser was diffracted according to the particle size of the clay.

2.3.2. X-ray Analysis

PANalytical X'pert Pro X-ray was used. The X-ray analysis helps in analyzing the purity of the clay and in determination of the compounds associated with the clay.

2.3.3. Cation Exchange Capacity (CEC)

CEC was measured with methylene blue absorption method.

2.3.4. Zeta-potential

Malvern Zetasizer 2000 was used to measure the zeta potential of the water-clay suspensions. The water-clay (2 wt % clay) suspension was centrifuged for 10 minutes at 4000 rpm. Afterwards, the zeta potential was measured by injecting the suspension into the Zetasizer.

2.3.5 Rheology

The rheological behavior of the clay-water suspensions were measured with Brookfield MODEL DV-III + Programmable Rheometer with a spindle SC4-18. The rheological behavior of 2 wt % clay-water and clay-DMF suspensions and 5 wt % clay-DMF suspensions were measured to understand the differences in the rheological behavior of the clays and to understand the differences of the behavior between different solvents.

2.3.6. BET Surface Analysis

ASAP Micromeritics 2010 was used to determine the BET surface area of the hectorite and montmorillonite.

2.3.7. Visual Examination

The colloidal view of the cellulosic material was observed by visual investigation. The change in the suspension of cellulose in the water after certain passes of homogenization could be easily observed.

2.3.8. Optical Microscopy

The fibrillation could be observed with optical microscopy as well. Leica DC300 optical microscopy was used to characterize the fibrillation of the cellulose.

Leica DS 480 optical microscopy was used to observe the dispersion of the carbon fibers in the polyurethane matrix. 100 times magnification was used to observe the PU-Carbon fiber composites.

2.3.9. Scanning Electron Microscopy (SEM)

Scanning electron microscopy, JEOL 5410 was used at 5 kV.

The fibril structure was characterized with SEM (Hitachi S-4300) operated at 6 kV.

The samples were coated with gold in order to have conductive samples to measure under SEM and avoid charging.

2.3.10. Transmission Electron Microscopy (TEM)

For preparation of TEM sample, polymer nanocomposite was dissolved in the DMF with a concentration of $2.5*10^{-5}$ g/mL. Then the solution was poured onto water with a pastor pipette with 5 drops. The polyurethane was coagulated on the water. The pieloform coated TEM grids are put on this polyurethane nanocomposite in water and waited there for 3 seconds. Then the grid was let to dry for 10 minutes in air. The sample was ready for observing with TEM. JEOL JEM 1011 operated at 80 kV was used to conduct TEM observations.

2.3.11. Fourier Transform Infrared Spectroscopy (FTIR) Analysis

FTIR analysis was conducted with Perkin Elmer FT-IR Spectrometer to investigate the polyurethane structure and to determine if there is any free NCO present in the polymer matrix.

2.3.12. Mechanical Properties, Tensile Testing

For the determination of mechanical properties, the tensile testing was applied to samples because the studied material is generally subjected to axial longitudinal forces. Two different tensile testing equipments were used. The polyurethane-clay and polyurethane-carbon fiber composites were tested with Shimadzu AGS-J 10 kN tensile testing machine. The dimensions of the samples were 10*100*0.1 mm. The maximum strength was measured. The cellulose composites were tested with Mini-Mat 2000 (Rheometric Scientific Ltd, Leatherhead, UK) at 22°C with dimensions of 0.1×5×50 mm.

2.3.13. Dynamic Mechanical Analysis (DMA)

The Perkin Elmer was used to measure the polyurethane-clay and polyurethane-carbon fiber composites. The tested material had dimensions of 0.1×10×40 mm. The material was heated from -100 ^{0}C to +100 ^{0}C with a heating rate 3 ^{0}C/min. The applied frequency was 1 Hz. The polyurethane-cellulose composites were measured by using Dynamic Mechanical Thermal Analyzer DMTA V (Rheometric Scientific Ltd, Leatherhead, UK). It was used to measure the dynamic modulus of the PU and composite materials at

different temperatures. Materials were tested using tensile mode. The sample size was 0.1×5×40 mm. The frequency was 1 Hz and the heating rate was 2 °C/min.

2.3.14. Thermal Gravimetric Analysis (TGA)

Perkin Elmer Diamond TG/DTA was used for TGA analysis. The measurements were done from +50 ^{0}C to +1200 ^{0}C with a heating rate of 100^{0}C/min. The analysis was used to determine the solid content left when the polymer was heated up to 1200 ^{0}C.

2.3.15. Contact Angle Measurement

KSV Cam200 device was used to determine the hydrophilicity of the polyurethane. Water was used as wetting liquid to determine the hydrophilicity.

3. RESULTS AND DISCUSSION

3.1 Characterization of Hectorite

The hectorite used in the preparation of polyurethane nanocomposites was characterized and the same procedure was carried out for the montmorillonite (MMT) clay, and their properties were compared. During the characterization studies, the liquid medium used was water, DMF and ethylene glycol.

3.1.1. Particle size analysis

Firstly, the particle size distributions were exhaustibly measured to understand the particle size of the clay in order to be able to obtain successful nanocomposites. Communition was performed by crushing and two stage milling. In the first step, the hectorite clay in the form of large stones was crushed to smaller particles. Afterwards, these smaller particles were reduced to an average size of 9.5 micron meter (average, 50 %) with disc milling. The particle size of the hectorite was measured and given in the Figure 3.1.

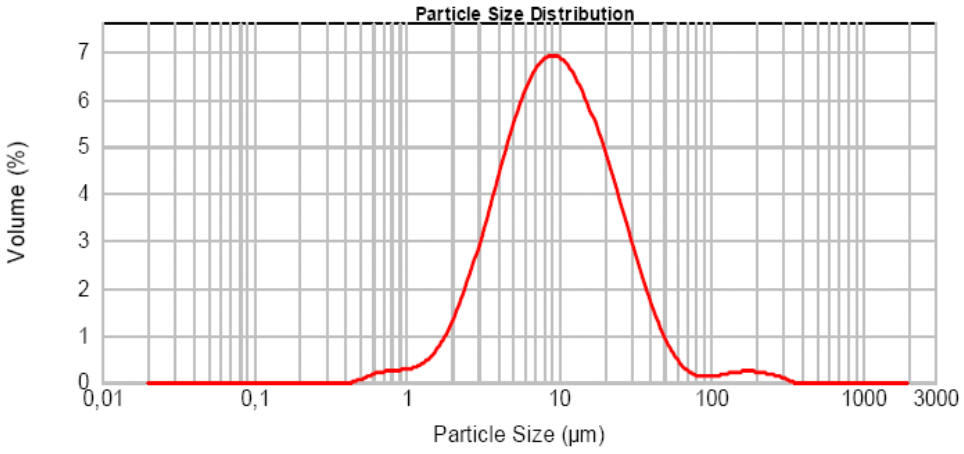

Figure 3.1: The particle size distribution of the HEC after disc milling

Different ball milling times were tested such are: 5 hours (5 h), 10 hours (10 h) and 16 hours (16 h). With 5 hours milling, an average particle size of 2.37 micronmeter, with 10 hours of milling 1.95 micronmeter and with 16 hours of milling 1.981 micronmeter was achieved (shown in Figure 3.2). Thus, the optimum milling time was 10 hours.

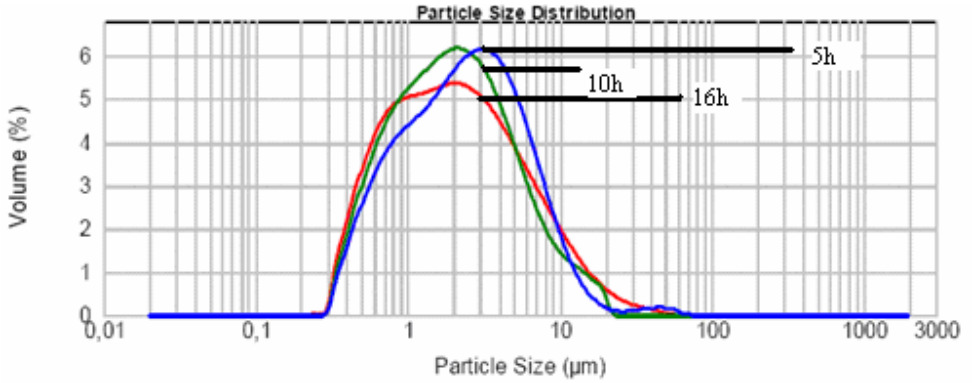

Figure 3.2: The particle size distribution of the HEC after different ball milling times

After these investigations, it was observed that the clay in the ball milling mixture with ethanol could not be recovered after milling because of the agglomeration of the clay particles. For this reason only disc milling was used and it was observed that the particle size was not so important when preparing nanocomposites of polymers with clays due to the exfoliation and separation of the clay layers in the polymer matrix.

The particle size of the MMT was determined as well. The average [d(0.5)] particle size of the montmorillonite was 6.79 micronmeter (shown in Figure 3.3.) obtained with disc milling. The final average particle of the hectorite size was measured as 1.95 micron meter. The distribution of the particle size is also very critical. The distribution of the hectorite is much more uniform than MMT. As the particle size decreases the interaction of the clay particles increases.

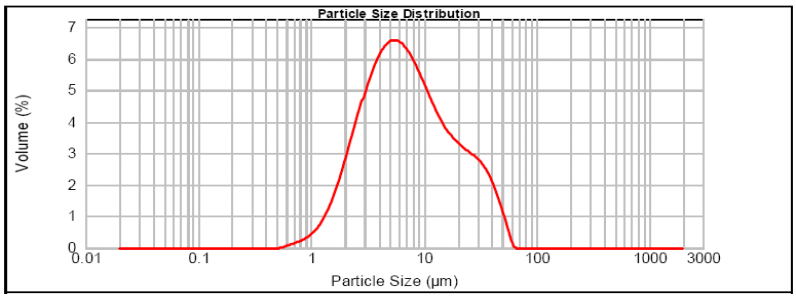

Figure 3.3: The particle size distribution of the MMT after milling

After measuring the particle size, the characterizations of the hectorite and montmorillonite were done to be able to characterize the hectorite and compare the hectorite with the montmorillonite. The results are given in Table 3.1.

Table 3.1: Characterization of hectorite and comparison with montmorillonite

	Hectorite	**Montmorillonite**
CEC meq/100g	95	53
Zeta(ξ) mV	-13	-17.2
Mobility (μ)µmcm/Vs	-1.34	-1.02
Yield Value(τ_B) Pa	0.06	-0.01
Viscosity(η_{pl}) mPa.s	1.64	1.22
Average Particle Size, µm	1.95	6.80
BET Surface Area, m^2/g	163.5	140.3

3.1.2. Cation exchange capacity

The cation exchange capacity (CEC) is a very critical value to be used in many different applications. It determines the capability of the clay to exchange the cations. This is also important for polymer nanocomposites enabling to obtain exfoliated structures. This first observation was in accordance with the values given in the literature in the introduction part of the thesis. As shown in Table 3.1, the value of CEC for hectorite was found 95 meq/100g. Even though hectorite is not purified, it has really very high CEC value. The high CEC is very important for swelling in water. The higher value enables to prepare organoclay much easier letting the organic modifiers to enter into the clay galleries.

3.1.3. Zeta potential

The zeta-potential value gives the charge of the particles suspended in certain solvents. In order to determine the zeta potential of HEC and MMT, water was used as the solvent. The best values to obtain good dispersion of the particles are either below -25 or above +25 mV. As seen in Table 3.1, for these clays, the values are not in that region but good exfoliated structures were obtained. The values of both clays are not much different. These values display flocculating structure of dispersions. The zeta potential is an electrical potential in the double layer at the interface between a particle, which moves in an electric field, and the surrounding liquid. The surface charge property can be characterized by the zeta potential and the stability of a clay solution can be measured depending on its value.

3.1.4. Rheological measurements

During the measurements, the clay was dispersed in water. In order to have good dispersion of the clay, which can easily disperse in the solvent, the yield values is critical. It should be lower than 1. Here, for both type of clays, it is very low value showing the dispersibility of the clay. The hectorite has a positive value which shows that the hectorite is better.

The viscosity values were obtained using the Brookfield rheometer. The graph is given in Figures 3.4. The viscosity value of the hectorite is higher. The higher the viscosity, the better the clay suspension is in terms of higher shear forces generated to obtain better clay-solvent dispersions.

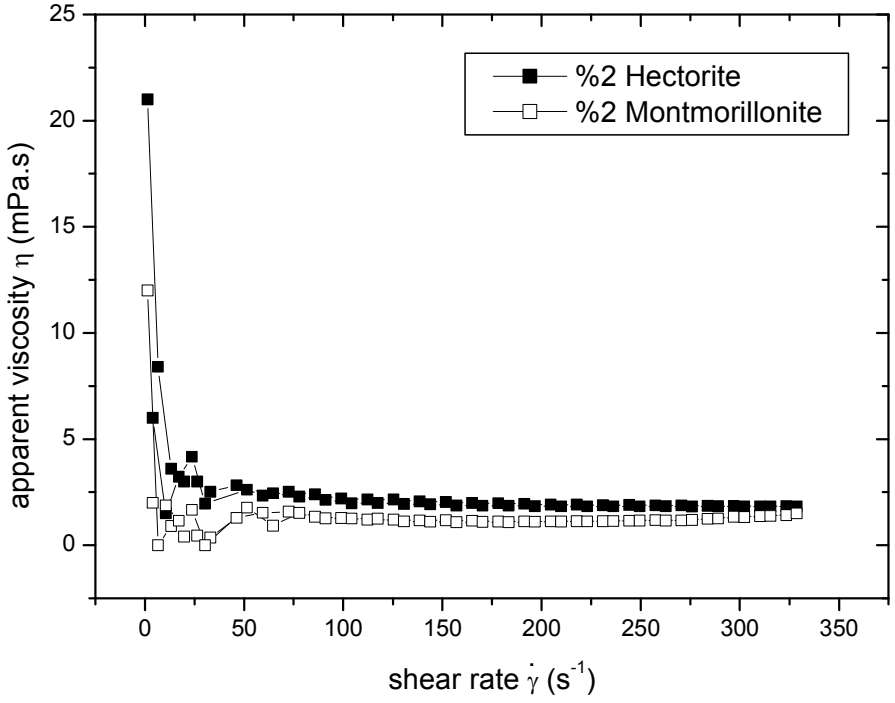

Figure 3.4: The viscosity of HEC and MMT

The critical value of stress for shifting from solid to liquid behavior defines the yield value τ_y. Yield stress value is directly related to the attractive energy and the separation distance between the particles. The gel state is characterized by the increase of the yield stress value. The degree of thixotropic or antithixotropic behavior was measured by the area of the hysteresis loop. The area between the increasing and decreasing curves defines the thixotropic area. The hysteresis loop area of the flow curves, known as thixotropy, is a reversible time-dependent flow. As seen in Figure 3.5, the behavior of the HEC is thixotropic whereas MMT is not thixotropic. The main reason of HEC being thixotropic is the smaller size of the particles. The smaller particles enable to interact better and have higher surface area.

The shear stress versus shear rate for HEC and MMT dispersions are shown in Figure 3.5. Hectorite dispersion showed non-Newtonian flow at a concentration of 2 %. Above a certain value of shear rate, the flow curve becomes linear. Pseudoplastic flow

behavior of colloid dispersions can be described by the Bingham model. The suspensions have Bingham plastic properties and Bingham flow model was applied. The flow behavior of any system (dispersion) is described in terms of the relationship between the shear stress (τ) and the shear rate ($\dot{\gamma}$). The shear rate is defined as the change of shear strain per unit time, and the shear stress as the tangential force applied per unit area. The ratio of τ to $\dot{\gamma}$ is called viscosity. Viscosity is a measure of the resistance to flow of the fluid. The plot of the shear stress vs. the shear rate is called a consistency curve. The resistance of the suspension to flow can therefore be considered as consisting of two parts: a Newtonian part in which the shear stress is proportional to the shear rate and a non-Newtonian part in which the shear stress is constant irrespective of the shear rate.

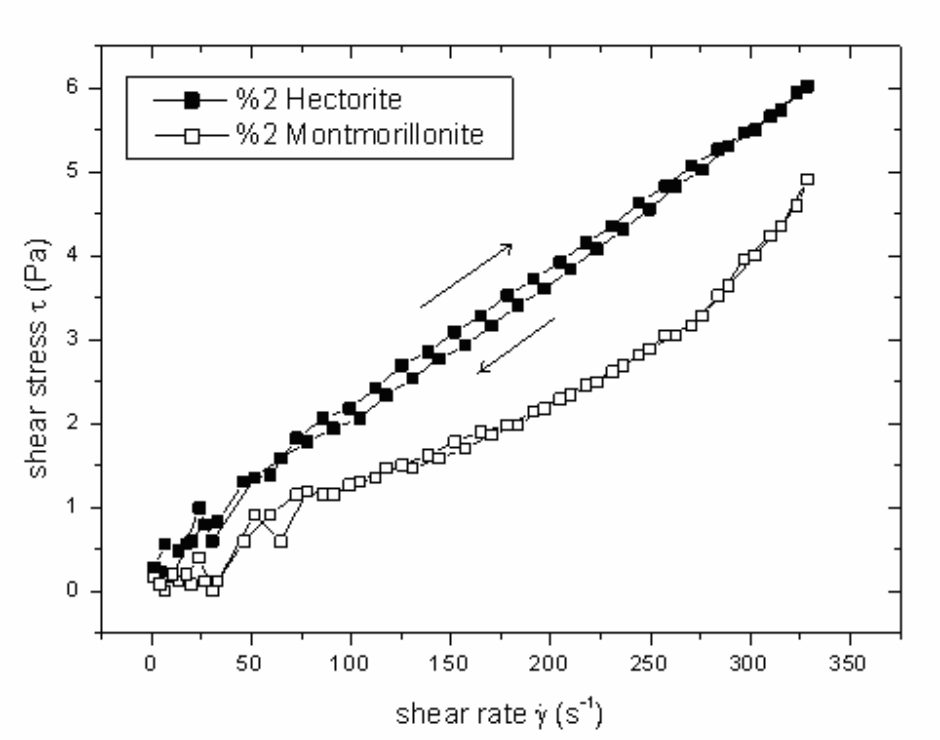

Figure 3.5: The rheological behavior of HEC and MMT

3.1.5. BET analysis

The BET analysis to measure the surface area of the hectorite was done. It was determined that the surface area of HEC and MMT is 163.5 and 140.3 m^2/g, respectively. This also shows the better properties of the hectorite compared to MMT.

3.1.6. Chemical and mineralogical analysis

The results of chemical analysis for HEC and MMT are given in Table 3.2. As shown in Table 3.2, the HEC contains Li which is unique property of the HEC. This creates very important rheological and thixotropic advantage of the HEC compared with the other clays.

Table 3.2: The Chemical Analysis of HEC and MMT

Sample	Ignition Loss	SiO_2	Al_2O_3	Fe_2O_3	TiO_2	CaO	MgO	Na_2O	K_2O	Li_2O
MMT	11.15	61.7	16.45	1.72	0.09	2.1	6.08	0.17	0.34	-
HEC	21.50	50.57	0.80	0.09	0.02	14.49	11.70	0.10	0.10	0.45

The hectorite was analyzed mineralogically and it was found that the hectorite is 90 % pure having 5 % calcite as impurity. From the mineralogical analysis, the MMT has 95 % purity with 3 % calcite.

3.2. Preparation of Organoclay

3.2.1. Results of organic modifiers

For preparation of organoclay, traditional organic modifiers, DTABr and HDTABr were used in order to increase the d-spacing of the hectorite. After using cationic modifier, anionic modifiers were used, namely ALS and SDS. Also LiCl was used in order to affect the Li content of the hectorite but neither of them increased the d-spacing values of the hectorite.

3.2.1.1. DTABr

The change in d-spacing values, zeta potential and viscosity values with change in the concentration of this organic modifier is given in the Figure 3.6 and Figure 3.7. Firstly

DTABr was used to delaminate the clay. The results showed that it was not successful for delaminating the clay and no improvements were observed with this organic modifier for d-spacing values.

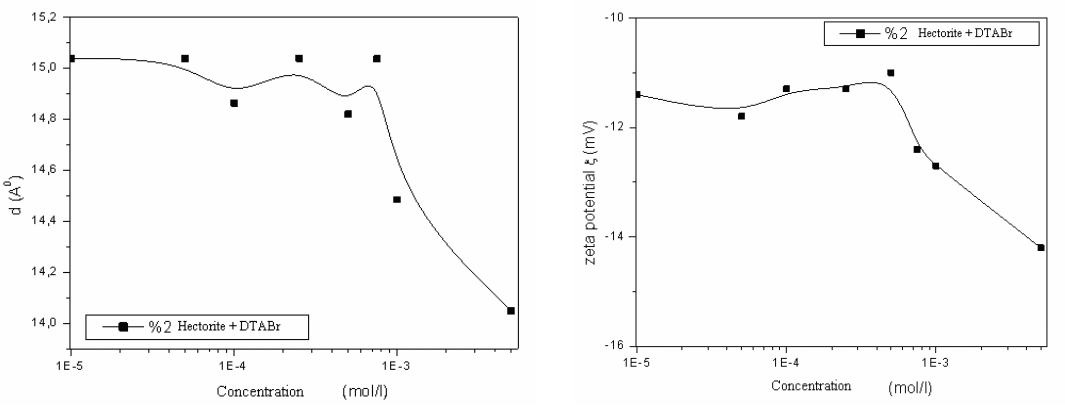

Figure 3.6: The d-spacing values and zeta potential values with change in the concentration of organic modifier

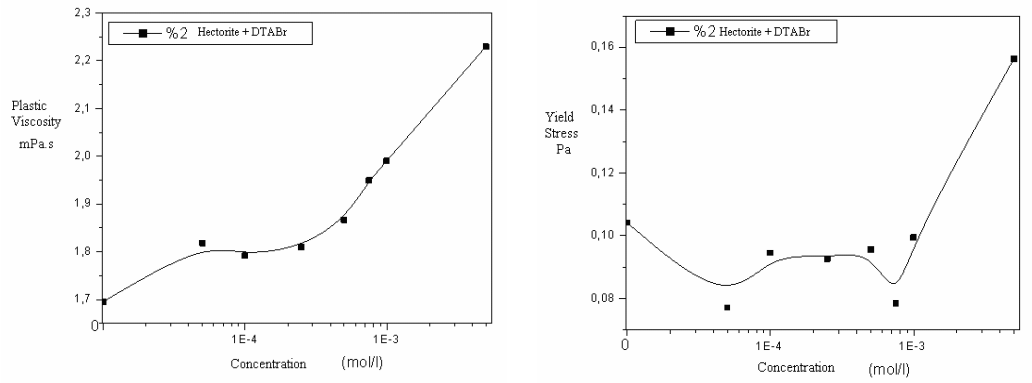

Figure 3.7: The plastic viscosity and yield stress change in the concentration of organic modifier

3.2.1.2. HDTABr

HDTABr with differing pH values were used to change the d-spacing and zeta-potential values. The results are summarized in Table 3.3.

Table 3.3: The effect of HDABr on HEC at different concentrations and acidity

Sample	Zeta Potential (mV)	D spacing (A^0)
HEC pH 2,5	-14.1	15.21
$5,10^{-3}$HDABr/HEC pH 2,5	-15,6	13,8
$5,10^{-3}$HDABr/HEC natural pH	-14.1	13.8
HEC pH 11,2	-40.0	12.7
$5,10^{-3}$HDABr/HEC pH 11,2	-28.1	13.8

No significant improvement was observed as well. Although the zeta-potential of HEC was measured as -40.0 mV at pH=11.2, the significant change was not determined for the value of d-spacing.

3.2.1.3. Other organic modifiers and LiCl

Anionic modifiers, ALS and SDS and also LiCl were tested to see the effects of the delamination.

It was understood that these did not help as well. The values of the d-spacing are 1.576 nm for HEC-LiCl, 1.535 nm for ALS-HEC and d-spacing could not be measured for SDS-HEC.

The X-ray analysis was used to determine the swelling capacity and the delamination of the clay. Organic solvents and water were used to swell the clay. It was found out that the clay is delaminated in water and organic solvents without using organic modifier. As shown in Table 3.3, water delaminated the clay much more than the organic solvents. This is consistent with the findings of Olejnik et al [54] who have found that the maximum swelling was obtained with water when they tested montmorillonite. The results are given in Table 3.4.

Table 3.4: The swelling of HEC in different solvents

Sample	d-spacing
Hectorite	1.538 nm
HEC, swollen in ethylene glycol	1.765 nm
HEC, swollen in DMF	1.960 nm
HEC, swollen in water	2.354 nm

The increase in the d-spacing values is very critical in the preparation of the nanocomposite. To increase the d-spacing values, generally organic modifiers were used. The organic modifiers enter between the layers of the clay and cause easy dispersion of the clay in the polymer matrix. In this study, the organic solvents penetrated between the clay layers and acted as organic modifier. Thus the clays were delaminated. Water helps to swell the hectorite as well. This is very important especially for water based polymer systems. Wypych [55] has done similar observations with kaolin clay. Kaolin was reacted with dimethyl sulfoxide (DMSO) and delaminated kaolin was obtained. It was observed that the value of d-spacing increased from 0.716 nm to 1.121 nm.

Graber and Mingelgrin [56] have proposed a model for this swelling behavior of clays in certain solvents. They have formed a model based on the solution theory of the polymers. They have used the solubility parameters of the solvents and the clays. They determined the maximum swelling in the presence of N-methylformamide. They obtained very significant swelling values for DMF as well.

The swelling of montmorillonite with DMF was done as well. The results of X-ray analysis and the shift in the peak angle can be seen in the Figure 3.8.

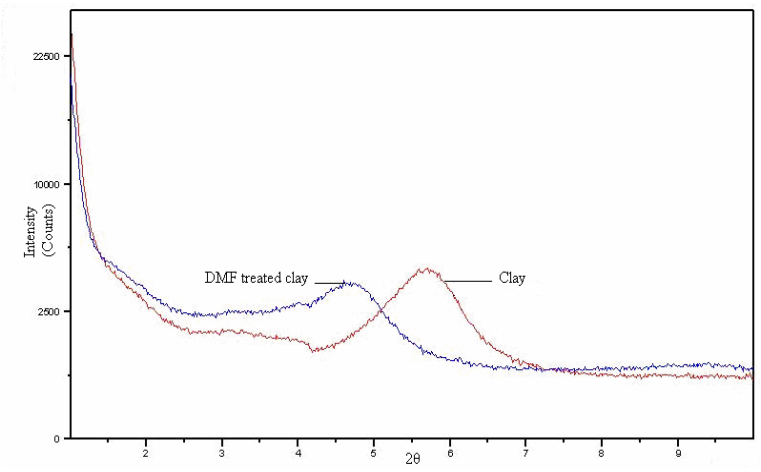

Figure 3.8: The shift of clay peak with DMF

The X-ray patterns of treated clay and the DMF treated clays are shown in Figure 3.8. The shift in d-spacing values is clearly observed.

3.3. Concluding Remarks on Clay Characterization:

This study is the first step in clay based polymer composite studies. Two different natural clays of Turkish origin were used. One of them was montmorillonite and the other was hectorite. Among these two, hectorite showed better properties than the montmorillonite for nanocomposite preparation.

In order to investigate the effect of organic modifiers, the organoclay was prepared. Conventional organic modifiers used for MMT were not successful for hectorite. The organic modifiers did not change the d-spacing values of the hectorite. On the contrary, the organic solvents such as ethyleneglycol, DMF and water were used to increase d-spacing values of the hectorite. The DMF has swollen the montmorillonite clay as well. DMF acted as the organic modifier.

3.4. Characterization of PU-Hectorite Nanocomposites

3.4.1. X-ray analysis

The X-ray patterns are given in Figures 3.9-3.14. By X-ray analysis, it can be concluded that the nanocomposites were obtained at all concentrations of hectorite in the

polyurethane matrix. All samples prepared at different clay concentrations showed the same behavior. None of them gave the clay peak at $2\theta = 6.5^0$. This is the most important finding of this research. This result shows that the compatibility between the polymer and the clay is very well. One of the reasons is the interaction of clay and DMF. As explained in the previous chapter, the interaction of the clay, hectorite with solvents such as water and DMF is very important. The easy swelling character of hectorite brings the delamination of the clay before interacting with the polymer-solvent solution. The interaction of the clay and the solvents, especially DMF, was shown by Graber et al [56]. For preparation of polymer-clay nanocomposite, the hydrophilicity of the polymer is one of the most important parameters. Hydrophilic polymers are compatible with the clay due to the hydrophilic character of the clay as well. As the polyurethane used in this study is hydrophilic, polyurethane clay nanocomposites were prepared successfully.

The stirring time was also very critical to obtain the exfoliated structures. Below four hours, the exfoliation could be achieved repeatedly. But after 4 hours, namely 4.5 hours, 6 hours, 12 hours and 24 hours exfoliated structures were observed with X-ray.

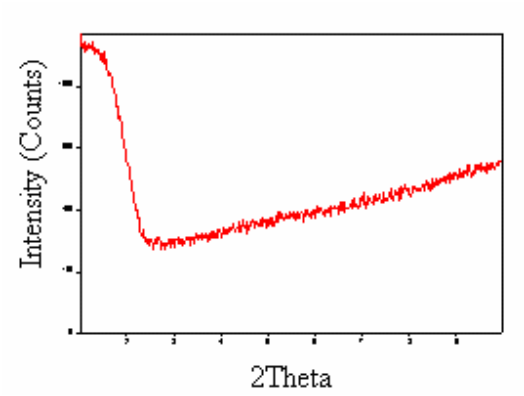

Figure 3.9: X-ray D. pattern of PUH1

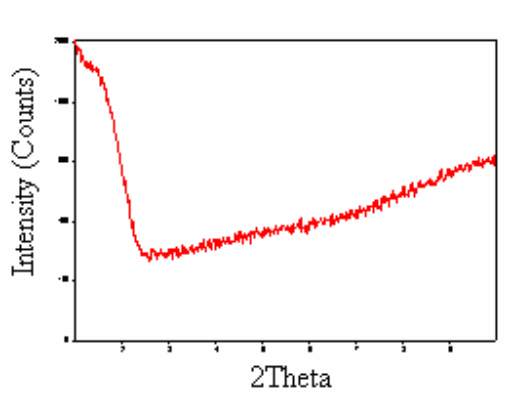

Figure 3.10: X-ray D. pattern of PUH3

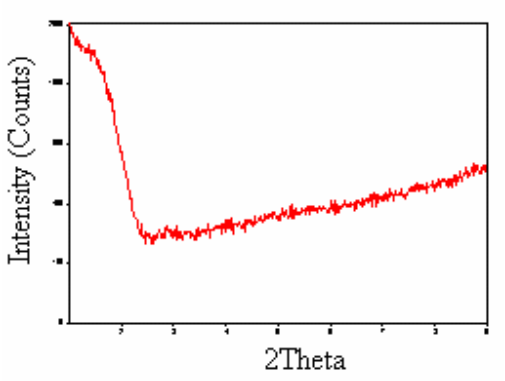

Figure 3.11: X-ray D. pattern of PUH5

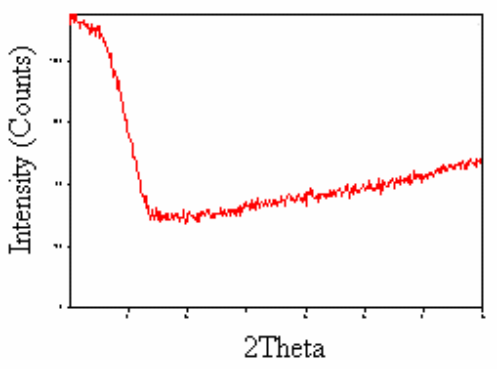

Figure 3.12: X-ray D. pattern of PUH7

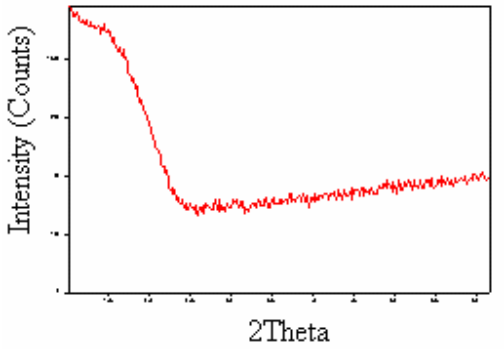

Figure 3.13: X-ray D. pattern of PUH10

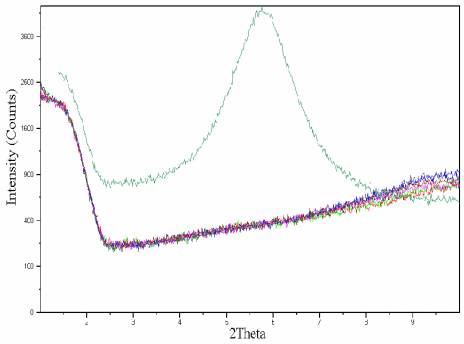

Figure 3.14: X-Ray D. patterns of HEC and PUHEC combined

3.4.2. Contact angle measurement

The contact angle of polyurethane with water was found as 63.73^0 (Figure 3.15). Since the value of the contact angle is smaller than 90^0, it can be concluded that the polyurethane is hydrophilic.

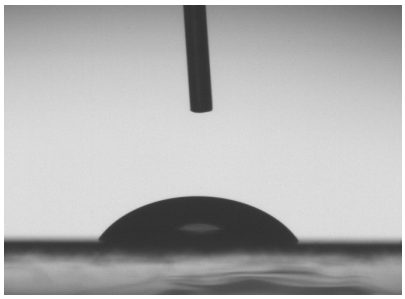

Figure 3.15: Contact angle of water on PU surface

3.4.3. FTIR analysis

The FTIR peaks of the hectorite (Figure 3.16), the polyurethane (Figure 3.17) and the nanocomposites (Figures 3.18-3.23) were used for explanation of nanocomposite structure.

As shown in Figure 3.20, silicate gives a characteristic peak at 998.30 cm^{-1}.

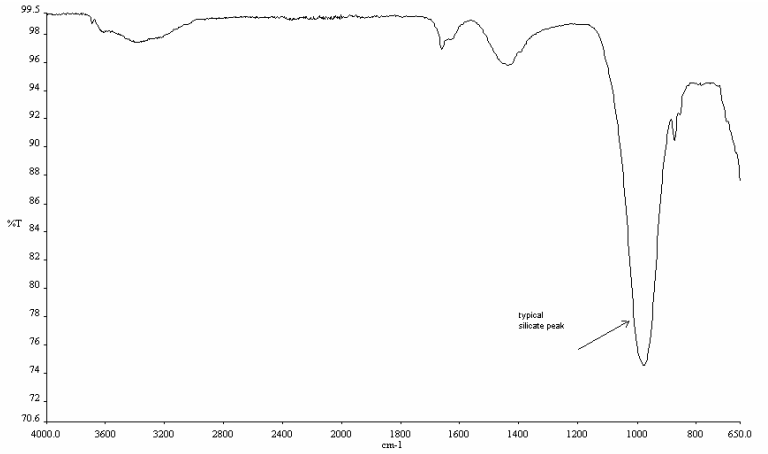

Figure 3.16: FTIR spectrum of HEC

The FTIR peaks of the polyurethane used in this study were given in Figure 3.17. The typical polyester polyol peaks were observed. At 1729 cm^{-1} ester bond, 1596 cm^{-1} aromatic bond, C=C and 1414 cm^{-1}, C-C bond were observed.

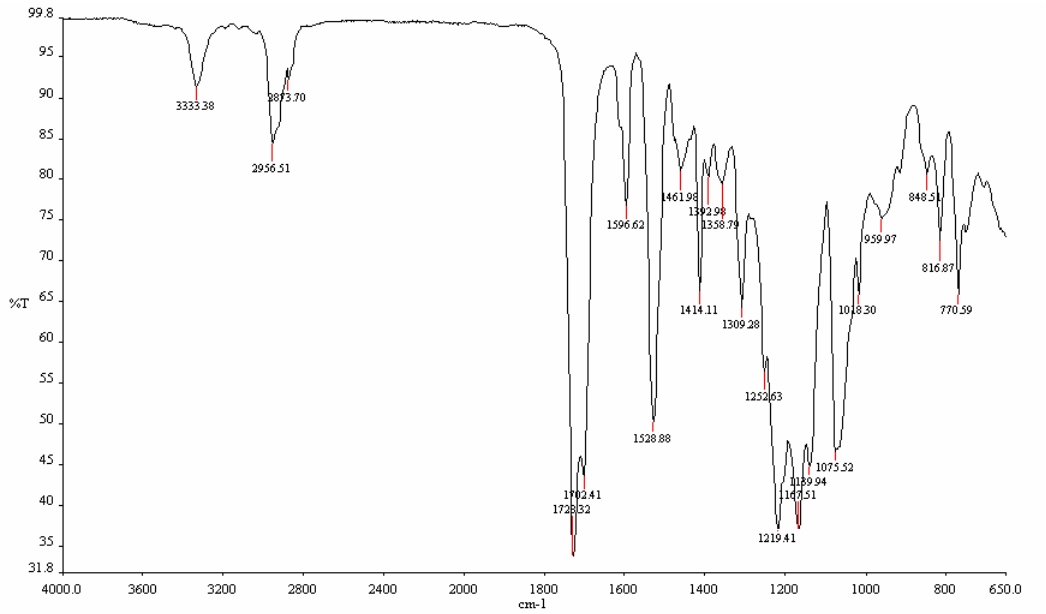

Figure 3.17: FTIR spectrum of polyurethane

In the Figures 3.18-3.23, the FTIR peaks of nanocomposites of the PU and the clay are shown.

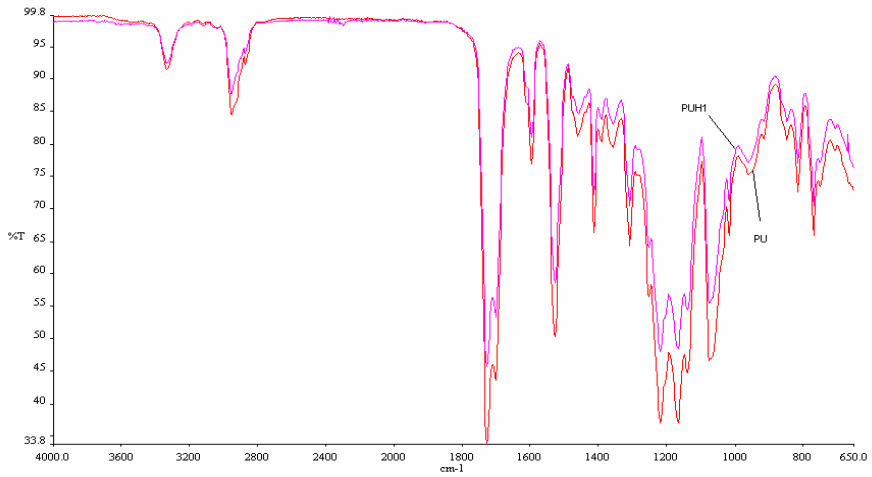

Figure 3.18: FTIR spectrum of PUH1

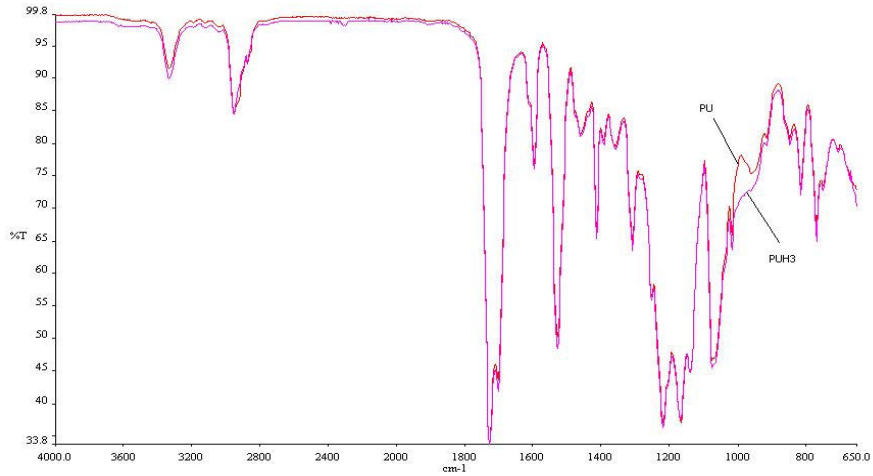

Figure 3.19: FTIR spectrum of PUH3

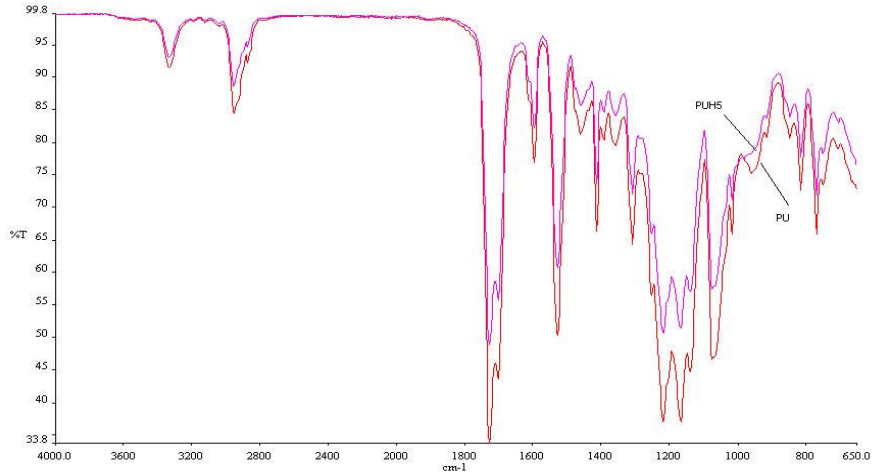

Figure 3.20: FTIR spectrum of PUH5

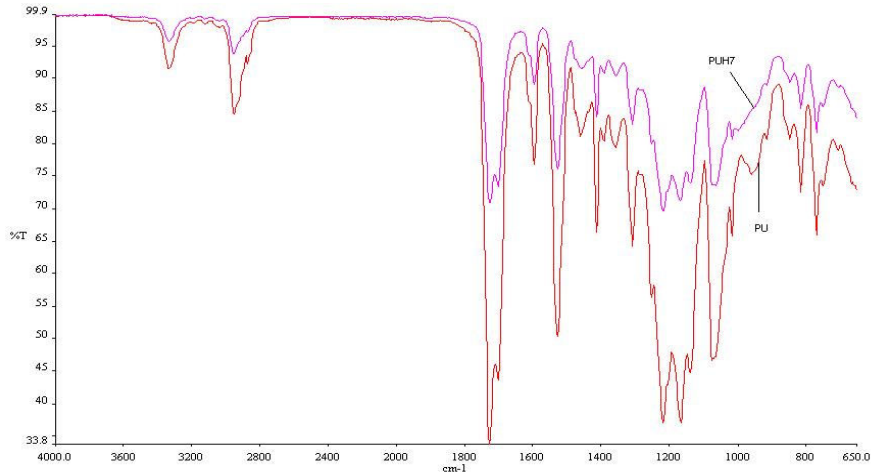

Figure 3.21: FTIR spectrum of PUH7

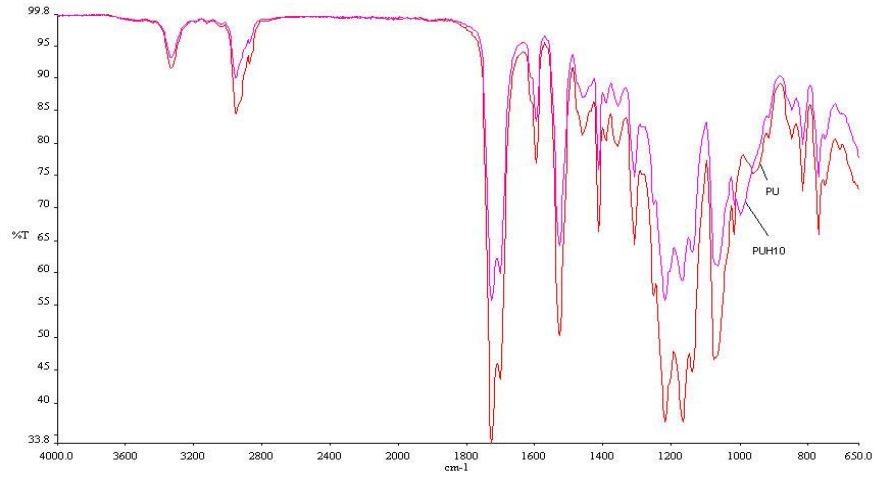

Figure 3.22: FTIR spectrum of PUH10

Figure 3.23: FTIR spectrum of PUH15

With 1 % hectorite addition, the polyurethane structure is maintained. After 1 % hectorite content, with 3 % addition and more, one of the peaks (at 959.97 cm^{-1}) disappears in the polyurethane structure. Takeichi and Guo [23] stated that at 947 cm^{-1} there is C-O out of plane deformation. Wu et al [57] has stated that at 937 cm^{-1} there is O-H out of plane stretching. This shows that the C-O-H bond in the polyurethane structure is destroyed due to the OH bonds of the hectorite.

On the other hand after 5 % the clay peak appears in the FTIR analysis at 998.30 cm^{-1}. The peak height increases at 10 and 15 wt %.

3.4.4. Mechanical testing

The results of the tensile test are given in the Figure 3.24.

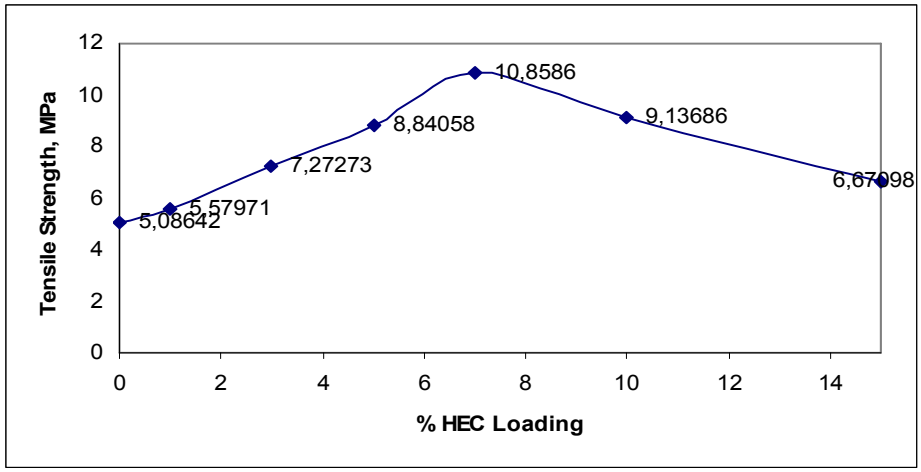

Figure 3.24: The mechanical properties of the PU and PU-HEC nanocomposites

As shown in Figure 3.24, the mechanical properties of nanocomposites prepared were strongly influenced by the content of HEC. Tensile strength increased with increasing HEC content in the range of 1-7 wt %. Compared to the pure PU, the tensile strength of the 7 wt % HEC containing PU nanocomposites was higher than 113,48 %. When the HEC content was higher than 7 wt %, tensile strength of nanocomposite decreased. This is consistent with the data obtained by W.J. Choi et al [58] and Ni et al [59]. They have observed also a peak value among the clay nanocomposites. This result is very important due to the use of the natural clay which is neither purified nor organically modified.

The increase in the mechanical properties was attributed to the individual hectorite platelets dispersed into the polyurethane matrix. The interfacial interaction of the hectorite and the polyurethane was very important in order to increase the mechanical properties. The hydrogen bonding between the hectorite and the polyurethane is very critical in order to increase the mechanical properties in the nanocomposites [60]. The hydrogen bonding is enhanced with hydrophilic polyurethane and the hydrophilic hectorite clay. Above certain level of clay loading, the maximum strength decreased.

3.4.5. Dynamic mechanical analysis

The DMA results of pure polyurethane and polyurethane-clay nanocomposites are shown in Figures 3.25-3.31.

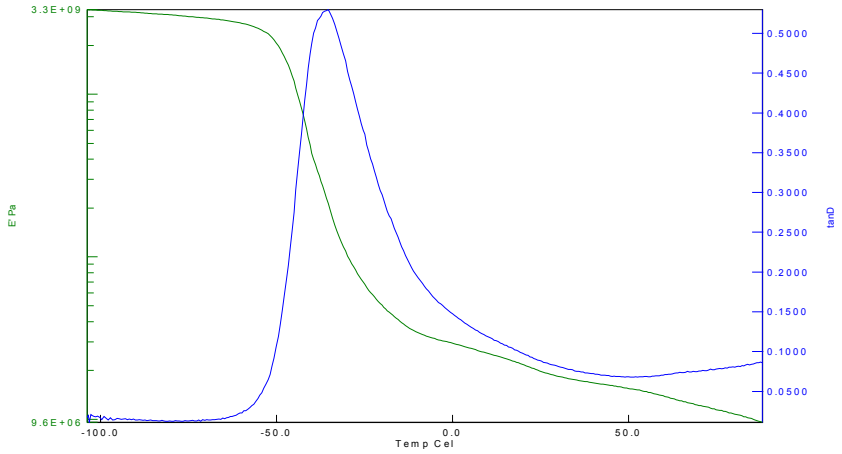

Figure 3.25: DMA of PU

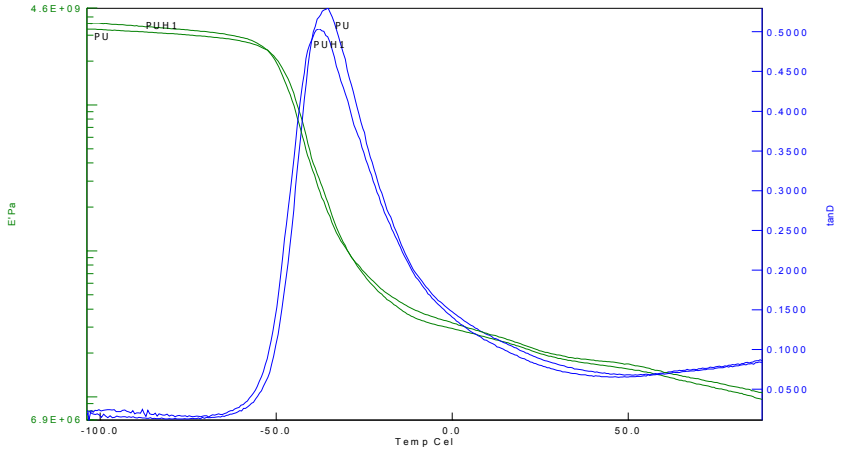

Figure 3.26: DMA of PUH1

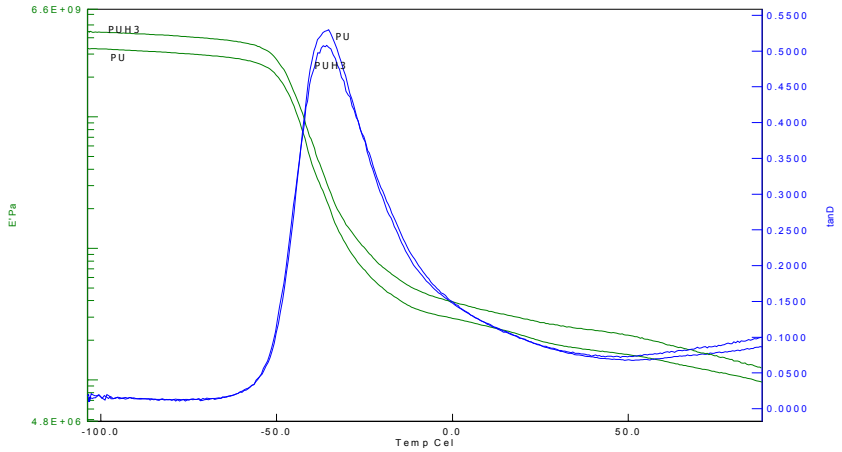

Figure 3.27: DMA of PUH3

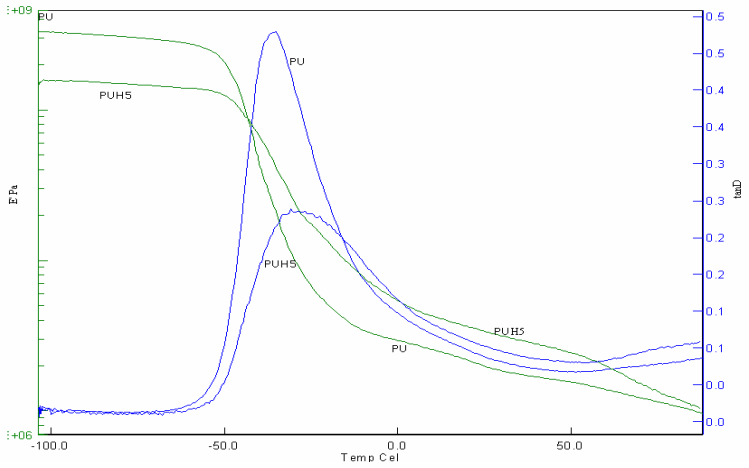

Figure 3.28: DMA of PUH5

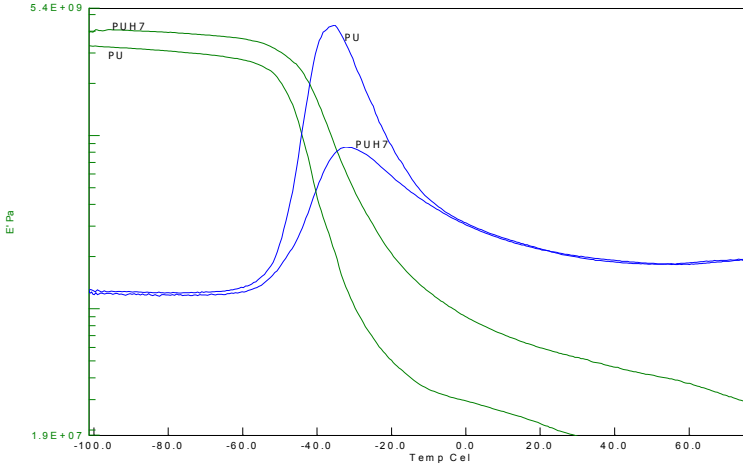

Figure 3.29: DMA of PUH7

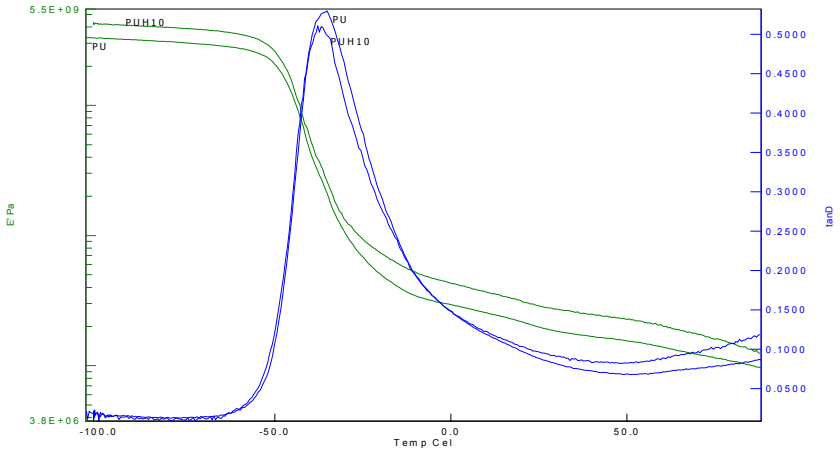

Figure 3.30: DMA of PUH10

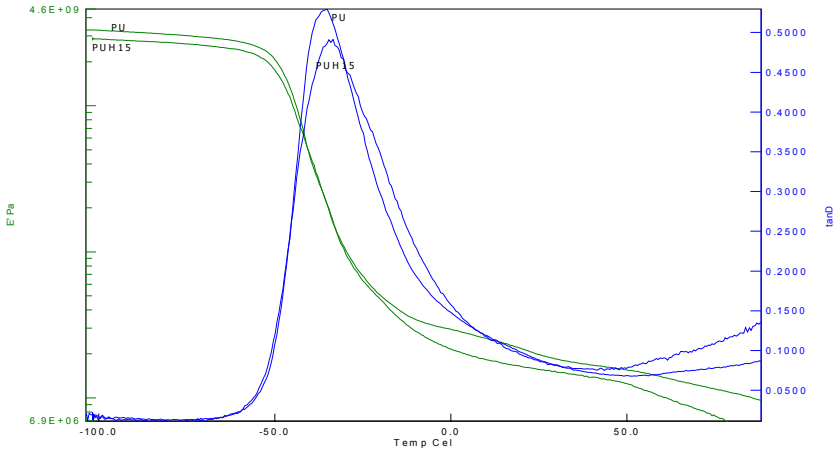

Figure 3.31: DMA of PUH15

Figure 3.26 shows the behavior of neat polyurethane. The polymer starts to soften at -52.4 ^{0}C measured by the onset value of tan delta. This the α transition of the polymer which means the glass transition temperature. The materials modulus values decrease very sharply as a consequence of the glass transition. Afterwards, the polymer comes to a rubbery linear region after the glass transition. The material continues to lose strength upon heating but the slope is less than the glass transition period.

When the polymer is reinforced with the clay the modulus values increase which is in agreement with the tensile testing. The modulus values of the nanocomposites are higher

than the pure polymer at all temperatures except the nanocomposite containing 15 % hectorite. The modulus value of the PUH15 is lower than the other due to the aggregation of the clays in the polyurethane matrix. The storage modulus values are higher especially above the glass transition temperature (Tg) of the polyurethane matrix.

The value of modulus increased with increased HEC content in the range of 1-7 wt %. The high strength of 7 % was confirmed with the tensile testing as well. For 10 % hectorite the modulus values are significantly higher than that of the pure polymer at all temperatures being less than the 5 and 7 %. For 15 % nanocomposite, due to the high content of HEC particles, the modulus values of the nanocomposite is less than that of the pure polymer. The modulus values are lower for all the temperatures.

When we investigate the tan delta peaks, it is observed that the tan delta peaks do not shift significantly. This shows that the nanocomposites do not alter Tg value of the pure polyurethane determined by the onset of tan delta. Another important phenomenon in the tan delta peak is the height of the tan delta peak. As the polymer loses its flexibility and it gets more rigid, and the chains lose their elasticity, this is reflected in the tan delta peaks. For all the compositions of the nanocomposites, the height of the tan delta peak decreases. Especially for the high strength compositions 5 and 7 %, the height decreases significantly.

3.4.6. TGA

The Figure 3.36 shows the combined TGA graph of the polyurethane nanocomposites formed with HEC. The thermal stability did not change much but the residue left after heating increases with the increase in the clay concentration.

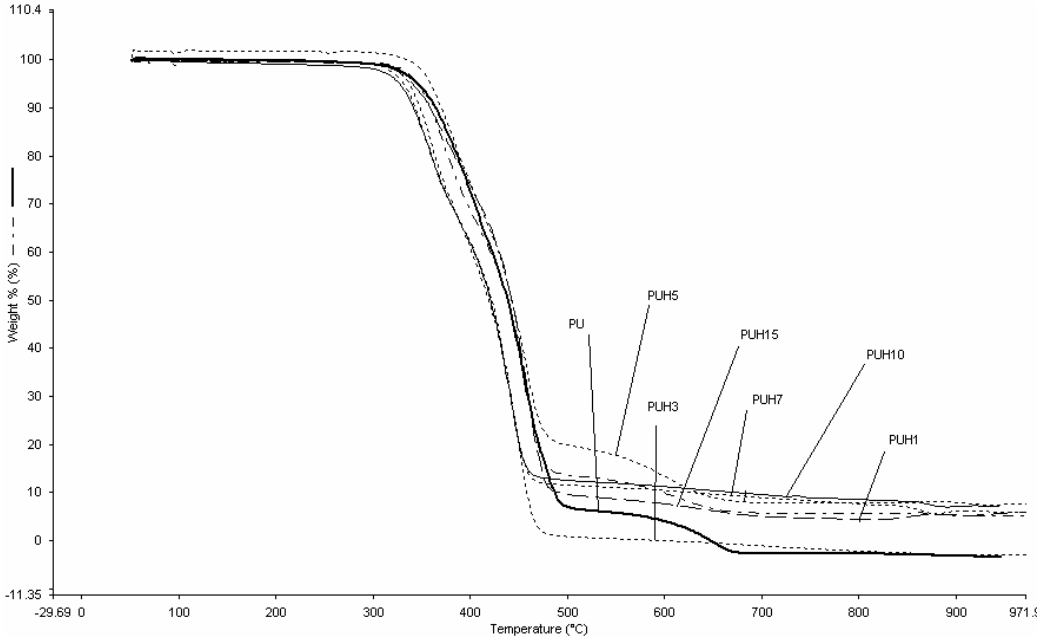

Figure 3.32: TGA thermograms of PU and nanocomposites

3.4.7. SEM

From the Figures 3.33-3.38, it was observed that the clay particles can not be seen in SEM images. This supports the exfoliation comments with X-ray analysis. For the final investigation of the structure for nanocomposites, TEM was used to observe individual plates of the clay.

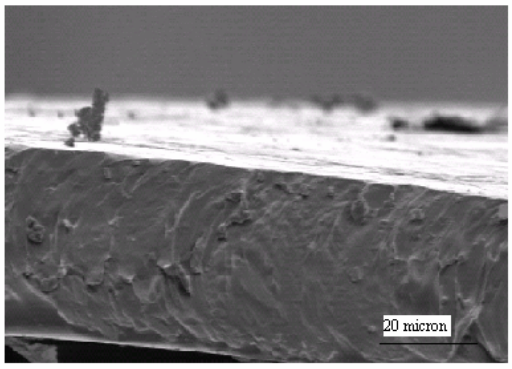

Figure 3.33: SEM image of PU

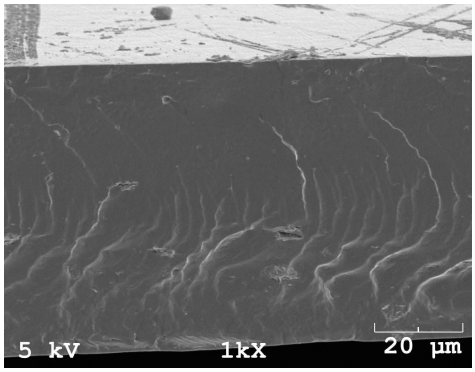

Figure 3.34: SEM image of PUH1

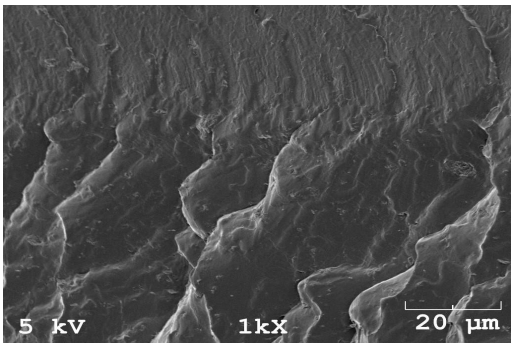

Figure 3.35: SEM image of PUH3

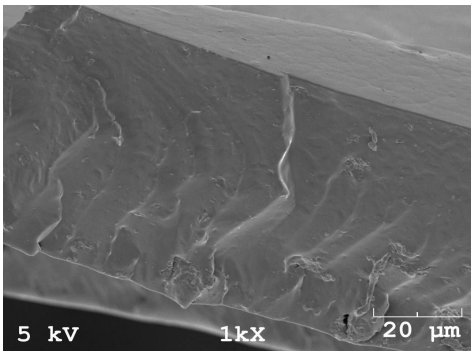

Figure 3.36: SEM image of PUH5

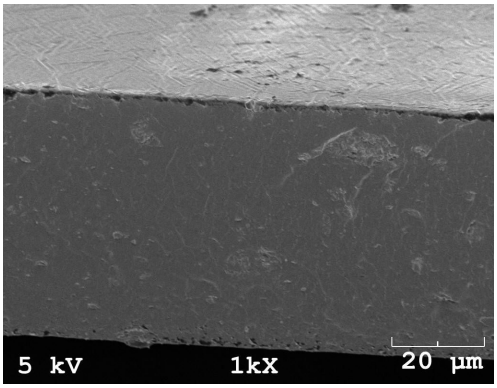

Figure 3.38: SEM image of PUH7

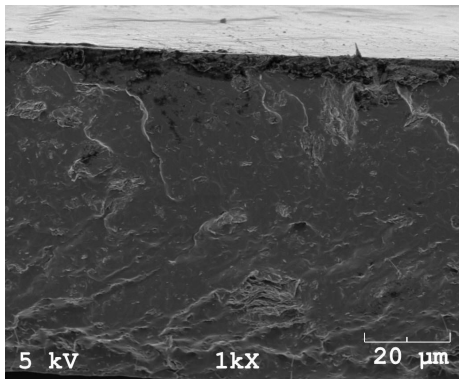

Figure 3.39: SEM image of PUH10

3.4.8. TEM

From the TEM observations (Figures 3.39-3.42), it is clearly observed that the hectorite is exfoliated in the polyurethane matrix. As the hectorite content increased, the clay thickness increased as well. The structures are still exfoliated but they are that much thin as 3 %. In this study, even with 15 % clay, exfoliated structures could be obtained which is very hard to obtain after 5 % clay addition.

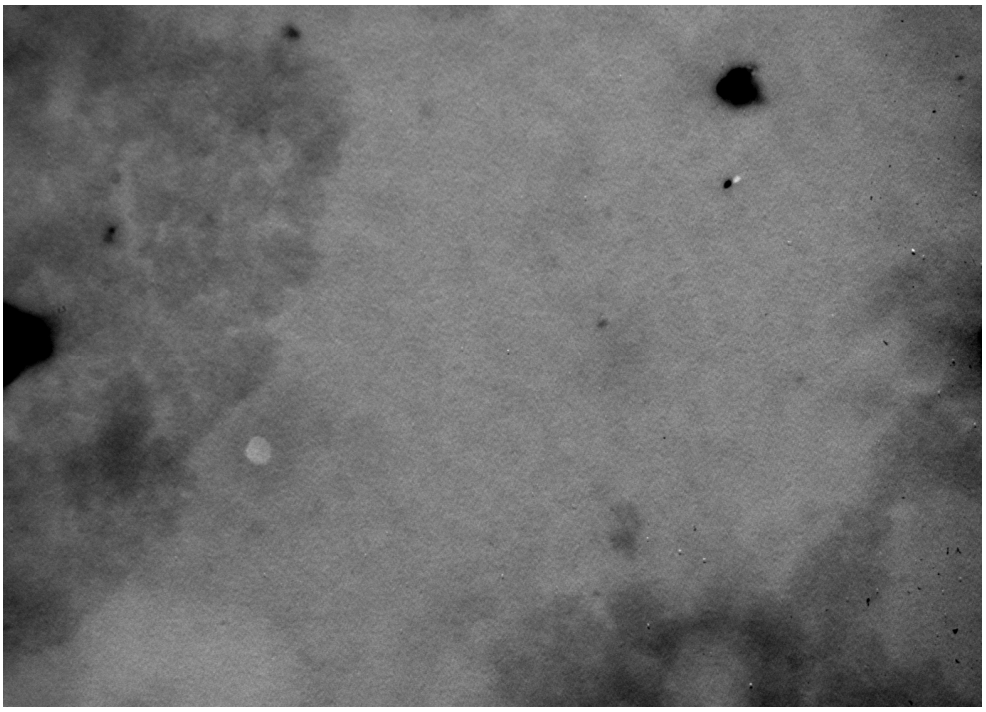

Figure 3.39: TEM image of PU

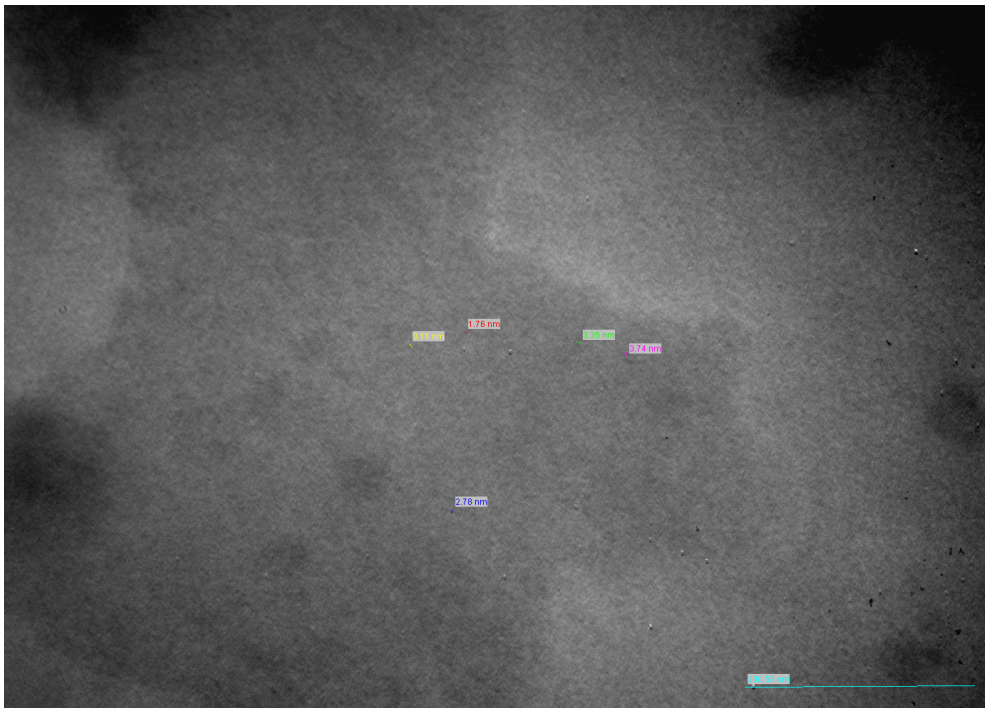

Figure 3.40: TEM image of PUH3

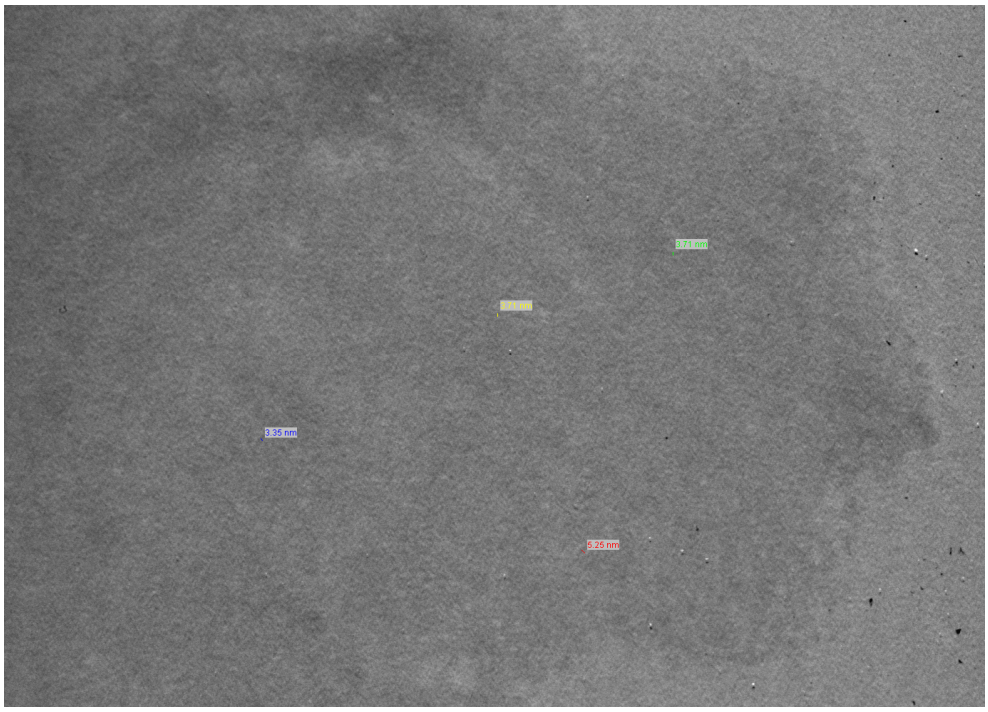

Figure 3.41: TEM image of PUH7

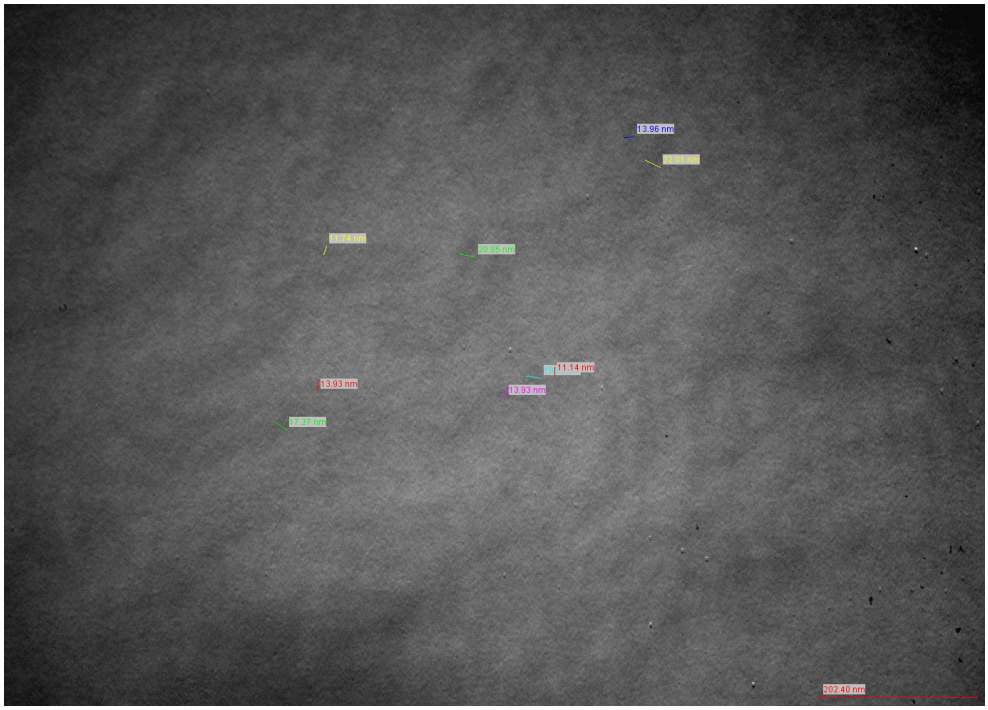

Figure 3.42: TEM image of PUH15

3.5. Preparation of PU-Montmorillonite Nanocomposites and Comparison with Hectorite

Polyurethane-Montmorillonite (MMT) nanocomposites were prepared as a comparison to PU-HEC nanocomposites. The PU-MMT nanocomposites were characterized structurally, mechanically and thermally. The results are given below.

3.5.1. X-ray analysis

The X-ray patterns are shown in Figure 3.43. The exfoliation is obtained with the montmorillonite material in the polyurethane matrix as well. At all concentrations, the partial exfoliation was achieved. The combined graph is given as well. This exfoliation is due to the hydrophilic nature of the polyurethane. The swelling character of the montmorillonite is very important as well. This study is also comparative to the nanocomposites prepared with the clay hectorite. They exhibit partially exfoliated behavior. This result is proved by TEM investigations as well.

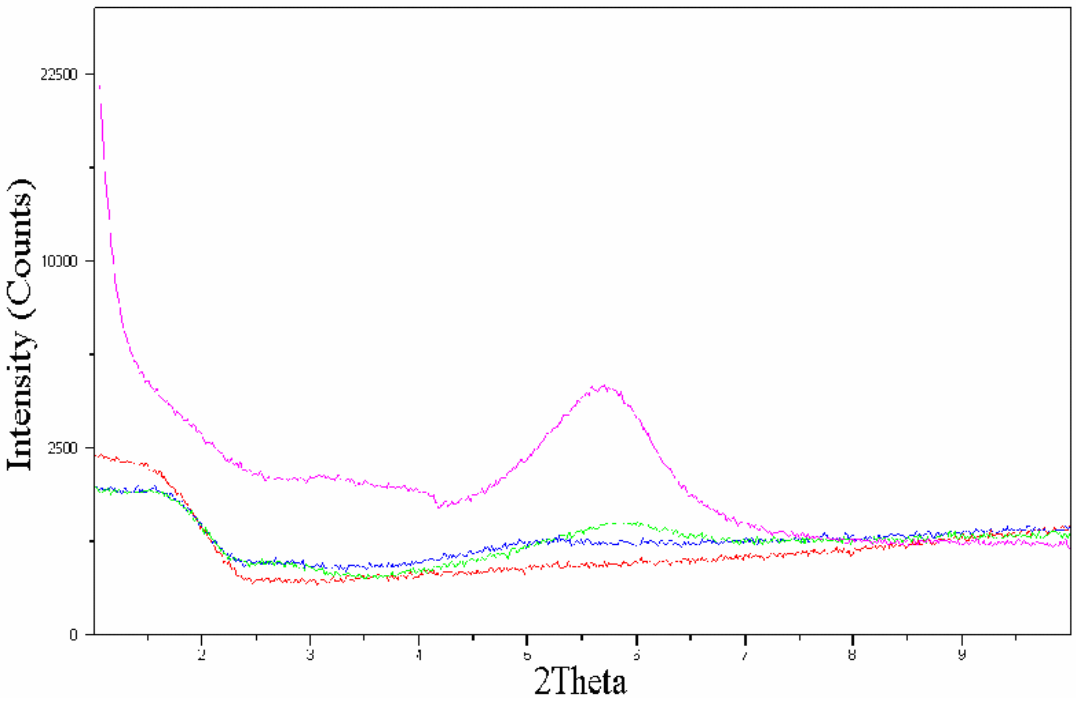

Figure 3.43: X-Ray D. pattern of PU and PU-MMT nanocomposites

3.5.2. FTIR analysis

The FTIR analysis was done for the PU-MMT nanocomposites (Figure 3.44). Similar results like PU-HEC nanocomposite were found. The PU structure is maintained except the 959.97 cm^{-1} peak. For MMT, there is one point different. For 3 and 5 % loading of the hectorite clay, that peak disappears but for the MMT clay the peak does not disappear and it is present in the nanocomposite. For 7 % the peak for OH group disappears again. The hectorite interacts with the polyurethane much better with compared to MMT.

With 7 % MMT the clay peak does not appear contradictory to HEC nanocomposites.

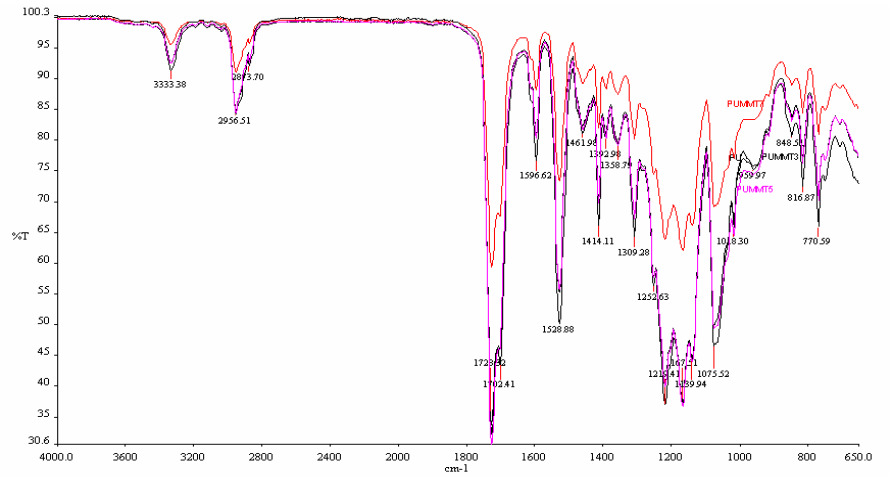

Figure 3.44: FTIR spectrum of PU and PU-MMT nanocomposites

3.5.3 Mechanical testing

The mechanical properties of the nanocomposites were measured with tensile testing shown in Figure 3.45. The reinforcing effect of the montmorillonite can be easily observed. The important parameter is the use of natural clay without any modification. So the cost of the preparation of the nanocomposite can be reduced dramatically. The montmorillonite is one of the most abundant type of clay. This shows that with a very cheap resource, the polyurethane can be reinforced.

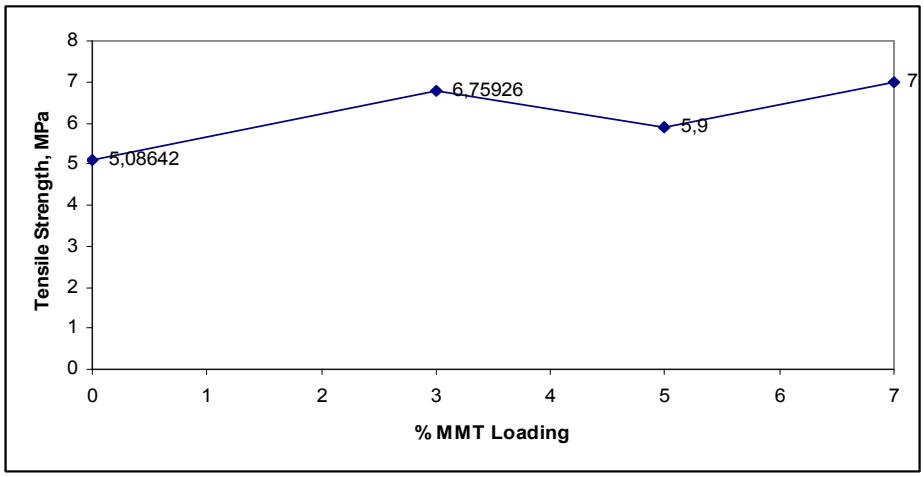

Figure 3.45: Mechanical properties of PU and PU-MMT nanocomposites

When we compare the properties of PU-MMT with PU-HEC, the results show that the use of hectorite causes higher strength than the use of MMT clay. This result shows the novelty of the nanocomposites prepared with the hectorite clay.

3.5.4. Dynamic mechanical analysis

The DMA results are shown in Figures 3.46-3.48.

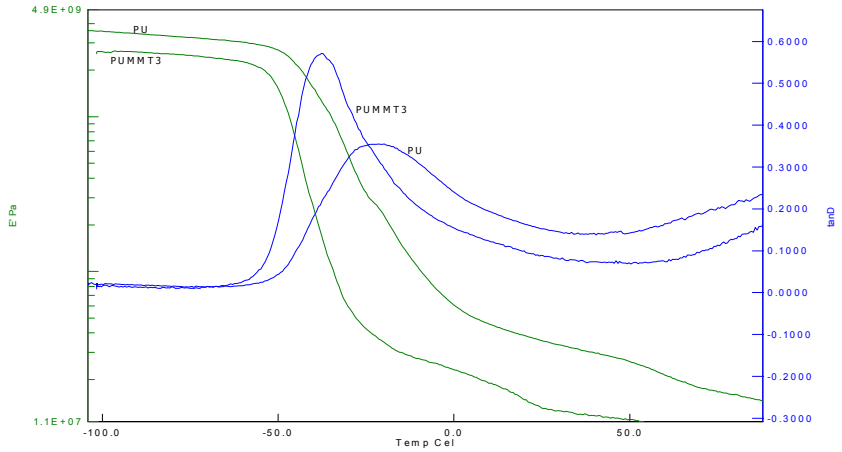

Figure 3.46: DMA of PU-MMT3

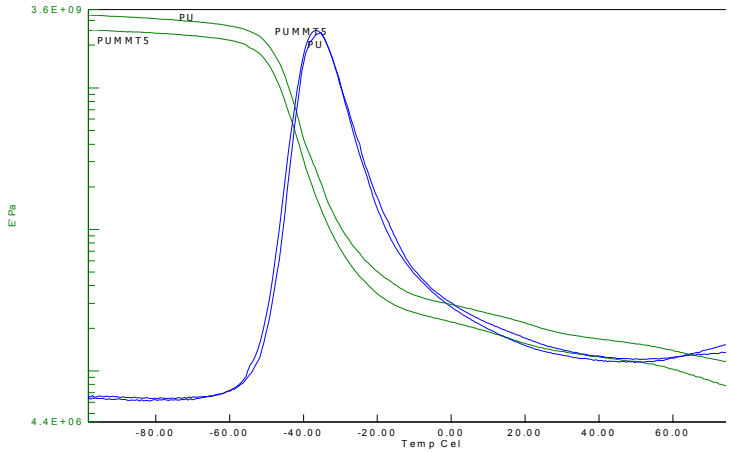

Figure 3.47: DMA of PU-MMT5

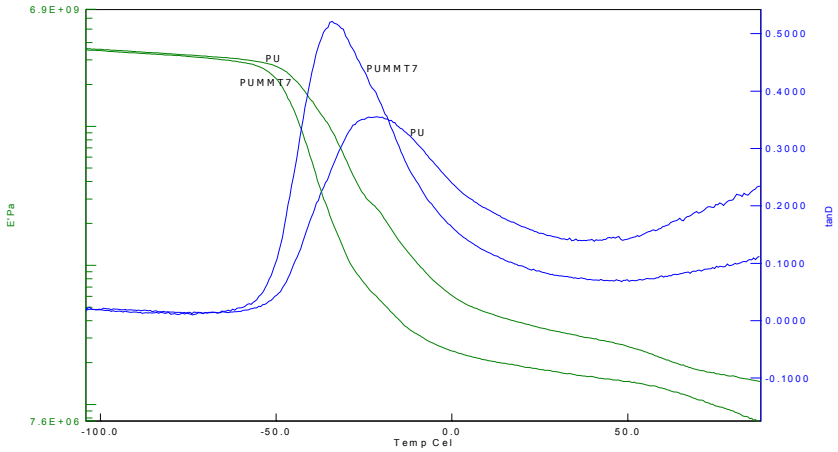

Figure 3.48: DMA of PU-MMT7

DMA curves for the PU-MMT nanocomposites are in accordance with the tensile testing. The results are not promising. The PU has higher modulus values than the nanocomposites except 7 % MMT concentration. The storage modulus of the nanocomposite at 3 % is lower than the polyurethane at all the temperatures. For 5 wt % MMT containing nanocomposite, the storage modulus is slightly higher than that of 3 % but it is still lower than the pure polymer. As a result of the mechanical and thermomechanical studies, it is clear that PU-HEC nanocomposites have better properties than that of PU-MMT nanocomposites.

For the tan delta curves, the Tg of the polymer and the nanocomposite is not very different indicating that the clay does not affect the glass transition temperature of the polymer. The change in the height of the curve reflects the change in the flexibility of the polymer chains. The height of the tan delta curves for the 3 % and 5 % nanocomposites increases. This shows that the nanocomposites became more elastic which is reflected as decrease in the elastic modulus. The 7 % MMT nanocomposite gave higher tan delta curves consisting with the modulus values.

3.5.5. TGA

The Figure 3.49 shows the combined TGA graph of the polyurethane nanocomposites formed with MMT. The final residue after heating increased with clay addition. The heat resistance increase is similar with the HEC as they are both mineral based materials.

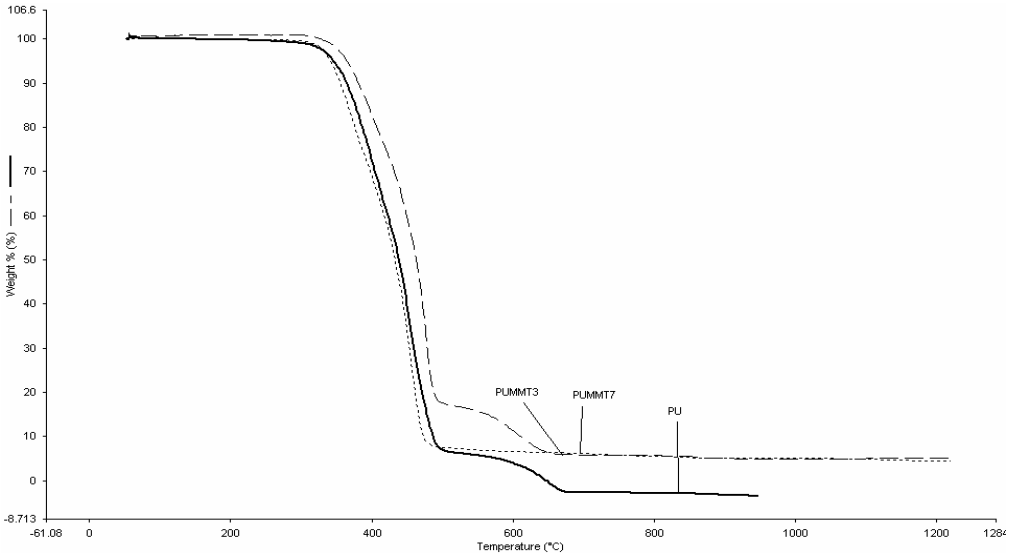

Figure 3.49: TGA thermograms of PU-MMT nanocomposites

3.5.6. TEM

The TEM observation with PUMMT7 is shown in the Figure 3.50. The clay platelets could not be distributed like PU-HEC nanocomposites. The PU-MMT nanocomposite is obtained partially exfoliated.

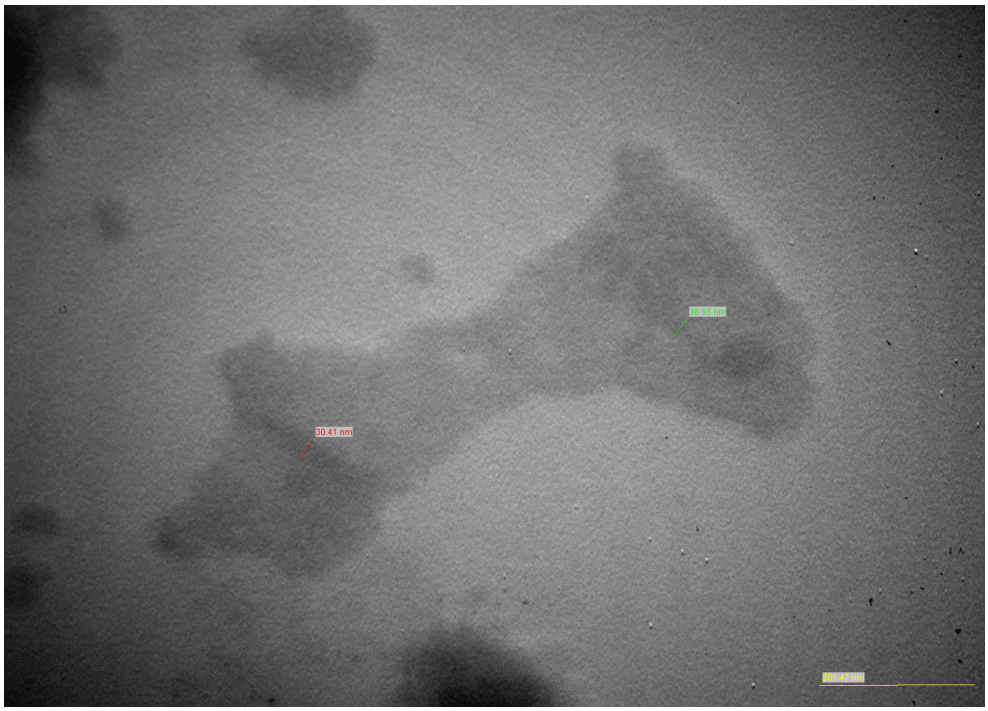

Figure 3.50: TEM image of PUMMT7

3.6. Preparation of PU-Laponite Nanocomposites and Comparison with PU-Hectorite Nanocomposites

In this part of the study, the polyurethane-laponite nanocomposites were prepared in order to compare with polyurethane-hectorite nanocomposites. The laponite is a synthetic commercial clay and it has a very similar structure of the natural clay hectorite. In this part of study, the major aim was to investigate the effectiveness of each clay. In the previous part, it was demonstrated that the hectorite has better properties than the MMT clay.

PU-laponite nanocomposites could be prepared up to 5 wt % of laponite. Above 5 wt % of laponite in DMF, the laponite agglomerated in DMF. The agglomerated laponite formed with 7 and 10 % could not be dispersed in DMF by the method used for hectorite preparation.

3.6.1. X-Ray analysis

With expertise gained in the production of exfoliated structures of polyurethane and the natural clay hectorite, the polyurethane-laponite nanocomposites were prepared with the same method. The results of the X-Ray patterns are given in Figure 3.51-3.54. As shown, the composites did not give the characteristic clay. This shows that the composites have exfoliated structures.

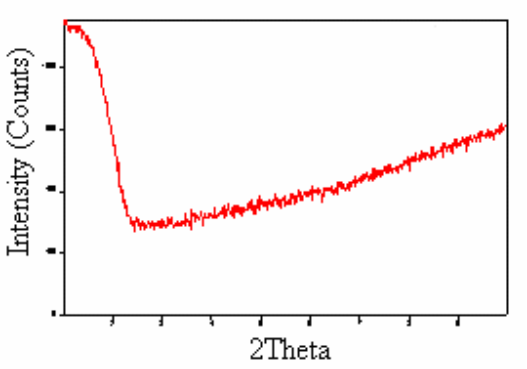

Figure 3.51: X-ray D. pattern of PUL1

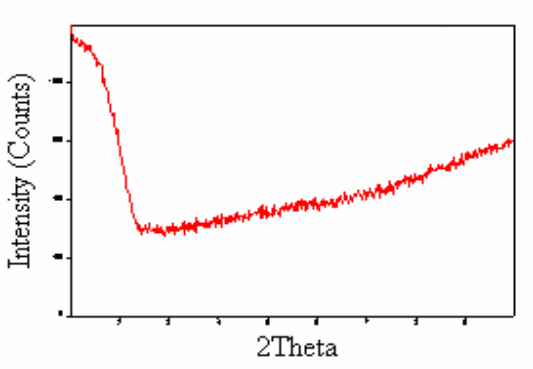

Figure 3.52: X-ray D. pattern of PUL3

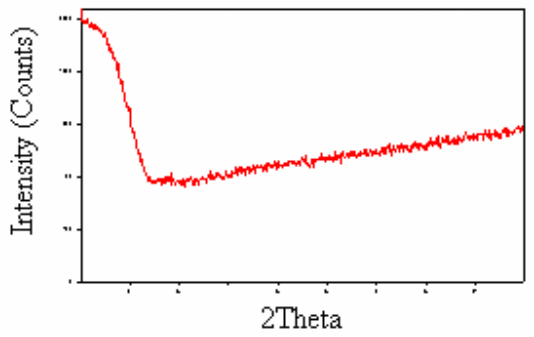

Figure 3.53: X-ray D. pattern of PUL5

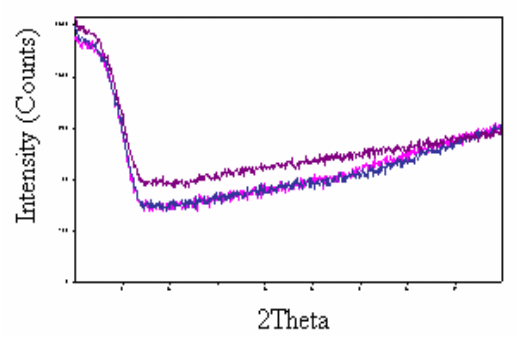

Figure 3.54: X-ray D. pattern of PUL- Combined

3.6.2. FTIR analysis

The FTIR analysis of the polyurethane and the nanocomposites is in Figure 3.55. The laponite does not affect the structure so much except one peak at 959.97 cm^{-1}. The peak of the polyurethane disappears.

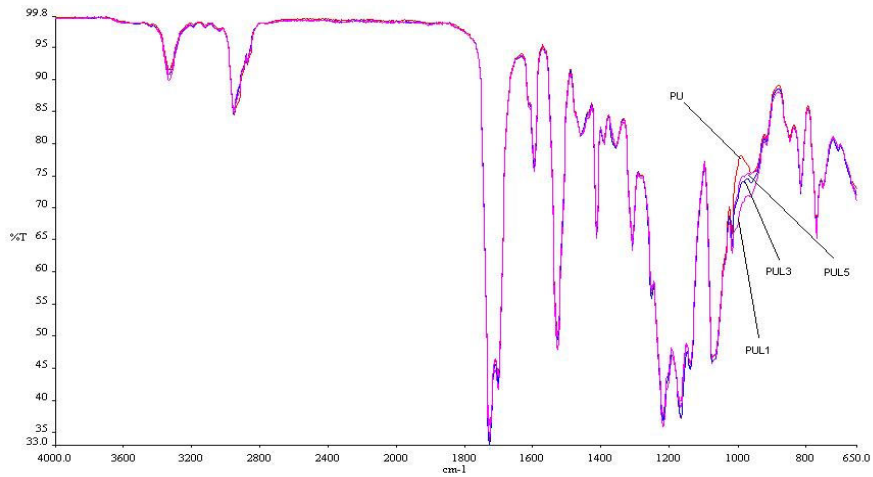

Figure 3.55: FTIR spectrum of PU-laponite nanocomposites

3.6.3. Mechanical testing

The mechanical properties of polyurethane and polyurethane-laponite nanocomposites are shown in Figure 3.56.

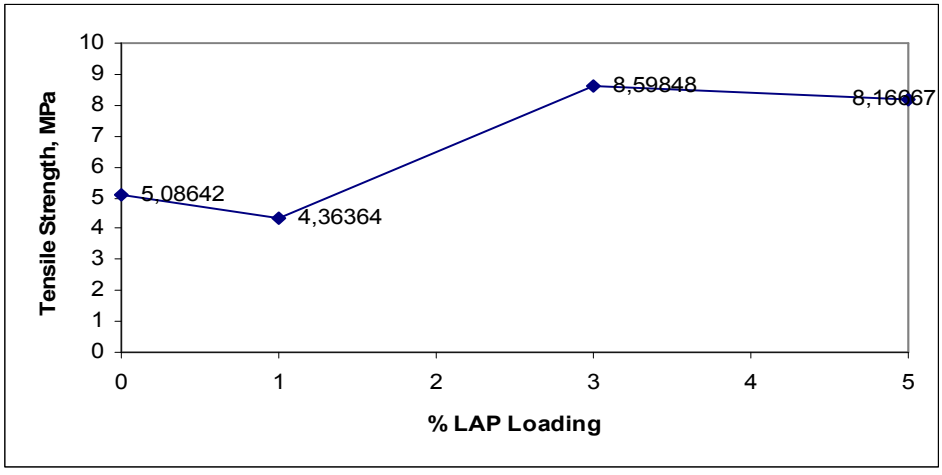

Figure 3.56: Mechanical properties of PU and PU-laponite nanocomposites

As shown from the graph, the optimum clay content for polyurethane-laponite nanocomposite is 3 wt % laponite. Compared to the pure PU, the tensile strength of 3 wt % laponite containing nanocomposite increased 69 %. Also nanocomposites could not be prepared above 5 wt % laponite addition due to the agglomeration. The good interaction of the laponite with PU is obtained like in PU-HEC nanocomposites. The hydrogen bonds were formed. 3 % loading of the laponite and HEC in PU matrix is one of the most important result of this study. The laponite with much fine and pure structure compared to hectorite is slightly above the PU-HEC nanocomposite. The maximum tensile strength which could be obtained was much higher with the natural clay, HEC. This shows the better performance of the PU-HEC nanocomposites compared with PU-laponite nanocomposites. Moreover, the processability of hectorite was much easier than that of laponite in this PU-DMF system due to the agglomeration of laponite particles. It is suggested that if the hectorite could be purified, then the properties of the PU-HEC could be even better which shows the important use of natural clay.

3.6.4. Dynamic mechanical analysis

The DMA results of the PU-Laponite nanocomposites are given in the Figures 3.57-3.59.

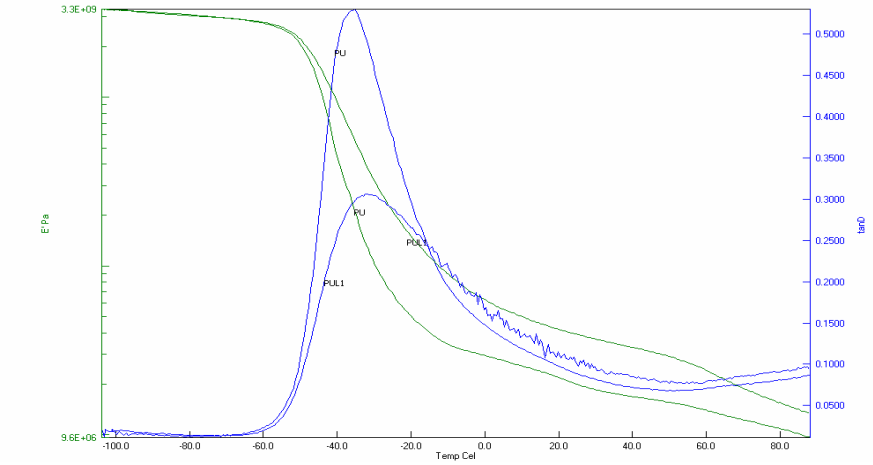

Figure 3.57: DMA of PU and PUL1

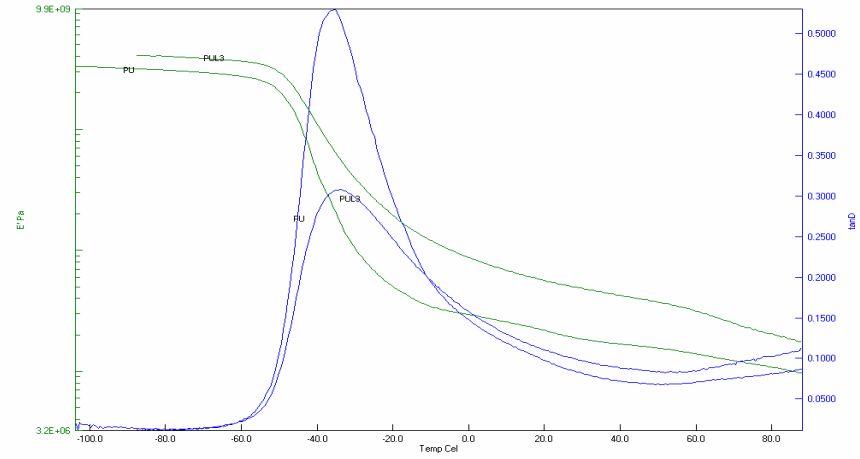

Figure 3.58: DMA of PU and PUL3

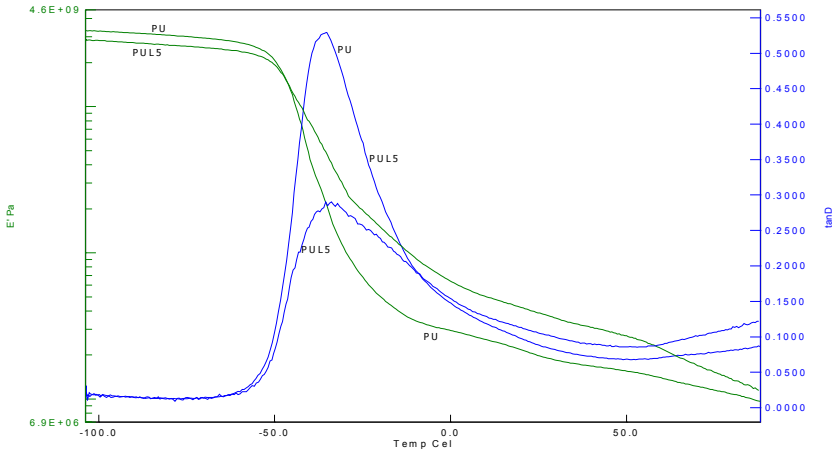

Figure 3.59: DMA of PU and PUL5

DMA was used to investigate the dynamic mechanical behavior of the nanocomposites prepared from two types of clays, HEC and MMT.

For the 1 % laponite, the starting modulus values of PU and the PUL1 nanocomposite are similar which is very consistent with the mechanical testing as the maximum tensile strength was almost the same as the pristine polymer. Mechanically, the pure polymer and the nanocomposites are similar but upon heating, the modulus values are higher for the nanocomposites. This gives nanocomposites thermal stability and higher modulus values at higher temperatures. This property enables the polymer to be used for special

applications requiring high mechanical strength or this increases the material life time under mechanical loading for long time.

As shown in Figures 3.57-3.59, the height of tan delta peak decreased with increasing laponite content in polymer composites. It is well known that tan delta peak is associated with the motion of polymer chains. The increasing filler content makes the polymer harder. The mobility of polymer chains decreases with increasing filler content. The same trend was observed by adding laponite to polyurethane.

3.6.5. TGA

The Figure 3.60 shows the combined TGA graph of the polyurethane nanocomposites formed with laponite. The final residue left after heating to 1200 ^{0}C increases with increase of the laponite content. This is also very similar to the PU-Hectorite materials. The 5 wt % of laponite showed better thermal stability than the other nanocomposites. Although the mechanical property of 3 wt % laponite-PU nanocomposite is higher than that of 5 % wt laponite-PU nanocomposite, the final residue left is better for 5 wt % laponite-PU nanocomposites.

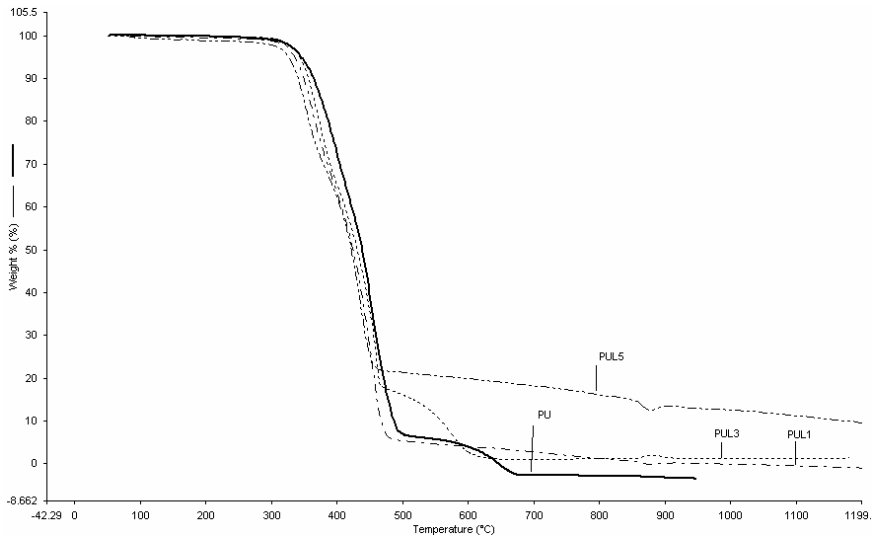

Figure 3.60: TGA thermograms of PU and PU-laponite nanocomposites

3.6.6. SEM images

SEM images show the excellent exfoliated structure of the polyurethane-laponite nanocomposites (Figure 3.61). For 1 %, 3 % and 5 % of laponite, the particles could not be observed which means that the clay platelets are so finely dispersed in the matrix.

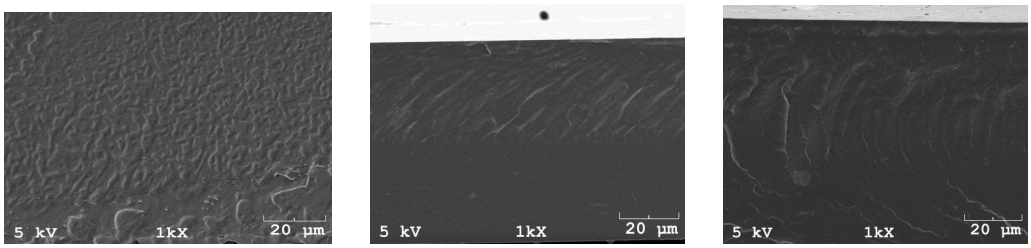

Figure 3.61: SEM image of PUL1, PUL3, PUL5 respectively

3.6.7. TEM images

TEM images of PU-Laponite nanocomposites with 3 and 5 wt % are shown in Figure 3.62 and 3.63. It was observed that the dispersion is quite well like hectorite but the thickness of the clays dispersed in the polymer matrix was much better for hectorite. The hectorite was dispersed much thinner than the laponite which shows the better dispersion of the clays. From these TEM images, it is possible to say that some clay platelets were intercalated.

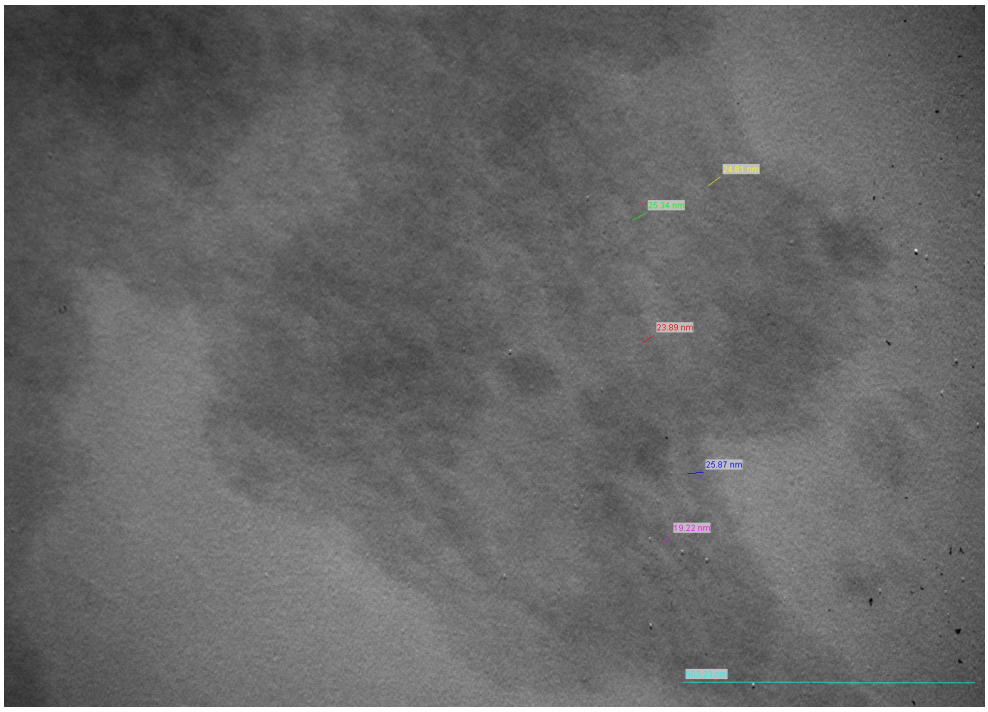

Figure 3.62: TEM image of PUL3

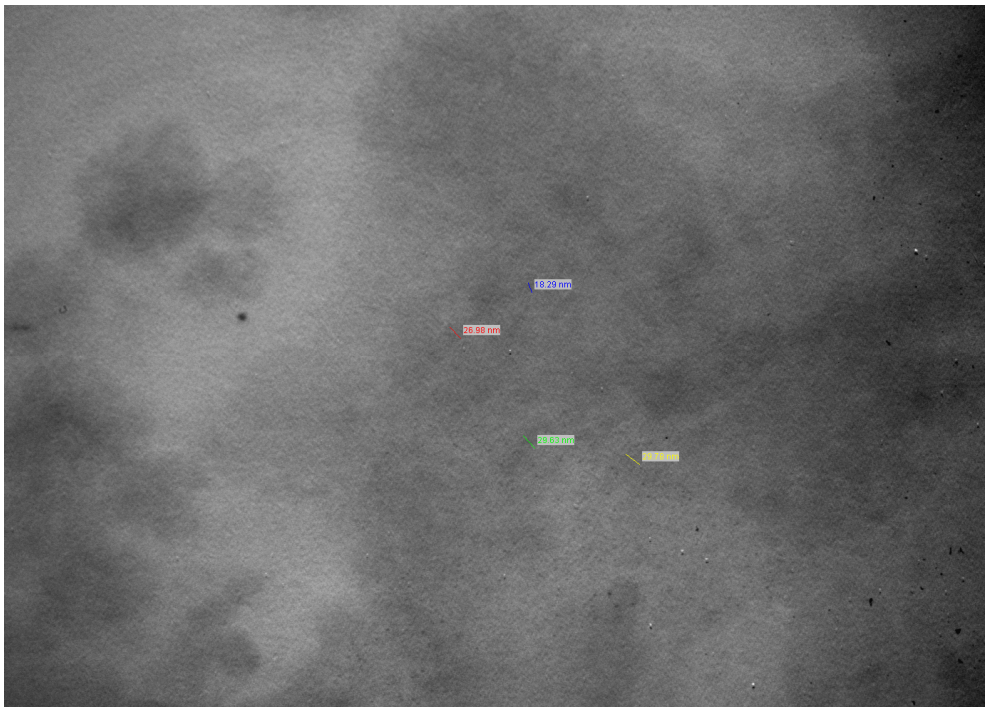

Figure 3.63: TEM images of PUL5

3.7. Concluding Remarks on PU-HEC, PU-MMT and PU-Lap. Nanocomposites

In this study very novel polyurethane hectorite nanocomposites were prepared with exfoliated structure. No organic modifier was used. As a comparison, PU-MMT nanocomposites were prepared to investigate the properties of the PU-HEC nanocomposites using the same polyurethane. It was observed that the mechanical properties of PU-HEC nanocomposites are better than PU-MMT nanocomposites. The synthetic clay, laponite was also used for the preparation of PU nanocomposites but the successful results were not obtained above 5 wt % laponite content. On the other hand, the mechanical properties of the laponite nanocomposite and hectorite nanocomposite are very similar. The optimum laponite concentration was found as 3 wt % from the results of mechanical testing and DMA.

As a result of this study, it is suggested that hectorite was successfully used in the preparation of polyurethane-clay nanocomposite as compared with MMT and Laponite. Additionally in the view of economic aspect, hectorite should be preferred because it was possible to use it without purification and modification.

The improvements are very detrimental for industrial applications. In this research, completely industrial polyurethane was used. That makes the research applicable specifically to this material. Further investigations can enlighten the use of these results for other polyurethane products such as adhesive, foam and biomedical

3.8 Polyurethane-Silane Coated Hectorite Nanocomposites

The aim of the preparation of silane coated hectorite and using it in the nanocomposite preparation was to improve the interaction of the polymer and the clay. Since the best results were obtained for polyurethane-hectorite nanocomposites, only hectorite was coated with silane and used in nanocomposite formulation. Silane coupling agents have been used for long time in the composite industry. There are different approaches for the use of silane coating. One approach is to delaminate the clay and use it as organic

modifier. The other approach is to use it as surface improver between the polymer and the inorganic phase. The latter approach was the main aim of this study.

Hectorite was coated with three different silane coupling materials. The same preparation technique was used for three coupling materials.

In the first part of this study, the silane grafting was analyzed by FTIR, X-Ray and TGA.

3.8.1. X-Ray analysis

The effect of silane coating on the d-spacing of the hectorite clay is given in the Figure 3.64. It is observed that the silane coating did not increase the d-spacing of the clay and instead it has decreased the d-spacing of the clay. This was reflected in the polymer nanocomposites.

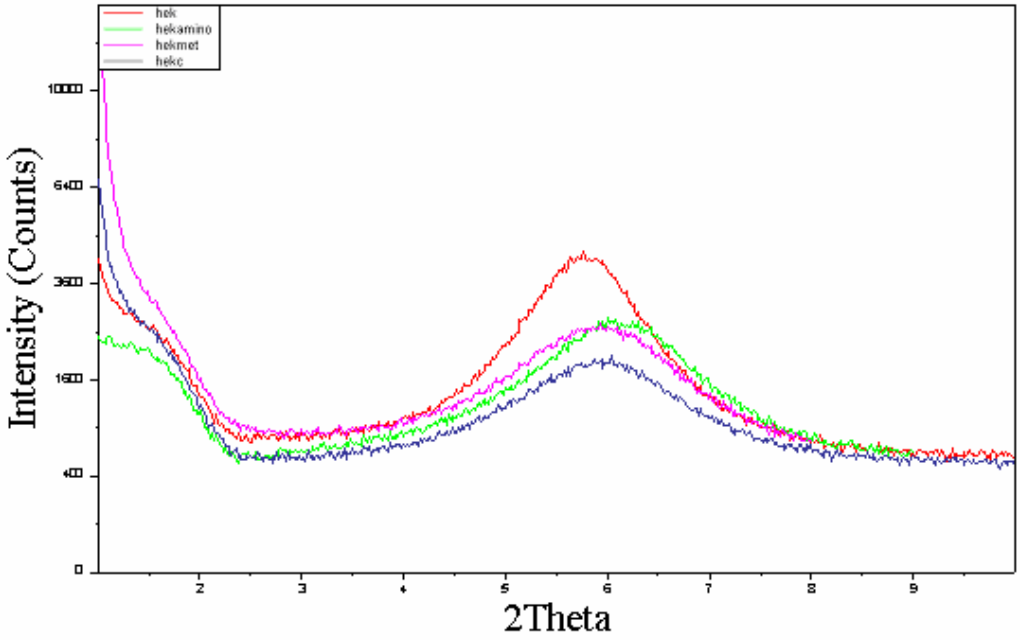

Figure 3.64: The X-ray D. pattern of silane grafted hectorite

Hek: Hectorite

Hekamino: 3- Aminopropyltriethoxysilane coated hectorite (amino silane)

Hekmet: Gamma-methacryloxypropyltrimethoxysilane coated hectorite; (met silane)

Hekc: Glycidoxypropyltrimethoxysilane coated hectorite (glycid silane)

3.8.2. FTIR analysis

With the three different silanes, the grafting is observed with FTIR as shown in the Figure 3.65. As shown the hectorite peaks are same for the entire range except the 2936 cm^{-1} peak representing CH_2 stretching of the silanes. This shows the grafting.

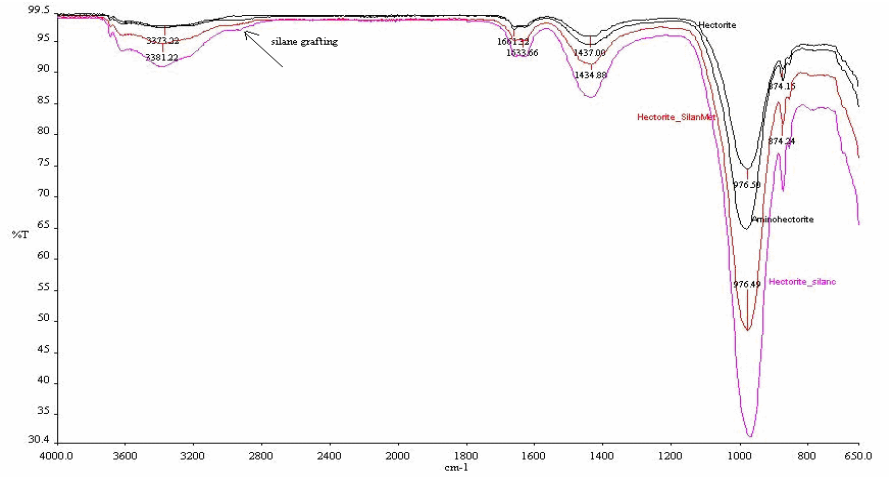

Figure 3.65: FTIR spectrum of silane grafting obtained from this study

The silane grafting is observed with FTIR by different researchers. He et al [35] observed the 3-APS (3-Aminopropyltriethoxysilane) silane grafting on the hectorite and montmorillonite clays with FTIR. They observed change at 2936 cm^{-1} on both clays which are shown in the Figure 3.66.

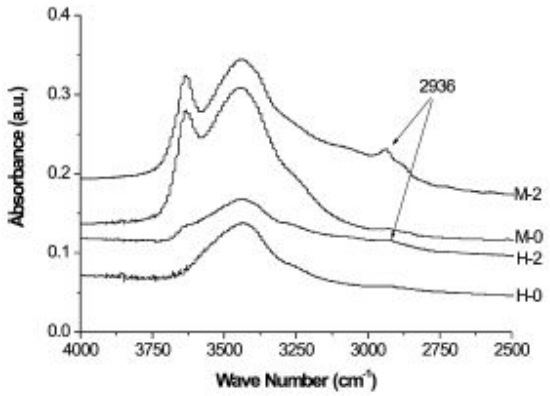

Figure 3.66: FTIR spectrum of silane grafting taken from literature [35]

Also Giannelis et al [61] also detected the same stretching at the same wave length. They have used the same 3-APS silane for the synthetic hectorite, laponite.

They have obtained the following FTIR peaks shown in Figure 3.67.

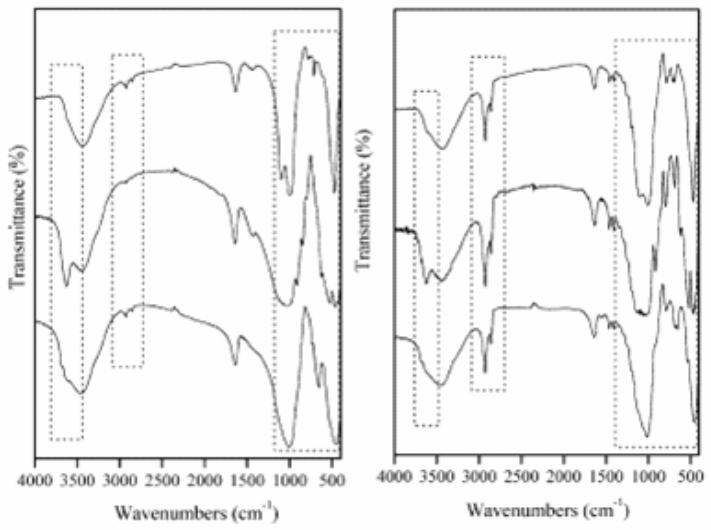

Figure 3.67: FTIR spectrum of silane grafting [62]

The same observation is done in this study as well. With the three different silanes, the grafting was observed with FTIR as shown in the following figure.

The Figure 3.67 shows that the hectorite peaks are same for the entire range except the 2936 cm^{-1} peak. This shows the grafting.

3.8.3. TGA

The Figure 3.68 is the TGA graph of the hectorite and the silane coated hectorite.

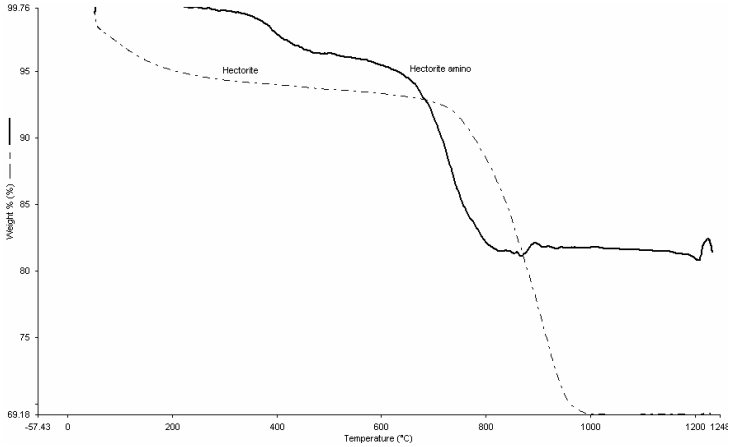

Figure 3.68: TGA thermograms of silane grafted hectorite

He et al [35] and Giannelis et al [61] investigated silane coated hectorite with TGA as well. He et al obtained similar curves to the curves of this study. They determined that there was no decomposition up to 800 ^{0}C for hectorite without silane.

In the case of silane coated hectorite, they determined two important temperatures. The first one was 209 ^{0}C which shows the vaporization of the physical bound silane. The other one was 550 ^{0}C. At that temperature grafted silane was decomposed. Giannelis also observed similar transitions for the silane coated laponite.

3.8.4. Preparation of silane coated hectorite polyurethane nanocomposites

In the first part of this study, it was found that polyurethane nanocomposite with 7 wt % hectorite showed the best mechanical properties. For this reason, silane coated hectorite was used for the preparation of nanocomposite with 7 wt % filler. In order to determine the effect of silane type on the mechanical properties of nanocomposite, three silane coupling agents were used to coat the hectorite.

3.8.4.1. X-ray analysis

X-ray diffraction patterns of polyurethane nanocomposites prepared from three different silane coated hectorite are given in the Figure 3.69. As shown, met silane coated hectorite was not successful for obtaining nanocomposites as the specific clay appeared in X-ray pattern. The d-spacing of the hectorite layers was decreased. This was reflected in the x-ray analysis.

.Both amino silane and glycid silane grafted hectorite PU nanocomposites were identified as exfoliated by the X-ray analysis.

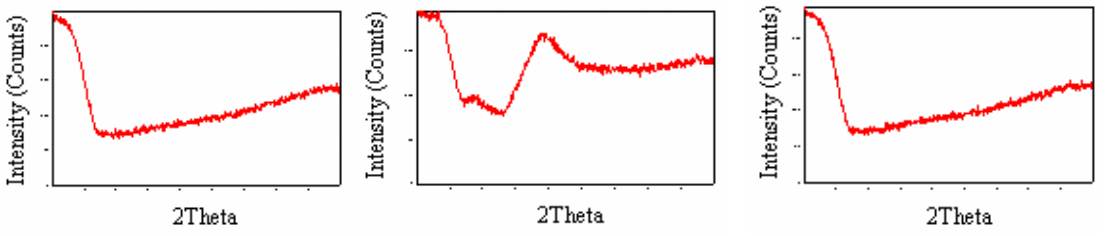

Figure 3.69: X-Ray D. patterns of hectorite-polyurethane nanocomposites with three different silanes, PU-Amino7, PU-Met7 and PU-Glycid7 respectively.

3.8.4.2. FTIR analysis

In the Figure 3.70-3.72, the similar FTIR spectrum was observed with silane and without silane coated hectorite nanocomposites. In these studies, the 959.97 cm^{-1} peak disappeared again. Also the 998.30 cm^{-1} peak also appeared for the three type silane grafted nanocomposites.

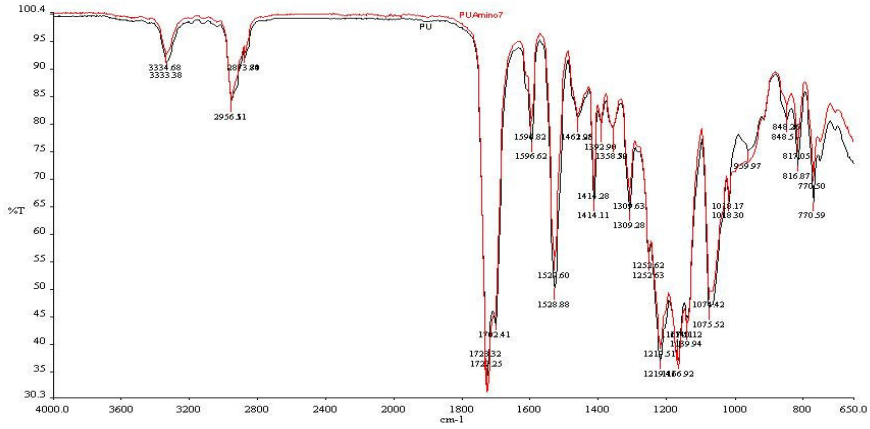

Figure 3.70: FTIR spectrum of PU and PUAmino7 nanocomposites

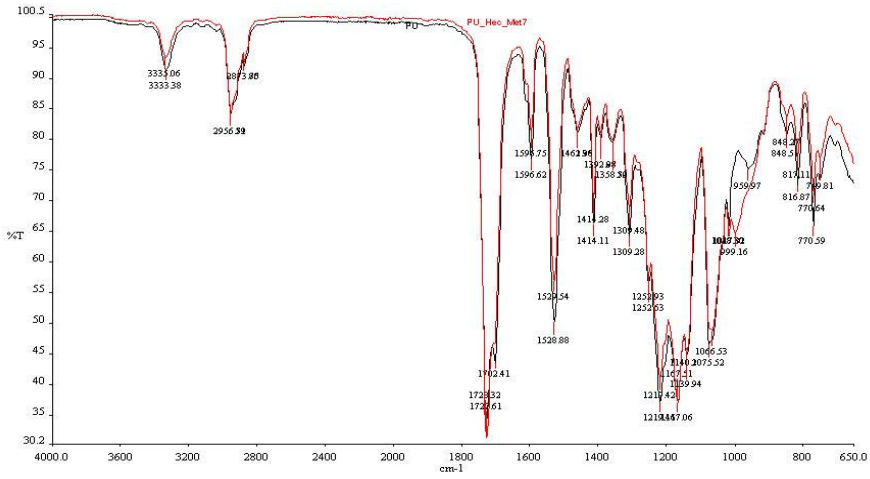

Figure 3.71: FTIR spectrum of PU and PUMet7 nanocomposites

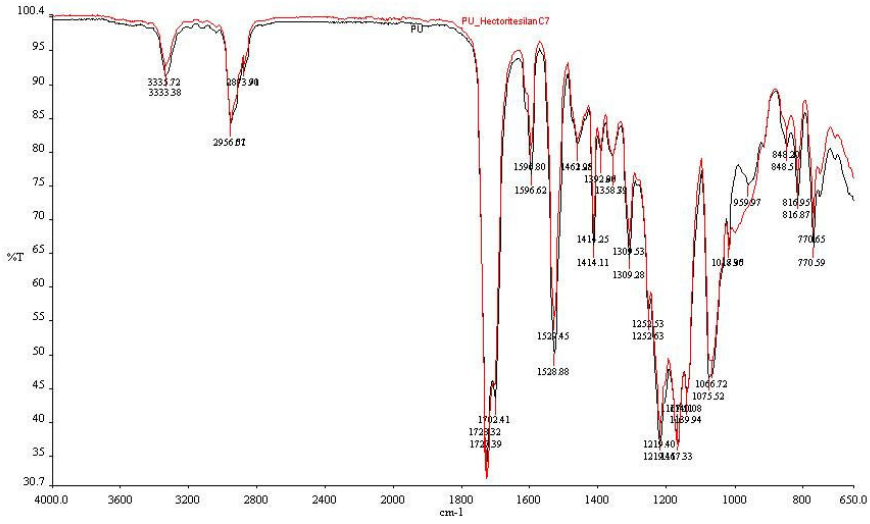

Figure 3.72: FTIR spectrum of PU and PUGlycid7 nanocomposites

3.8.4.3. Mechanical testing

The mechanical properties of three different silane coated hectorite PU nanocomposites are given in the Table 3.5.

Table 3.5: Mechanical properties of three different silane coated hectorite-PU nanocomposites

Sample	Tensile Strength (MPa)
PU	5.09
PUAmino7	8.48
PUMet7	8.04
PUGlycid7	6.45
PUH7	10.86

It was observed that the best reinforcement was achieved with the amino silane. The other two were not successful because the maximum strength of the silane grafted nanocomposites was lower than the uncoated of the hectorite. This is related with the shrinkage of the clay layers with the silane modification of the clay which was observed in x-ray analysis.

3.8.4.4. Dynamic mechanical analysis

The DMA graphs of silane coated hectorite PU nanocomposites are given in Figures 3.73-3.75.

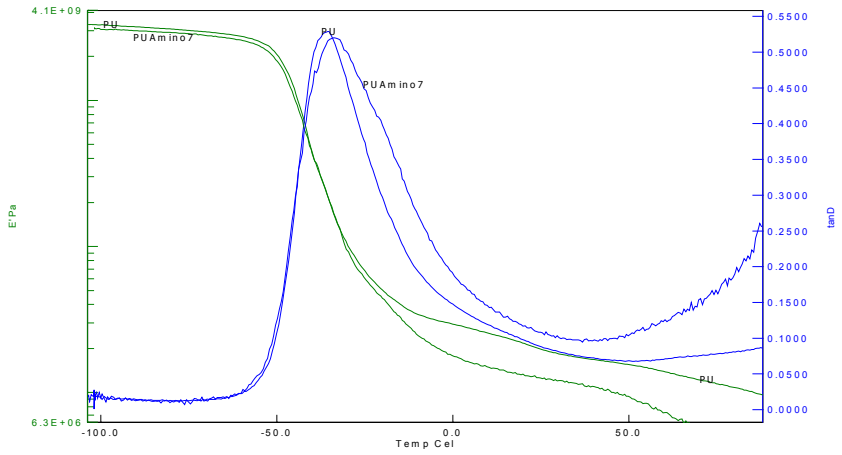

Figure 3.73: DMA of PUAmino7

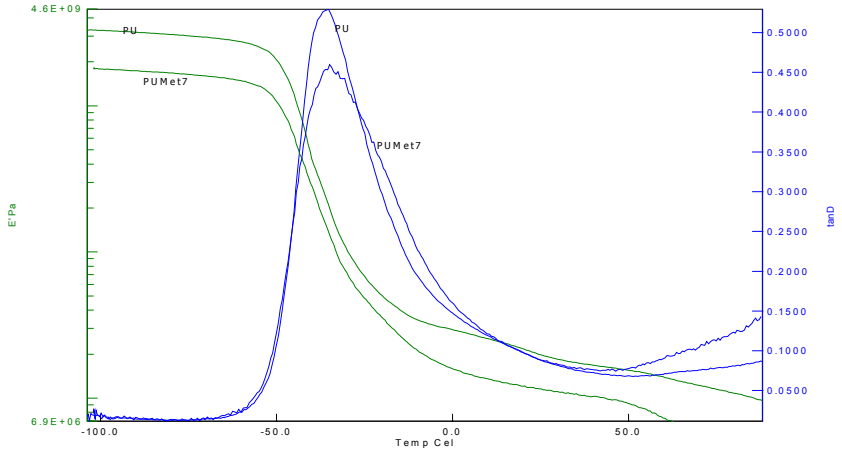

Figure 3.74: DMA of PUMet7

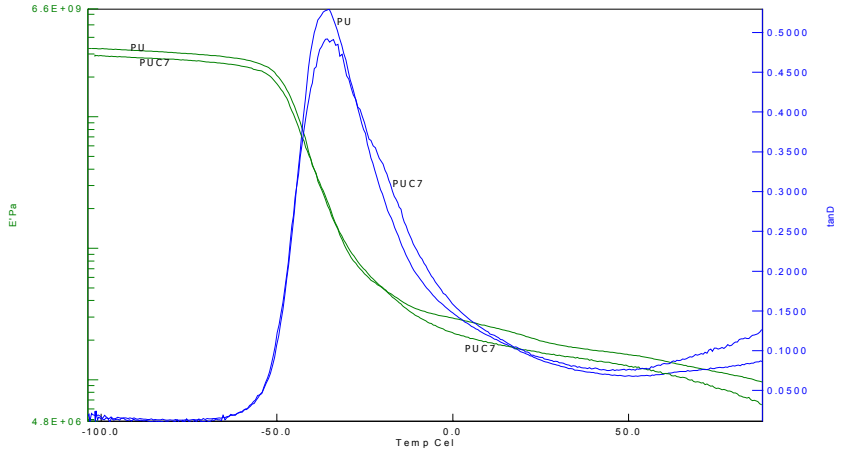

Figure 3.75: DMA of PUGlycid7

For all the silane grafted clay nanocomposites, the modulus values were lower than the pure polymer at all temperatures. This shows that the reinforcing is not so effective like the uncoated hectorite.

The flexibility of the polymer chains did not change much but the tan delta of the peak shifted to the right which shows the better interaction of the clay and the polymer.

3.8.4.5. TGA

In the Figure 3.76, TGA graph of the PU and PU-silane coated hectorite nanocomposites is given. It is clearly observed that with 7 % percentage of the clay, the final residue left

after heating is higher than the pure polymer for all the nanocomposites prepared with the three silanes.

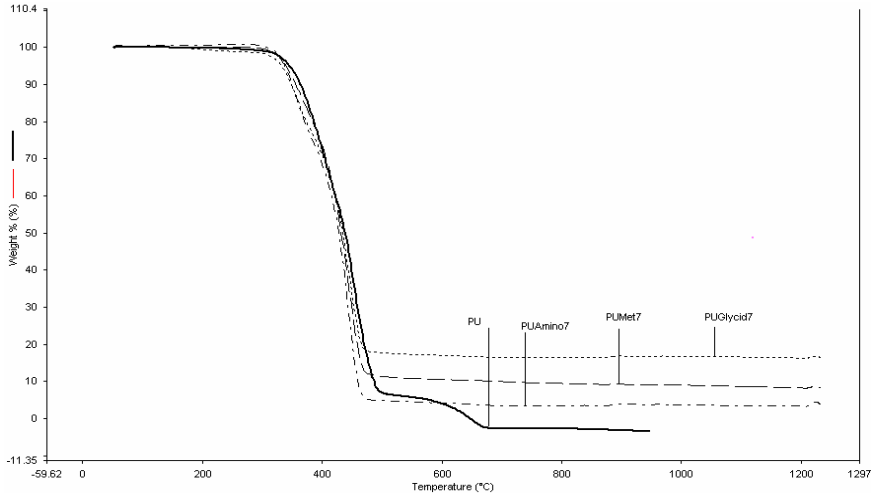

Figure 3.76: TGA thermograms of PU-silane grafted hectorite nanocomposites

3.8.5. Preparation of PU-amino silane grafted hectorite nanocomposite

As compared, the properties of nanocomposites prepared from three different types of silane coated hectorite, it was determined that amino silane was the best silane for the PU-hectorite nanocomposites. Then a series of amino silane modified hectorite nanocomposites were prepared. The concentration of clay was chosen between 1 to 10 wt %.

3.8.5.1. X-Ray analysis

The X-ray analysis was performed for the samples with 5 different silane grafted hectorite loading. X-ray diffraction patterns of the samples are given in Figures 3.77-3.79. As shown, all samples did not give the characteristic peak except the sample with 10 wt % of silane coated hectorite.

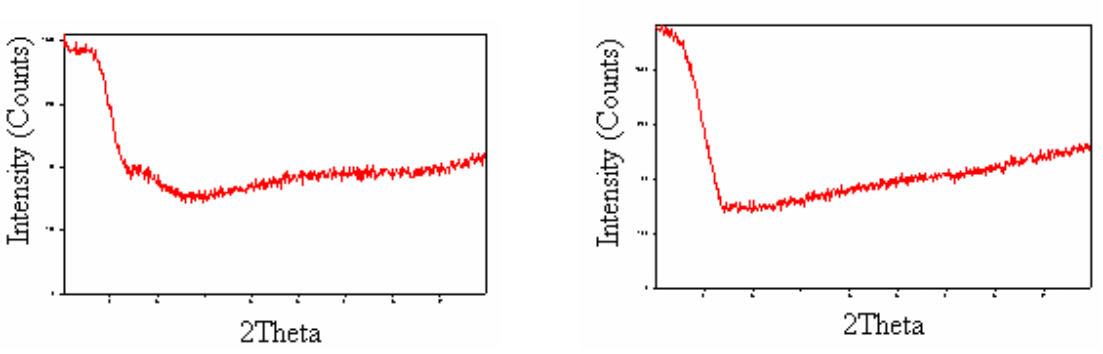

Figure 3.77: X-Ray D. pattern of PUAmino1 and PUAmino3, respectively

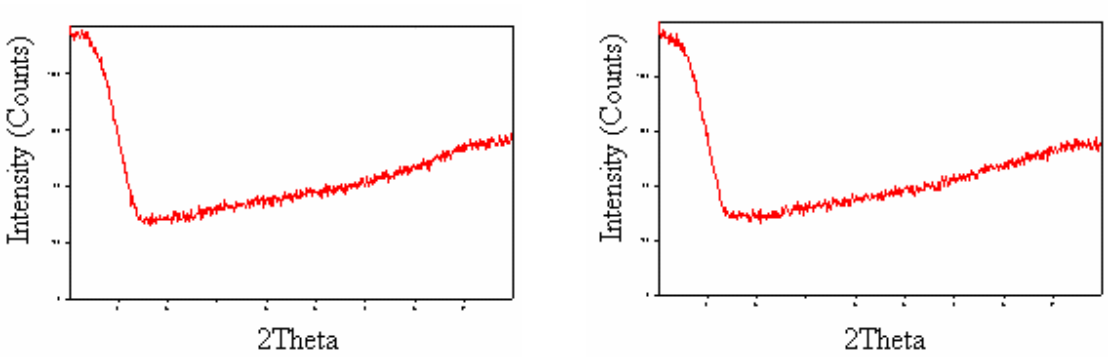

Figure 3.78: X-Ray D. Pattern of PUAmino5 and PUAmino7, respectively

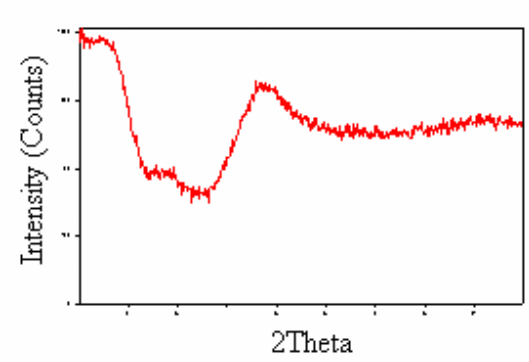

Figure 3.79: X-Ray D. pattern of PUAmino10

3.8.5.2. FTIR analysis

FTIR analysis for the 5 different nanocomposites were performed (Figures 3.80-3.82). Again, it is observed that the 959.97 cm^{-1} peak of the polyurethane disappeared after 1 %. But here in this study, the clay peak did not appear like the pure hectorite studies. In the

pure hectorite studies, it was observed that at 998.30 cm^{-1} the clay peak appears very slightly.

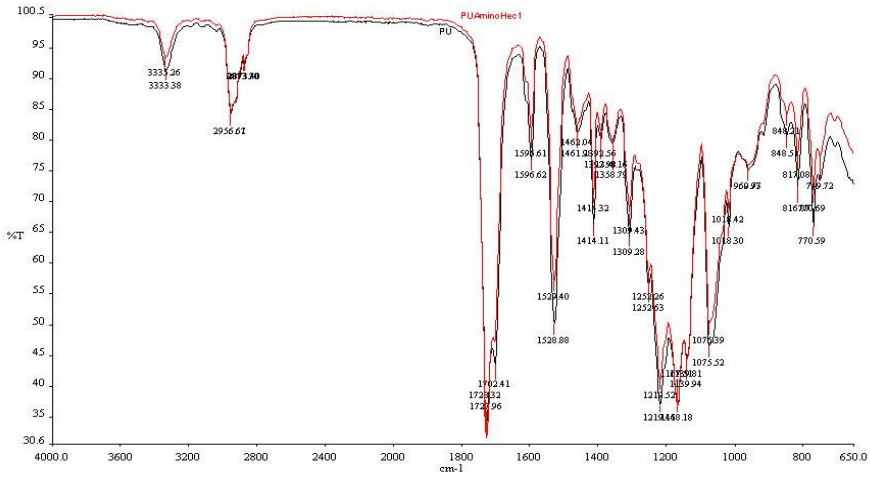

Figure 3.80: FTIR spectrum of PU-PUAmino1

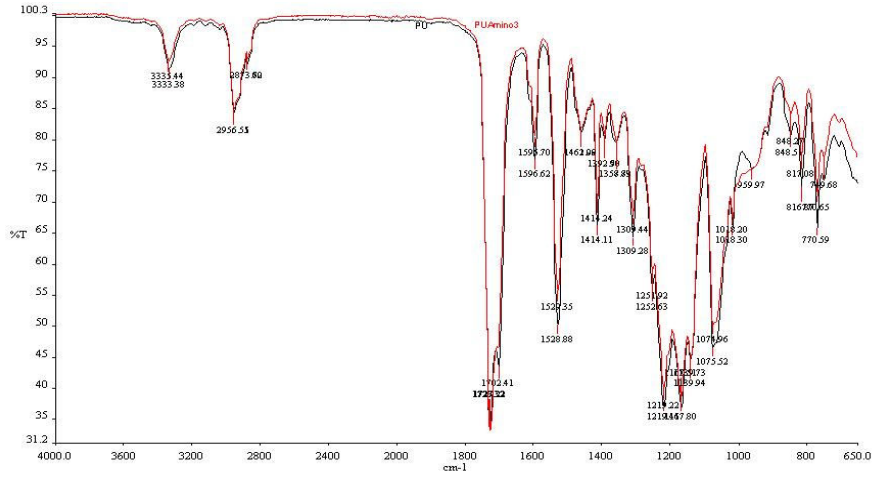

Figure 3.81: FTIR spectrum of PU-PUAmino3

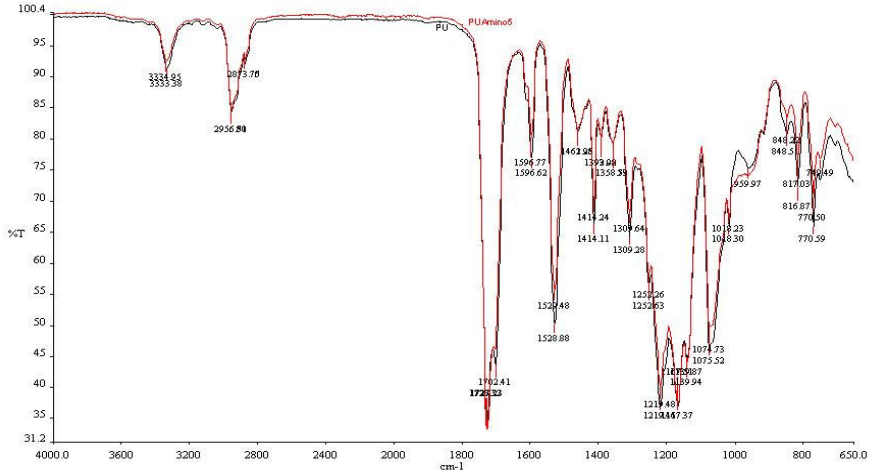

Figure 3.82: FTIR spectrum of PU-PUAmino5

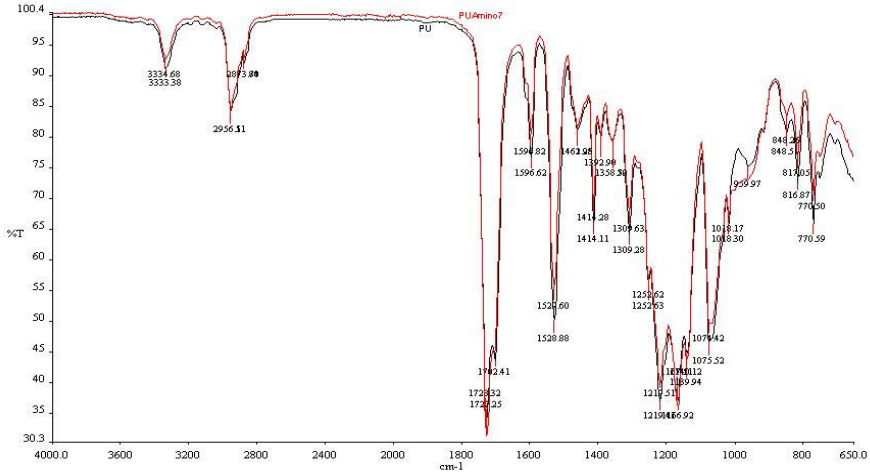

Figure 3.83: FTIR spectrum of PU-PUAmino7

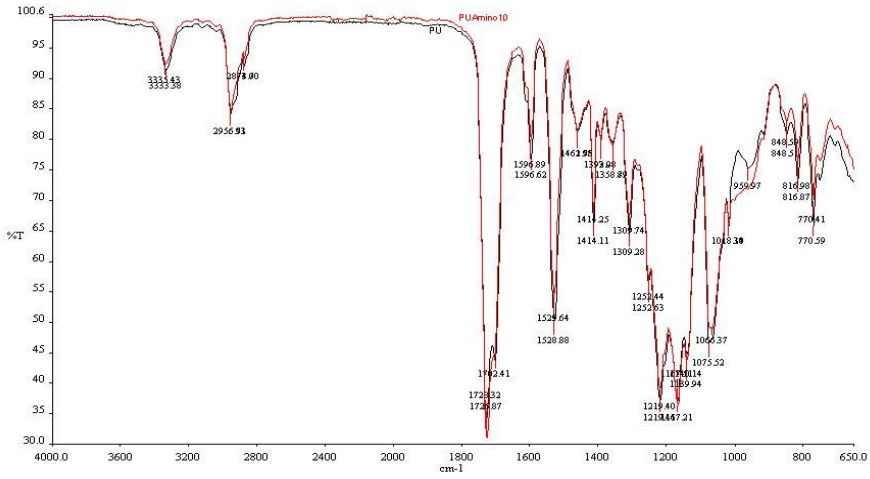

Figure 3.84: FTIR spectrum of PU-PUAmino10

3.8.5.3 Mechanical testing

In this study, the major goal was to improve the mechanical performance of the polyurethane matrix. The silane grafting was used to make even better properties compared to the improved PU-HEC composites. In this study, the results are promising for the mechanical properties. But the results are not that much better than the PU-HEC composite. Except 1 % the value is close. This is due to the contraction of the hectorite. The ease of good dispersed clay platelets disappears. The results become slightly lower than the pristine polymer. Further grafting procedures should be developed in order to produce very successful silane coated clays in order to produce better nanocomposites.

Table 3.6 Mechanical properties of PU-amino hectorite nanocomposites

Sample	Tensile Strength (MPa)
PU	5.09
PUAmino1	6.50
PUAmino3	4.78
PUAmino5	7.81
PUAmino7	8.48

3.8.5.4. Dynamic mechanical analysis

As the mechanical properties and other tests showed that the silane grafting did not improve the performance of the composite and instead it is inferior to the pure hectorite composites, the DMA results are not very promising as well, as shown in Figures 3.83-3.87.

The modulus values are very close to the polyurethane but not better. For pure hectorite, the results were better in terms of modulus values. Again this is related with the slight contradiction of the clays. The modulus values would be better if the clay could swell instead of contract.

The most important result of this study was the shift in the tan delta peaks. The shift in the tan delta peaks clearly indicates good interaction and compatibility of the two phases in the composite materials especially. The tan delta peaks have shifted for all the compositions which show the better interaction of the polyurethane and hectorite due to the silane grafting. For the hectorite samples, the tan delta peaks were very similar. For laponite samples, the height of the tan delta was lower giving material rigidity but the tan delta peaks did not shift for laponite composites as well. But here, the shift of the tan delta is very promising. So more work should be done to improve the silane grafting.

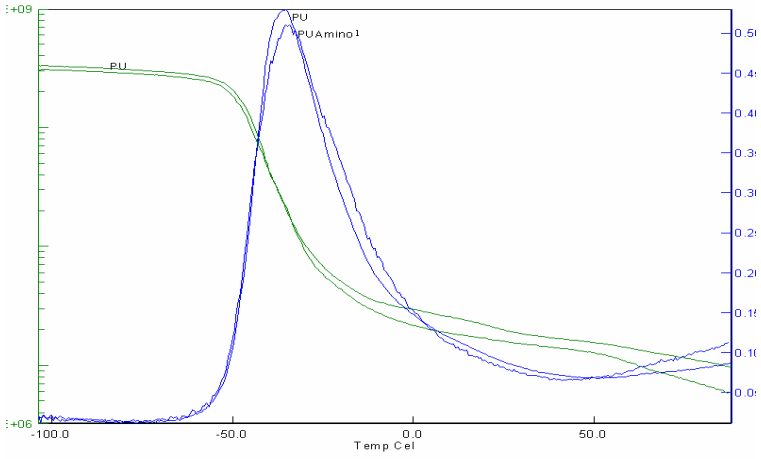

Figure 3.85: DMA of PU and PUAmino1

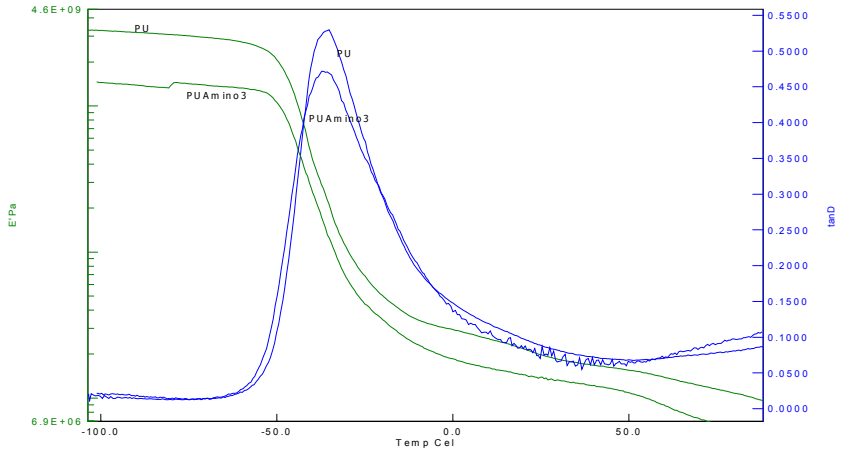

Figure 3.86: DMA of PU and PUAmino3

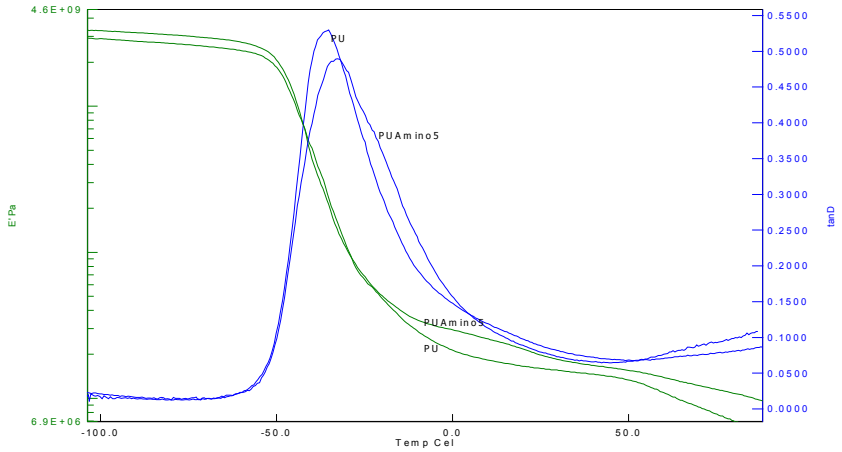

Figure 3.87: DMA of PU and PUAmino5

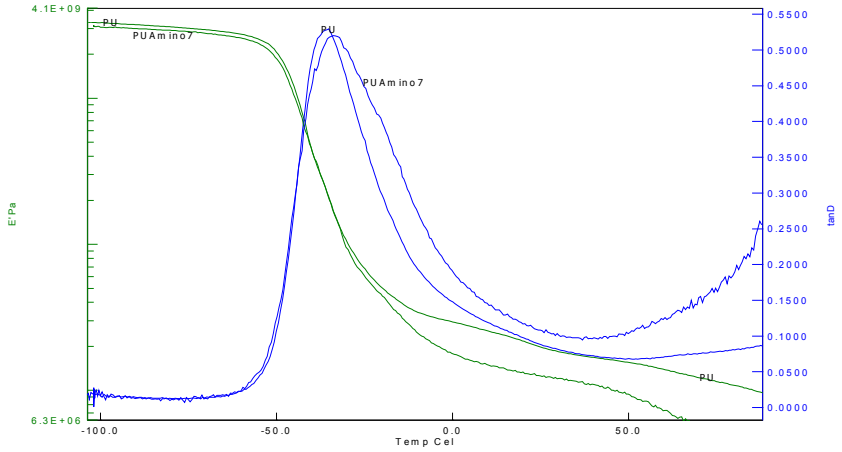

Figure 3.88: DMA of PU and PUAmino7

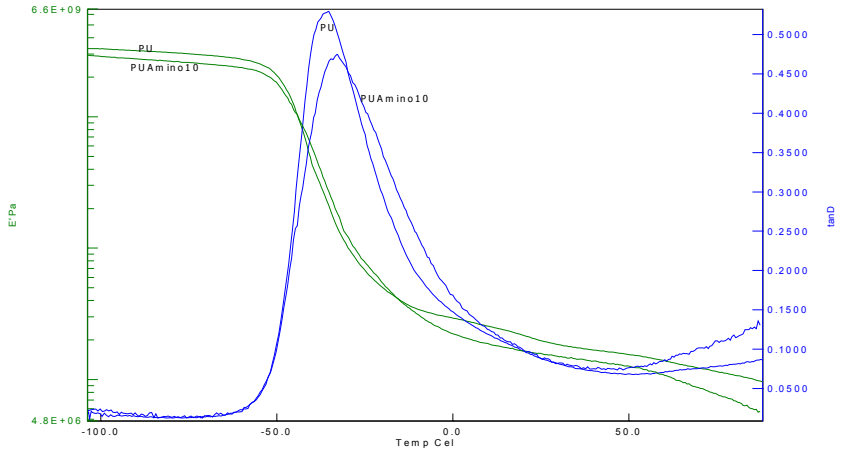

Figure 3.89: DMA of PU and PUAmino10

3.8.5.5. TGA

In Figure 3.88, TGA of the amino silane coated hectorite and PU nanocomposites are given. The final residue left increases as the clay concentration increases.

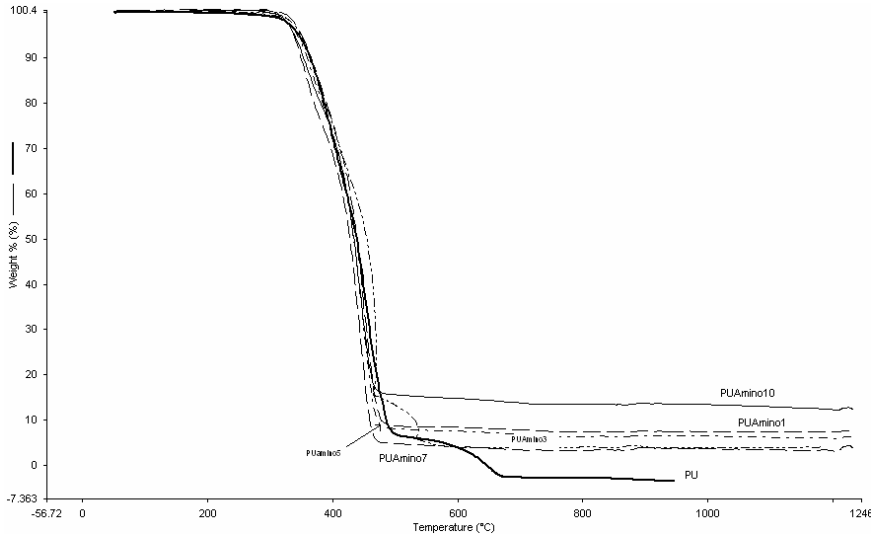

Figure 3.90: TGA thermograms of PU and PU-amino hectorite nanocomposites

3.8.6. Concluding remarks on silane coating for Hectorite in PU Nanocomposites

Three different types of silane coating agents were used for coating the hectorite in order to increase the reinforcing ability of the clay. Amino silane was the most effective silane for the preparation of hectorite nanocomposites. On the other hand, nanocomposites prepared from uncoated hectorite gave better mechanical properties than the nanocomposite with silane coated hectorite.

3.9. PU-Cellulose Nanocomposites

3.9.1. Preparation of microfibrils

It was observed that the higher pressure, 500 bar, was more effective for fibrillation than 250 bar, therefore 500 bar was used in this study. The critical parameter in the homogenization process was number of times the slurry would pass through the homogeniser. The time for one complete cycle was measured and 15 passes were calculated as 15 times the duration of one complete cycle. The fibrillation was done with 0.025 wt % cellulose slurry at 500 bar and was passed through the homogeniser 15, 30, 45, 60 times.

3.9.2. Visual examination

The change in dispersion of the cellulose suspensions after certain passes of homogenisation could be easily observed. Figure 3.89 shows the suspension after 15, 30, 45 and 60 passes. After 15 passes, the cellulose fibers were not homogenously dispersed in the water, a small improvement was observed after 30 passes. After 45 and 60 passes a more colloidal structure was obtained, the fibrils did not sediment as easily on the bottom of the beaker.

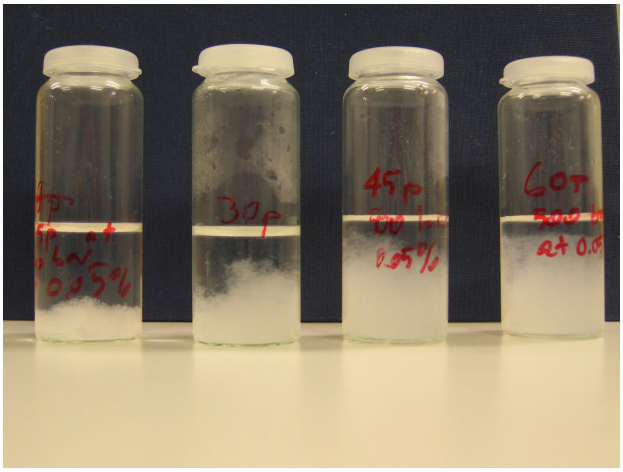

Figure 3.91: Colloidal suspensions of cellulose in water

3.9.3. Optical microscopy

The changes were also observed in the optical microscope. It can be easily seen in Figures 3.90 and 3.91 that the cellulose fibers in Figure 3.91 are smaller and more fibrillated after the homogenization process, compared to cellulose fibers in Figure 3.90. This observation further strengthens the statement of fibrillation of cellulose to nano scale.

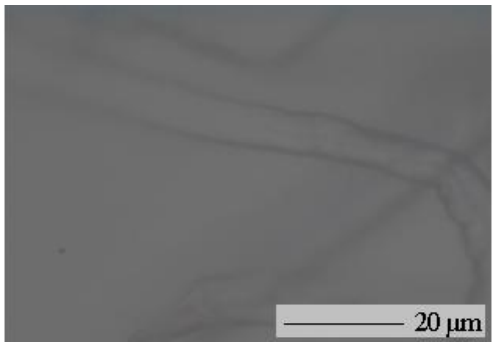

Figure 3.92: Cellulose fiber

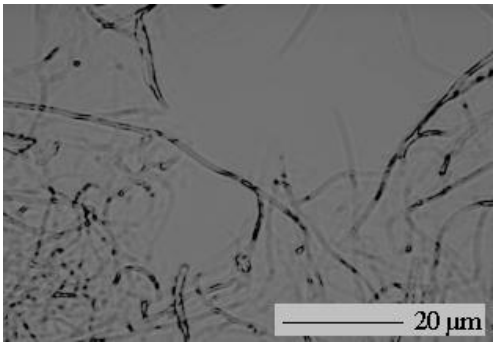

Figure 3.93: Cellulose fibril

3.9.4. Fibril structure

In Figures 3.92-3.97, three different materials are shown. Figures 3.92 and 3.93 show the cellulose fiber structure before the fibrillation process. Figure 3.92 shows the overview and Figure 3.93 shows a more detailed view of the cellulose fiber structure where it is possible to visualize the nanofibrils at the fiber surface. Figures 3.94 and 3.95 show the fibrillated cellulose after the homogenization process, The fibrillation

will occur on the individual fibrils which can be seen on the cellulose fiber in detail. The microscopy study showed that it is possible to fibrillate cellulose pulp fibers using a high pressure homogenizer.

Figures 3.94 and 3.95 show the fibrillated structures of the cellulose fibers after 45 passes through the homogenizer. It is possible to see the great difference between the Figures 3.96 and 3.97. The fibers are broken down to the smaller fibers and forming a network of fibrils. Figures 3.96 and 3.97 show the effect after 60 passes with further decreased fibril size compared to Figures 3.96 and 3.97. It is clearly shown that the homogenization process results in fibrillation of cellulose fibers resulting in small fibrils which are at least partly at nano size. The fibrillated structure can be observed within SEM pictures. The number of passes through the homogenizer does not affect the fibril size after 45 passes but the number of fibrils increased after 60 passes. This is the reason why the 60 passes was chosen as optimum in this study.

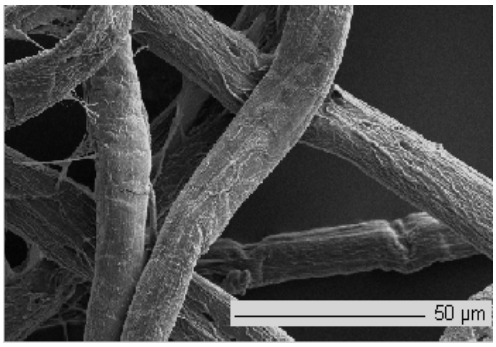

Figure 3.94: SEM image of cellulose fiber

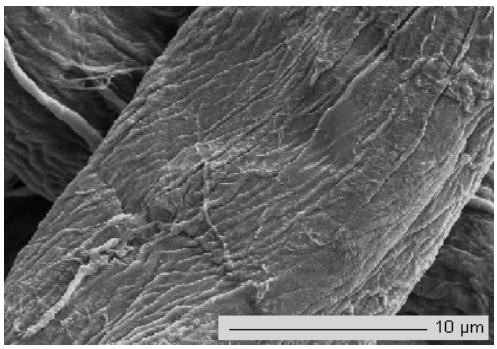

Figure 3.95: SEM image of cellulose fiber

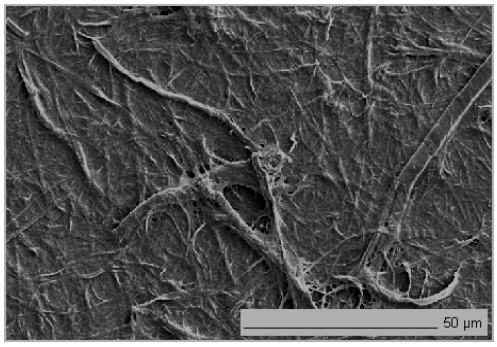

Figure 3.96: Cellulose fibril after 45 times homogenization

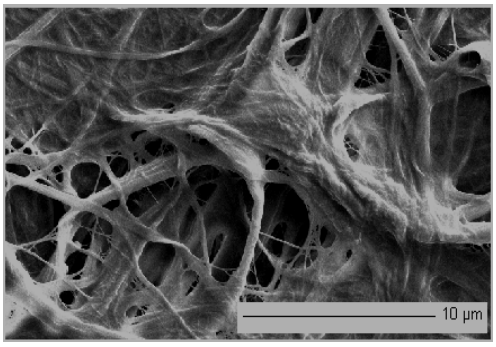

Figure 3.97: Cellulose fibril after 45 times homogenization

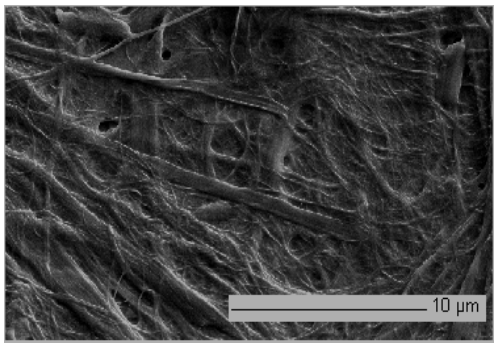

Figure 3.98: Cellulose fibril after 60 times homogenization

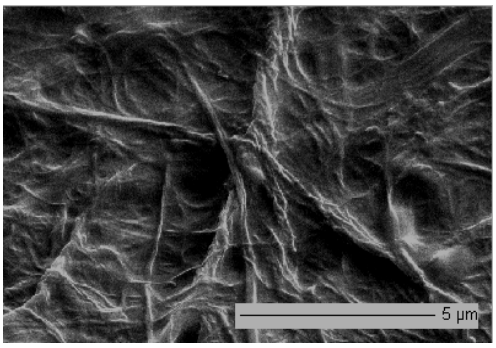

Figure 3.99: Cellulose fibril after 60 times homogenization

3.9.5. Mechanical and thermal properties

The mechanical properties of neat polyurethane and cellulose fiber polyurethane composites are shown in Table 3.7. The results show that the mechanical properties of composites were improved with an increase in cellulose fiber content. The increase in the tensile strength was significant which strengthen the hypothesis that polyurethane and cellulose are compatible as they are both hydrophilic, The strength of the PU-CF 2 was increased with 200 % compared with neat PU.

Table 3.7: Mechanical properties of pure PU and prepared composites

Sample	Tensile Strength (MPa)
PU	5.09
PU-CF 1	11.06
PU-CF 2	15.98
PU-CNF 1	5.47
PU-CNF 2	28.03

The microfibrils showed to be more effective reinforcement than the micro sized cellulose fibers. The strength was improved from 5 MPa for neat PU to 28 MPa (almost 500%) for the PU-CNF 2 composite. These results clearly show the effectiveness of nano size reinforcement. The cellulose nano fibrils will integrate within the polymer matrix much better due to the smaller size but this great improvement is also expected due to better properties of nano sized fibrils compared with the micro sized fibers. The increase of the probability of the cellulose linkages can be observed at the nano-scale as well having much smaller particle sizes [62].

In the earlier studies conducted on polyurethanes and cellulose based fibers all of them are reporting about the mechanical reinforcement [63]. Rials and Wolcott [64] tested the composites dynamic mechanical thermal properties comparing the modulus values and observed an increase in the mechanical properties of PU with wood fibers. Auad et al. [16] reported improved mechanical properties with the nanosize cellulose whiskers in PU matrix. On the other hand Nakagaito and Yano [65] reported increased mechanical properties with micro fibrillated cellulose fibrils (not bacterial, 2.4-27.9 %) in a phenol formaldehyde matrix. This study showed the importance of the fibrillation process forming microfibrils as nanosize reinforcements to make the nanocomposite materials much stronger than the composites with cellulose fibers in micro meter size.

Figure 3.98 and 3.99 shows the storage modulus and tan delta as a function of temperature for pure PU and the composites. The storage modulus in Figure 3.98 shows that both composites have higher modulus on the entire temperature range compared to pure PU and that the modulus does not drop after the PU softening temperature. The nanocomposite shows highest storage modulus during the entire temperature range, being approximately 2200 % higher than the neat PU matrix and about 150 % higher than the CNF composites at room temperature.

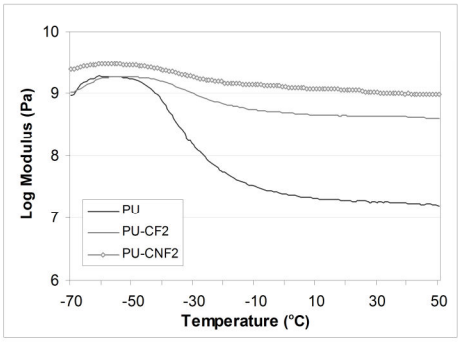

Figure 3.100: Storage modulus values

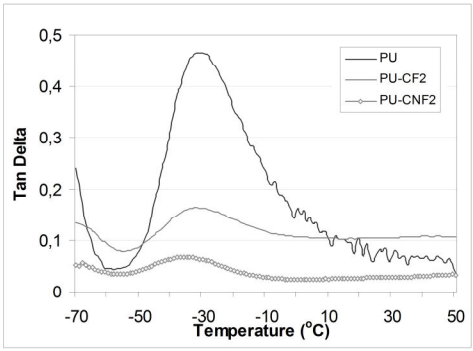

Figure 3.101 : Tan delta values

One of the most interesting results of this study was the large improvement in storage modulus of the nanocomposite compared with neat PU and cellulose fiber composites. This large improvement is expected to be a result of a percolation network formed by cellulose nano fibrils [62]. The strong hydrogen bonds between the cellulose molecules will lead to strong interaction between the fibers and fibrils thus results in much better composite properties compared with the pure PU at higher

temperatures. The other important effect is that the microfibrillated cellulose has flexibility. This property of the cellulose fibrils gives a tangling effect with the polymer matrix which will further increase the mechanical properties of the nanocomposite [66]. The composites with cellulose fibers and fibrils show much better temperature stability than PU at room temperature because of the percolating network effect and it is maintained even at higher temperatures.

Rials and Wolcott [64] prepared polyurethane-wood fiber composites and observed similar reinforcements with wood fibers but with much higher wood fiber content. They did not test with DMA in order to observe the behaviour of the composites with increasing temperature.

Also Nakagaito and Yano [65] used microfibrillated cellulose to increase the mechanical properties of the phenol formaldehyde but they did not perform DMA analysis neither.

This study has shown the importance of the microfibrillated cellulose in order to obtain composites with good mechanical properties and the increased stability at higher temperatures.

The tan delta of pure PU and the composites is shown in Figure 3.103. The shift in tan delta peak temperature can give an indication of the molecular interaction between two phases.

In this study, the tan delta peak did not show any shift indicating that there are no molecular interaction between the PU and cellulose. Therefore the reinforcing effect and thermal stability are associated mainly with the cellulose network and strong interaction of cellulose particles.

3.9.6. Concluding remarks on PU-cellulose fiber and cellulose fibril composites

Microfibrillated cellulose was obtained with a novel method using a high pressure homogenizer. The fibrils were characterized and identified to be very small, partly at nanosize by SEM analysis. Fiber/fibril mats were prepared by filtering the slurry and a film-stacking technique was used to prepare the composites. Transparent composite films were obtained with cellulose fibrils.

The mechanical and thermal properties of the matrix polymer (PU) and the prepared composites were investigated and the results showed that both cellulose fibers and

nanofibrils improved the mechanical properties of PU. The most remarkable results were shown in nanocomposites with 16.5 wt% fibril content. The strength was nearly 500 % and the E-modulus 3000 % better than the matrix polymer. Furthermore the storage modulus of the nanocomposites was improved and it was higher than PU in both elastic and plastic temperature range. When the storage modulus dropped the temperature of -52,4 °C for neat PU and the cellulose fiber composite at a temperature of -31 °C, the nanocomposites showed no significant drop in the storage modulus values even at higher temperatures.

Tan delta peak temperature was not changed for the composites compared to PU, which indicates no molecular interaction between the PU and cellulose.

With these improvements, the use of polyurethane and many other polymers can be expanded. The most important outcome of this study was to understand the importance of nanosize reinforcement for the polymers

3.10. Preparation of PU-carbon fiber

In investigating the carbon fiber reinforced polyurethane, the major aim was to compare the reinforcing effect of the carbon fiber with the nanoreinforcements obtained with clays and cellulose materials. The use of carbon fibers in industrial applications has increased because of its high mechanical properties. The goal was to understand if the carbon composites were better than the nanoreinforcing phases such as clay and cellulose. For this purpose, tensile testing, DMA, TGA and FTIR analyses were done and the results were compared with those of clay and cellulose based composites.

3.10.1 FTIR analysis

In the Figure 3.100-102, it is observed that the polyurethane structure is maintained with no change in the general spectrum. For PU-clay nanocomposites, the peak of 959.97 cm^{-1} disappeared indicating that the structure of the polymer was changed. Instead for carbon composites with the same loading, no change was observed in the structure. As the content of the carbon fiber is too low (the maximum loading was 3 %), the peaks of the carbon can not be seen as well. So the structure of the polymer is not altered. This makes the composite material much more valuable.

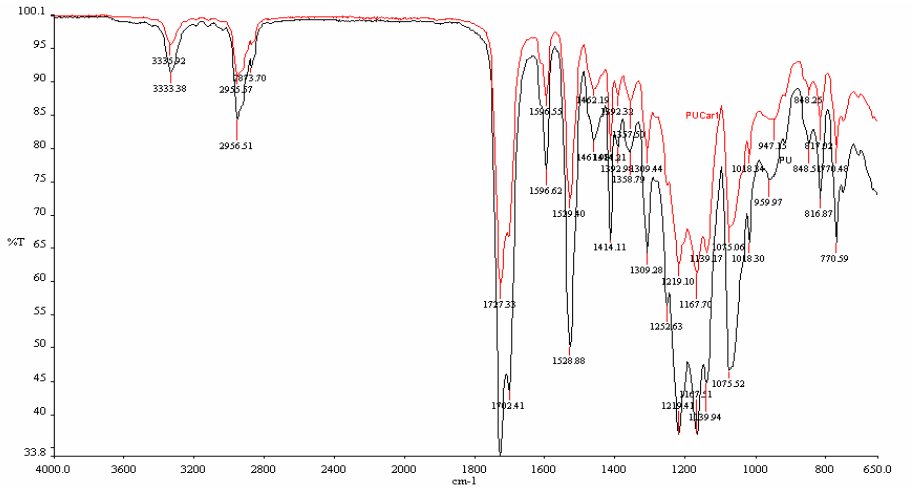

Figure 3.102: FTIR spectrum of PU and PUCar1

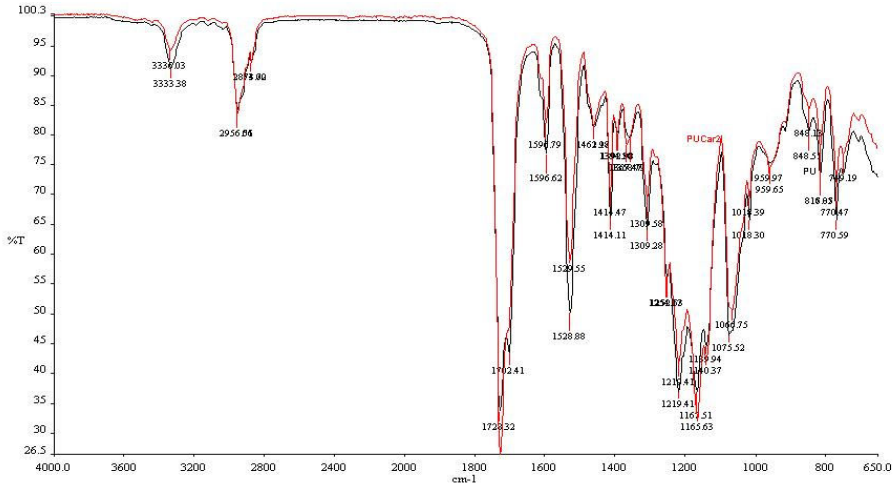

Figure 3.103: FTIR spectrum of PU and PUCar2

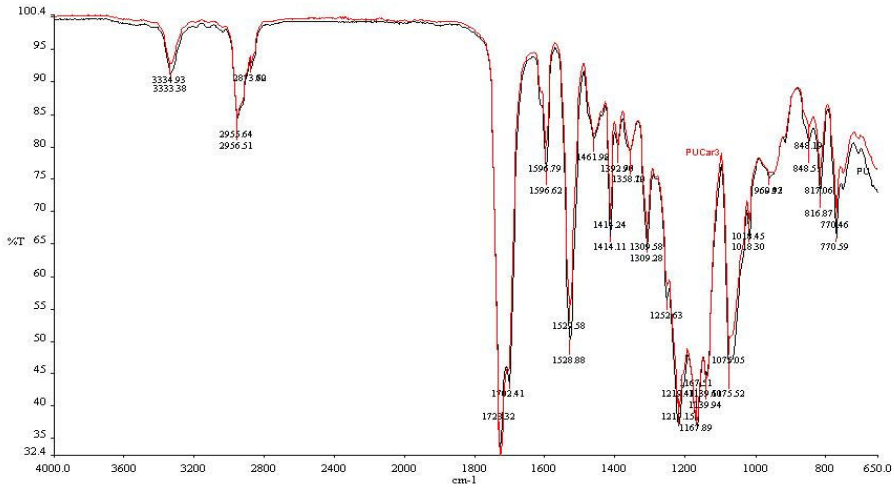

Figure 3.104: FTIR spectrum of PU and PUCar3

3.10.2. Mechanical testing

When the mechanical properties are investigated, the improvement in the mechanical properties is drastic. Mechanical properties of PU-carbon fiber composites are given in Table 3.8. As shown, tensile strength of composite increases with increasing carbon fiber content and leveling off towards 3 wt %. It is well known that the carbon has specific strength of 15 times higher than the steel. This high strength has also influenced the mechanical properties of the composite. The polymer has 5 MPa maximum tensile strength. Even 0.5 % loading of carbon fiber has increased the mechanical properties 128 % which is very significant.

At higher concentrations of the carbon fiber, the increase of the maximum mechanical properties was even higher. At 1 percent of carbon fiber, the increase was 217 % which is three times than the pristine polymer. It is really important to have so much increase with such 1 % carbon fiber in the polyurethane matrix. At 2 % of carbon fiber, the increase was 264 % and for 3 % of carbon fiber the increase was 293 % at which point the increase was leveling off. Above 3 % carbon fiber was not needed to test as the tensile strength was leveling off. In earlier studies [67], obtained improvement with short fiber was not this much impressive. In a later study [17], long fibers were used in order to obtain better reinforcement. The increase was also very high like the data obtained in this study. But the long fiber study is not very suitable method for industrial applications. In this study, with short fibers, the same improvements were obtained as the previous long fibers study. The reason for obtaining better reinforcement is due to the good interaction of the carbon fiber and

polyurethane and good distribution of the carbon fiber in the polyurethane structure. The second reason is that the carbon fibers are polar and the polyurethane is hydrophilic being polar as well. This polarity formed excellent composite materials.

Table 3.8: Mechanical properties of PU and PU carbon fiber composites

Sample	Tensile Strength (MPa)
PU	5.09
PUCar05	11.57
PUCar1	16.12
PUCar2	18.53
PUCar3	19.98

3.10.3. Dynamic mechanical analysis

When the viscoelastic behavior of micro composites prepared with carbon fiber was investigated by DMA, the values of storage modulus values were found to be higher than that of pure polymer after -52,4^{0}C, as shown in Figures 3.103-3.105. DMA results support the results of mechanical tests. This shows the superior performance of the composite material.

The polymer chain restriction can be clearly observed on the tan delta curves. The height of the tan delta curves decreased with increasing carbon fiber content because the carbon fiber increased the rigidity of the polymer chains.

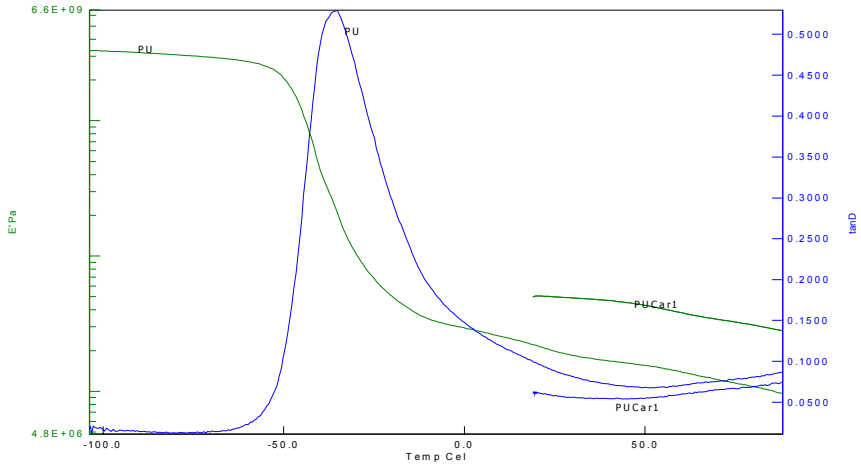

Figure 3.105: DMA of PUCar1

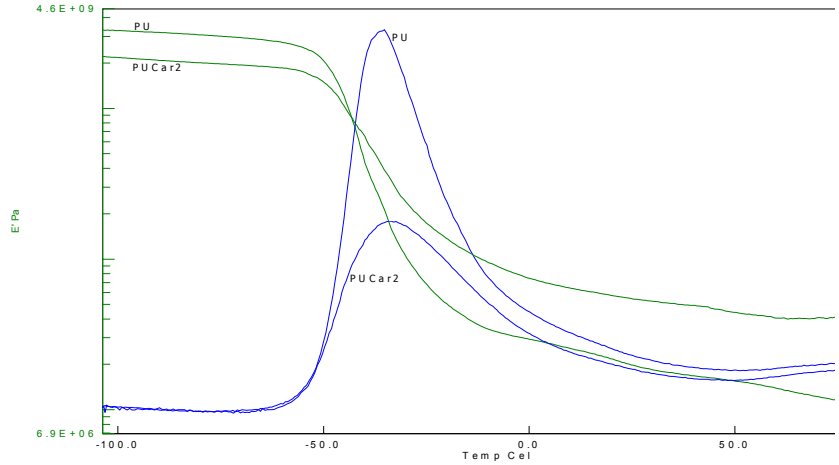

Figure 3.106: DMA of PUCar2

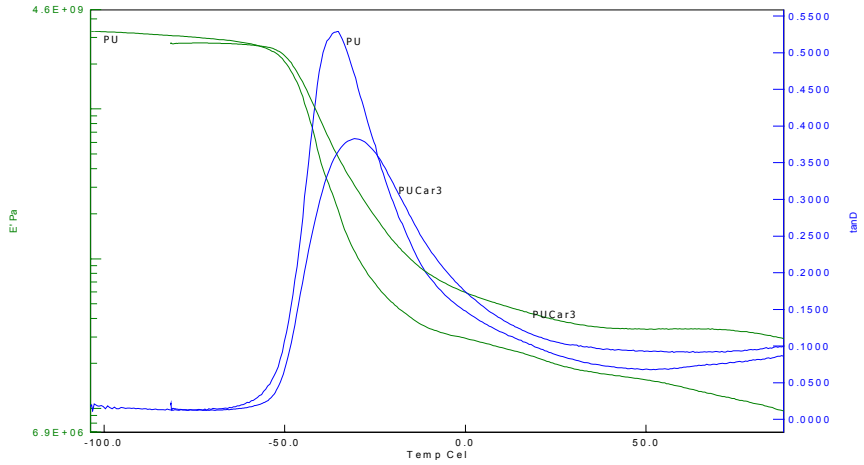

Figure 3.107: DMA of PUCar3

When the micron-meter carbon fiber reinforced polyurethane is compared with the nanocomposites of the polyurethane-clay, it was observed that even the minimum concentration of the carbon fiber (0,5 wt %) has higher strength than all the nanocomposites of clays including the silane coated and the synthetic forms of the clay hectorite. 3 % carbon reinforced PU has two times higher strength than the 7 wt % HEC- polyurethane nanocomposites.

On the other hand, nanocomposites prepared from clay are transparent and are not affected from the light. On the contrary of this property, composites obtained with carbon fiber were not transparent. Moreover, in this study, polymer-clay nanocomposites with exfoliated structures were obtained with no organic modifiers.

This makes the reinforcing material very cheap. So the choice of the reinforcing phase depends on the requirements and budget of the application.

When the carbon reinforcement is compared with the cellulose reinforcement, it was observed that the carbon fibers are better in terms of tensile strength even with much lower percentages. When the carbon fiber is compared with the cellulose fibrils, it was found that cellulose fibrils create higher tensile strength than the carbon fibers with 28 MPa compared to 19 MPa of carbon fibers. The concentration of carbon fiber is less than the nanosized cellulose fibrils so it can be stated that the effective reinforcement of the carbon fiber is better. Higher concentration of carbon fiber would be tested but this could not be achieved with solvent casting due to the difficulties in preparing the carbon-fiber reinforced polyurethanes.

When the DMA results are compared, it was observed that carbon fibers have higher modulus values than clays. On the other hand, cellulose material both at the micron and nano level is much better than the clay and carbon fiber.

3.10.4 TGA

The thermal stability of the composite materials was tested with TGA, as shown in Figure 3.106. It was clearly shown that the final residue increases with the incorporation of the carbon fiber to the matrix.

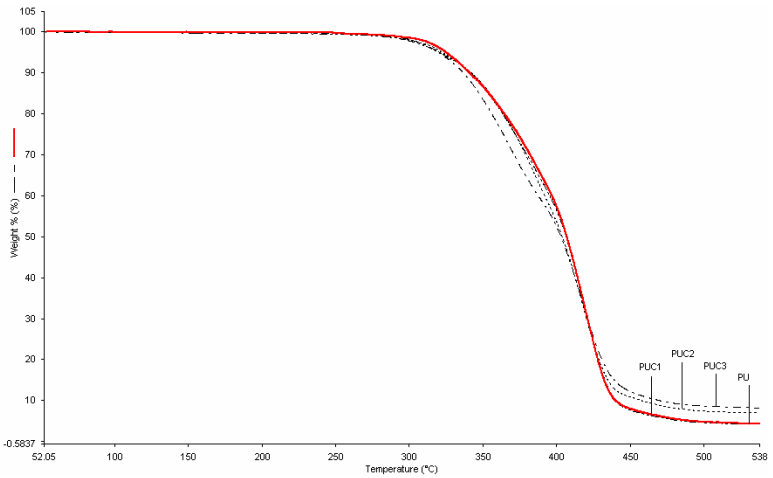

Figure 3.108: TGA thermograms of PU and PUCar composites

3.10.5. Optical microscopy

The dispersion of the carbon fibers were investigated with optical microscopy. Electron microscopy was not needed. The fibers could be easily observed with the optical microscope. The magnifications were 100* which was enough to observe homogenous distribution of the carbon fibers. The images of the 3 different compositions are given in Figure 3.107-3.109.

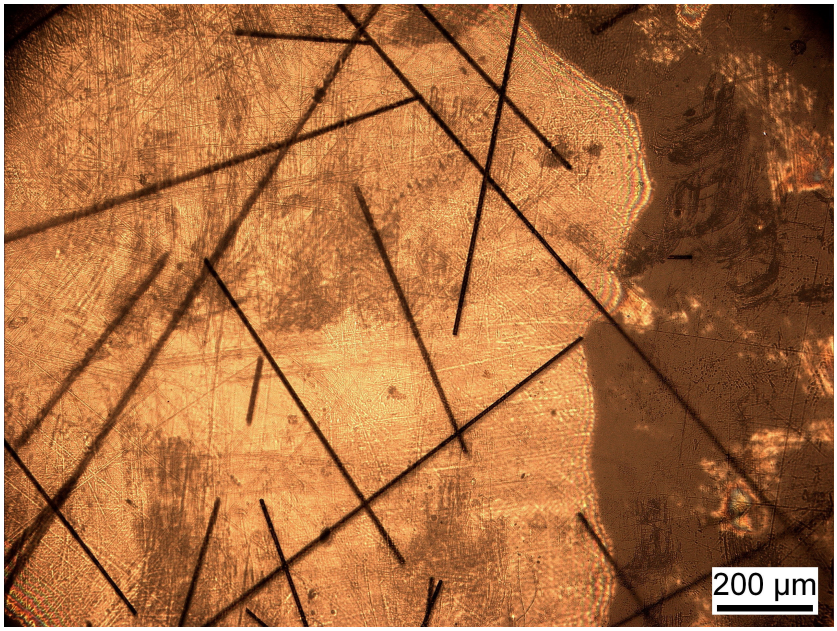

Figure 3.109: Optical microscopy of PU-carbon fiber1 composites

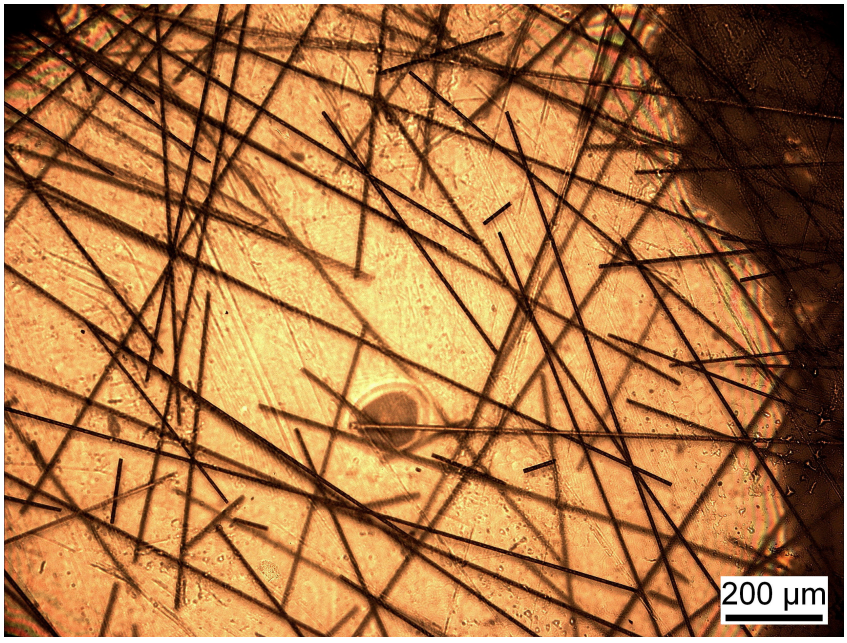

Figure 3.110: Optical microscopy of PU-carbon fiber2 composites

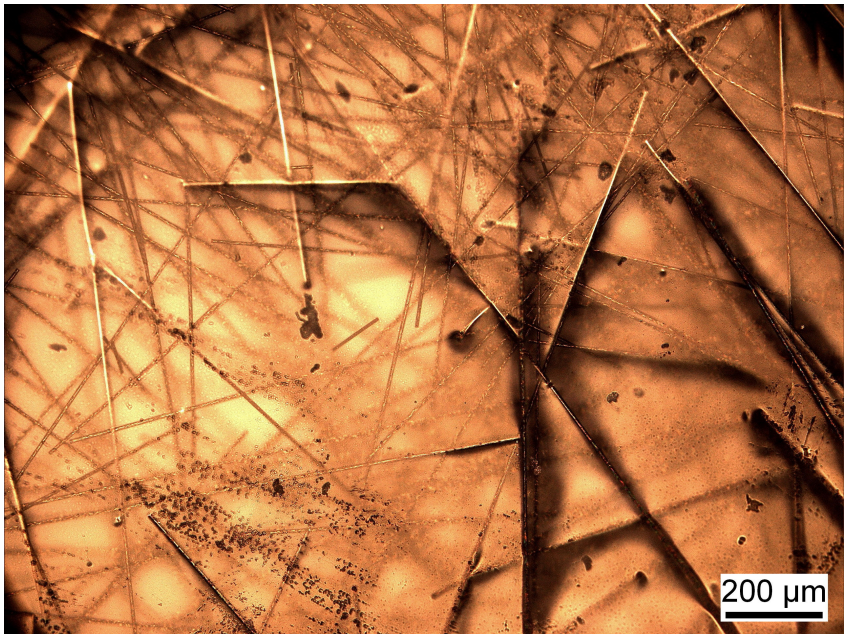

Figure 3.111: Optical microscopy of PU-carbon Fiber3 composites

From the figures it is clearly seen that the fibers are randomly distributed. The fiber distribution could be easily observed. There is homogenous distribution of the carbon fibers. The fibers are very fine and all have the same diameter which makes the composite material much better perform superior.

3.10.6. Concluding remarks on PU-carbon fiber composites

The effect of the carbon fibers on the mechanical properties of the polyurethane is very dramatic. They are much more effective than the clay nanocomposites prepared in this study for all the clay compositions. On the contrary, the TGA results show that the final residue is higher for the clay nanocomposites is better due to the nanosize interaction with the polymer. Cellulose fibers being natural resource, give higher strength than the carbon fibers to the polyurethane matrix. From DMA graphs, it was observed that the thermomechanical properties of the cellulose composites are better than those the PU-Carbon fiber composites.

4. CONCLUSION

The aim of this Ph.D study was to prepare polyurethane nano and microcomposites having good mechanical and thermal properties. Within the developments in the technology, nanoscale reinforcements have become possible which have many advantages compared to the micron sized reinforcements.

This study had three parts. The parts were arranged in an order of going from nanoscale to micron scale. In the first and most comprehensive part, the polyurethane was reinforced with the different nanoclays and with certain chemical modifications of the clays such as organoclay preparation and silane coupling. In the second part, cellulose was used as a reinforcing material at micro and nano size. In the last step, micron meter sized carbon fiber was used to increase the mechanical properties of the polyurethane.

The most important outcome of this study was to produce nanocomposites of polyurethane with clays without any modification. The swelling behavior of the clay in DMF and the hydrophilic nature of the polyurethane enabled to produce even 15 wt % exfoliated hectorite polyurethane nanocomposites. In order to use as comparison material, PU-MMT nanocomposites were prepared using the same preparation procedure of exfoliated structure of PU-HEC nanocomposites. Exfoliated structures were obtained as well. As compared, the properties of PU-HEC and PU-MMT nanocomposites, it was observed that hectorite based nanocomposites gave better results.

The preparing procedure of the PU-clay in exfoliated structure was implemented to the polyurethane laponite composites. Laponite, which is synthetic form of hectorite, has very similar chemical structure of the hectorite. It is synthetic form of the hectorite with no impurity in it. Again successful exfoliated nanocomposites were produced. The properties of the PU-HEC and PU-Lap were compared and it was observed that the PU-HEC is better than PU-Lap in terms of processability and the mechanical properties.

As a last step in the polyurethane-clay nanocomposites, the HEC was silane coated in order to improve the properties of the pure polymer. It was observed that the silane could be grafted to the structure slightly and improvements were not so important when compared with the HEC itself.

After all these, polyurethane-clay nanocomposites, polyurethane cellulose composites at the micron and nanoscale were prepared. The cellulose is also a natural resource and it is abundant in nature. The good thing about the cellulose is, it can be prepared at the micron and nano level. In this study both sizes of cellulose were used to reinforce the same polyurethane as in the first part of this study. The reinforcement was higher and the thermal properties were very good. One of the most important aspects of this study was to understand the difference between the micron and nano size reinforcement. The nano size reinforcements were much better than micron sized reinforcements in terms of the mechanical properties and thermal properties for polyurethane.

As the last step, the micron sized carbon fiber was used to determine the effect of the reinforcement. The results were much better than all the clay compositions in terms of mechanical properties. When the properties of the polyurethane-carbon fiber composites are compared with the cellulose based materials, the results were found between the micron sized and nano size cellulose.

To conclude this comprehensive work on polyurethane composites with 3 different reinforcing materials, it was observed that the best mechanical and thermal properties were achieved with cellulose material which can be prepared at the micro and nano level.

In Table 4.1., the values of tensile strength are given for all composites prepared in this study.

Table 4.1: Tensile Strength of all Composites Prepared in this Study

Sample	Tensile Strength, MPa
Polyurethane	5.09
Polyurethane-1 wt % Hectorite	5.58
Polyurethane-3 wt % Hectorite	7.27
Polyurethane-5 wt % Hectorite	8.84
Polyurethane-7 wt % Hectorite	**10.86**
Polyurethane-10 wt % Hectorite	9.15
Polyurethane-15 wt % Hectorite	6.68
Polyurethane-3 wt % Montmorillonite	6.76
Polyurethane-5 wt % Montmorillonite	5.90
Polyurethane-7 wt % Montmorillonite	7.00
Polyurethane-1 wt % Laponite	4.36
Polyurethane-3 wt % Laponite	8.60
Polyurethane-5 wt % Laponite	8.17
Polyurethane-7 wt % Silane A Coated Hectorite	8.48
Polyurethane-7 wt % Silane B Coated Hectorite	8.04
Polyurethane-7 wt % Silane C Coated Hectorite	6.45
Polyurethane-1 wt % Silane A Coated Hectorite	6.50
Polyurethane-3 wt % Silane A Coated Hectorite	4.78
Polyurethane-5 wt % Silane A Coated Hectorite	7.81
Polyurethane-8,5 wt % Cellulose Fiber	11.06
Polyurethane-18,7 wt % Cellulose Fiber	15.98
Polyurethane-7,5 wt % Cellulose Fibril	5.48
Polyurethane-16,5 wt % Cellulose Fibril	**28.03**
Polyurethane-0,5 wt % Carbon Fiber	11.57
Polyurethane-1 wt % Carbon Fiber	16.12
Polyurethane-2 wt % Carbon Fiber	18.52
Polyurethane-3 wt % Carbon Fiber	**19.98**

For further work, these findings can be used for other polyurethane applications. In the case of biomedical applications, these properties may be very important. The polyurethane clay composites can be expanded to work on extrusion of thermoplastic polyurethanes. The cellulose can be incorporated to the polyurethane during the synthesis of the polymer which can be even more effective. The carbon fiber study can be expanded to the different uses of carbon fibers such as sensor applications and the military applications.

REFERENCES

[1] http://composite.about.com/od/whatsacomposite, 28.11.2005

[2] **Vaia, R.A**., 2002. Polymer nanocomposites open a new dimension for plastics and composites. *The AMPTIAC Newsletter*, **6**, 17-24.

[3] **Callister W.D.**, 1994. Materials Science and Engineering, An Introduction. John Wiley & Sons, New York.

[4] **Soboyejo, W.,** 2002. Mechanical Properties of Engineered Materials, Marcel Dekker Inc., New York.

[5] **Jordan J., Jacobb K. I., Tannenbaum, R., Sharaf, M.A., Jasiuk, I.,** 2005. Experimental trends in polymer nanocomposites-a review, *Materials Science and Engineering* A, **393**, 1–11.

[6] http://www.efunda.com/formulae/solid_mechanics/composites/comp_intro.cfm, 29.11.2005

[7] **Shen, J., Zhang, Z., Wu, G.**, 2003. Preparation and characterization of polyurethane doped with nano-sized SiO_2 derived from sol-gel process, *J. Of Chem. Eng. Japan*, **36,** 1270-1275

[8] **Moon, S.Y., Kim, J. K., Nah, C., Lee, Y.S.**, 2004. Polyurethane/montmorillonite nanocomposites prepared from crystalline polyols, using 1,4-butanediol and organoclay hybrid as chain extenders, *European Polymer Journal*, **40,** 1615–1621.

[9] **Stevens, M.P.**, 1999. Polymer Chemistry, Oxford University Press, Oxford.

[10] **Ozkaynak, M.U., Atalay-Oral, C., Tantekin-Ersolmaz, B., Güner, F.S.**, 2005. Polyurethane films for wound dressing applications, *Macromol. Symp.,* **228**,177-184.

[11] www.basf.com, 15.03.2007

[12] www.bayer.com, 25.03.2007

[13] **Gorrasi, G., Tortora, M., Vittoria, V.**, 2005. Synthesis and physical properties of layered silicates/polyurethane nanocomposites, *Journal of Polymer Science: Part B: Polymer Physics*, **43**, 2454–2467.

[14] **Lee, S.H., Kim, S.H., Lim, H., Kim, B.K.**, 2006. Environmentally friendly glass Fiber and nanoclay reinforced polyurethane foam. *IUPAC International Symposium on Advanced Polymers for Emerging Technologies,* 10-13 October, Busan, South Korea.

[15] **Yao, K.J., Song, M., Hourston, D.J., Luo, D.Z.**, 2002. Polymer/layered silicate nanocomposite: 2 Polyurethane nanocomposites. *Polymer,* **43**, 1017-1020.

[16] **Auad, M.L., Contos, V.S., Nutt S., Aranguren M.I., Marcovich N.E.**, 2005. Polyurethane reinforced with nano/micro sized cellulose fibers. *Proceedings of COMAT 2005. International Conference on Science and Technology of Composite Materials*. Argentina.

[17] **Borda, J., Keki, S., Rathy, I., Bodnar, l., Zsuga, M.**, 2007. Novel polyurethane elastomer continuous carbon fiber composites: Preparation and characterization, *Journal of Applied Polymer Science,* **103**, 287–292.

[18] **Ray, S.S., Okamoto, M.**, 2003. Polymer/layered silicate nanocomposites: a review from preparation to processing, *Prog. Polym. Sci.*, **28,** 1539–1641.

[19] **Wang, Z., Pinnavaia, T. J.**, 1998. Nanolayer reinforcement of elastomeric polyurethane, *Chem. Mater.,* **10***,* 3769-3771.

[20] **Ray, S.S., Bousmina, M.**, 2005. Biodegradable polymers and their layered silicate nanocomposites: In greening the 21stcentury materials world, *Progress in Materials Science,* **50,** 962–1079.

[21] http://www.surrey.ac.uk/PRC/Research/nano.htm, 20.11.2005.

[22] **LeBaron, P.C., Wang, Z., Pinnavaia, T. J.**, 1999. Polymer-layered silicate nanocomposites: an overview, *Applied Clay Science,* **15,** 11–29.

[23] **Takeichi, T., Guo Y.**, 2003. Synthesis and characterization of poly(urethane-enzoxazine)/clay hybrid nanocomposites, *Journal of Applied Polymer Science*, **90**, 14, 4075–4083.

[24] **Rhoney, I., Brown, S., Hudson, N.E., Pethrick, R. A.**, 2004. Influence of processing method on the exfoliation process for organically modified clay systems: Polyurethanes, *Journal of Applied Polymer Science*, **91**, 1335–1343.

[25] **Xu, R., Manias, E., Snyder, A. J., Runt, J.,** 2001. New biomedical poly(urethane-urea)-layered silicate nanocomposites, *Macromolecules,* **34***,* 337-339.

[26] **Han, B., Cheng, A., Ji, G., Wu, S., Shen, I.J.,** 2004. Effect of Organophilic montmorillonite on polyurethane/montmorillonite nanocomposites, *Journal of Applied Polymer Science*, **91**, 2536–2542.

[27] **Alexandre, M., Dubois, P., Sun, T., Garces J. M., Jérôme, R.**, 2002. Polyethylene-layered silicate nanocomposites prepared by the polymerization-filling technique: synthesis and mechanical properties, *Polymer,* **43,** 2123-2132.

[28] **Chen, B., Evans, J.R.G.**, 2005. Thermoplastic starch–clay nanocomposites and their characteristics. *Carbohydrate Polymers*, **61,** 455–463.

[29] **Brindley, G.W., Brown, G.**, 1984. Crystal Structure of Clay Minerals and Their X-ray Identification, Spottiswoode Ballantyne Ltd., London.

[30] **Wheeler, P. A., Wang, J., Baker, J., Mathias, L.J.**, 2005. Synthesis and characterization of covalently functionalized laponite clay**,** *Chem. Mater.* **17***,* 3012-3018

[31] **Yang, R., Liu, Y., Wang, K.**, **Yu, J.**, 2003. Characterization of surface interaction of inorganic fillers with silane coupling agents, *J. Anal. Appl. Pyrolysis,* **70,** 413-425.

[32] **Leu, C. M., Wu, Z.W. and Wei, K. H.**, 2002. Synthesis and properties of covalently bonded layered silicates/polyimide (BTDA-ODA) nanocomposites**,** *Chem. Mater.* **14,** 3016-3021.

[33] **Vrancken, K.C., Possemierss, K.P., Van Der Voort, P., Vansant, E.F.**, 1995. Surface modification of silica gels with aminoorganosilanes. *Colloids and Surfaces A: Physicochemical and Engineering Aspects***, 98,** 235-241.

[34] **E.P. Plueddemann**, 1992. Silane Coupling Agents, Plenum Press, New York.

[35] **He, H., Duchet, J., Galy, J., Gerard, J.F.**, 2005. Grafting of swelling clay materials with 3-aminopropyltriethoxysilane, *Journal of Colloid and Interface Science,* **288,** 171–176.

[36] **Chen, G.X., Yoon, J.S.**, 2005. Nonisothermal crystallization kinetics of poly(butylenesuccinate) composites with a twice functionalized organoclay, *Journal of Polymer Science: Part B: Polymer Physics*, **43**, 817-826.

[37] **Chen, G., Yoon J.S***.,* 2005. Nanocomposites of poly[(butylene succinate)-*co*-(butylene adipate)] (PBSA) and twice-functionalized organoclay*, Polym. Int.,* **54,** 939–945.

[38] **Matinlinna, J.P., Özcan, M., Lassilaa, L.V.J., Vallittu P. K,** 2004. The effect of a 3- methacryloxypropyltrimethoxysilane and vinyltriisopropoxysilane blend and tris(3-trimethoxysilylpropyl) isocyanurate on the shear bond

strength of composite resin to titanium metal, *Dental Materials* **20**, 804–813.

[39] **Krystafkiewicz, A., Werner, R., Lipska, L.D., Jesionowski, T.**, 2005. Effect of silane coupling agents on properties of precipitated sodium–aluminium silicates, *Colloids and Surfaces A: Physicochem. Eng. Aspects* **267,** 19-23.

[40] http://www.chemblink.com/products/2530-83-8.htm, 21.12.2006.

[41] **Bledzki, A.K., Gassan, J.**, 1999. Composites reinforced with cellulose based fibres, *Prog. Polym. Sci.*, **24,** 221–274.

[42] **Nevell T.P., Zeronian S.H.**, 1985. Cellulose chemistry and its applications. John Wiley, New York.

[43] **Malainine, M. E., Mahrouz, M., Dufresne, A.**, 2005. Thermoplastic nanocomposites based on cellulose microfibrils from *Opuntia ficus-indica* parenchyma cell. *Composites Science and Technology,* **65,** 1520-1526.

[44] **Persenaire, O., Alexandre, M., Dege, P., Pirard, R., Dubois, P.**, 2004. End-grained wood-polyurethane composites, *Macromol. Mater. Eng.*, **289**, 895–902**,**

[45] **Garkhail, S. K., Heijenrath, R. W. H., Peijs, T.**, 2000. Mechanical properties of natural-fibre-mat reinforced thermoplastics based on flax fibres and polypropylene, *Applied Composite Materials,* **7,** 351–372.

[46] **Oksman**, **K.,** 2000.Mechanical properties of natural fibre mat reinforced thermoplastic, *Applied Composite Materials,* **7,** 403–414.

[47] **Nogi, M., Handa, K., Nakagaito, A. N., Yano, H.**, 2005. Optically transparent bionanofiber composites with low sensitivity to refractive index of the polymer matrix, *Applied Physics Letters,* **87**, 243-110.

[48] **Kulpinski, P.**, 2005. Cellulose nanofibers prepared by the *N*-methylmorpholine-*N*-oxide method**.** *Journal of Applied Polymer Science*, **98**, 1855–1859.

[49] **Bhatnagar, A., Sain, M.**, 2005. Processing of cellulose nanofiber-reinforced composites. *Journal of Reinforced Plastics and Composites*, **24,** 1259-1268.

[50] **Oksman, K., Kvien, I., Petersson, L., Bondeson, D., Mathew, A.P.**, 2005. Proceedings of COMAT 2005. International Conference on Science and Technology of Composite Materials, Argentina.

[51] E-Composites, Inc**.** Market Report, 2004. Growth Opportunities in Carbon Fiber Market 2004-2010, 2004.

[52] **Marsh, H., and Rodriguez-Reinoso, F.**, Sciences of carbon materials. University of Alicante Publications, Spain.

[53] **Kelly B.T.**, 1981, Physics of Graphite., Applied Science, London.

[54] **Olejnik, S.**, **Posner, A.M.**, **Quirk, J.P.**, 1974. Swelling of montmorillonite in polar organic liquids**,** *Clays and Clay Miner.,* **22**, 361.

[55] **Wypych**, **F.** 2004. Clay Surfaces: Fundamentals and Applications**,** Oxford Press, Oxford**.**

[56] **Graber, E. R., Mingelgrin, U.**, 1994. Clay swelling and regular solution theory, *Environ. Sci. Technol*., **26**, 2360-2365

[57] **Wu, N., Fu, L., Su, M., Aslam, M., Wong, K. C. and Dravid, V. P.**, 2004. Interaction of fatty acid monolayers with cobalt nanoparticles, *Nano Lett.,* **4**, 383-386.

[58] **Choia, W. J., Kimb, S. H., Kim, Y. J., Kim, S. C.**, 2004. Synthesis of chain-extended organifier and properties of polyurethane/clay nanocomposites, *Polymer,* **45,** 6045-6057.

[59] **Ni, P., Li, J., Suo, J., Li, S.**, 2004. Novel polyether polyurethane/clay nanocomposites: synthesized with organic-modified montmorillonite as chain extenders, *Journal of Applied Polymer Science*, **94**, 534–541.

[60] **Tien, Y.I., Wei, K.H.**, 2001. Hydrogen bonding and mechanical properties in segmented montmorillonite/polyurethane nanocomposites of different hard segment ratios, *Polymer,* **42,** 3213-3221

[61] **Bourlinos, A.B., Jiang, D.D. and Giannelis, E.P.**, 2004. Clay-organosiloxane hybrids: a route to cross-linked clay particles and clay monoliths, *Chem. Mater.,* **16***,* 2404-2410.

[62] **Samir M.A.S.A., Alloin F., Sanchez J.Y., Dufresne A.**, 2004. Cellulose nanocrystals reinforced poly(oxyethylene), *Polymer,* **45,** 4149–4157.

[63] **Rivera-Armenta J.L., Heinze T., Mendoza-Martnez A.M.**, 2004. New polyurethane foams modified with cellulose derivatives. *European Polymer Journal,* **40,** 2803-2812.

[64] **Rials T.G., Wolcott M.P., Nassar J.M.**, 2001. Interfacial contributions in lignocellulosic fiber-reinforced polyurethane composites, *J. Appl. Polym. Sci.*, **80,** 546-555.

[65] **Nakagaito A.N., Yano H.**, 2004. The effect of morphological changes from pulp fiber towards nano-scale fibrillated cellulose on the mechanical properties of high strength plant fiber based composites. *Appl. Phys. A*, **78**, 547–552.

[66] **Angles M N, Dufresne A.,** 2001**.** Plasticized starch/tunicin whiskers nanocomposite materials 2: Mechanical behavior, *Macromolecules,* **34,** 2921-2931.

[67] **Correa, R.A., Nunes, R.C.R.**, 1998. Short fiber reinforced thermoplastic polyurethane elastomer composites, *Polymer Composites,* **19***,* 152-155.

RESUME

After completing his Bachelor of Science degree in Metallurgical and Materials Engineering Department at the Middle East Technical University (METU) in 1999, he has decided to specialize on polymeric materials due to the rapid growing of the polymer industry. He has completed two different Master of Science degrees at METU. In his first master degree he has continued to work on the materials technology in the graduate department of Polymer Science and Technology with a thesis concentrated on biomedical polymeric composite materials. In his second master study, he has studied the managerial aspects of engineering in the graduate department of Engineering Management with a thesis cooperated with Turkey's biggest technology exporter company KORDSA.

During his master studies, he has worked as R&D Engineer at TTM Co. in order to develop novel polymer laminated steel sheets first time in Turkey which is used as refrigerators' front panel mainly. The products are now being exported to Sweden and many other European countries.

After working in the industry, he has decided to conduct Ph.D study in order to gain expertise in polymer composites in depth. During his Ph.D thesis, he has formulated novel nanocomposites to be used in commercial applications with the Flokser Co. During this study he was awarded a scholarship from the Norwegian Government for 5 months to work on polymer-nanocomposites.

Besides academic and industrial experience, he has been founder and shareholder for the company, KREON located in Technopark in Istanbul Technical University to give consultancy and develop new materials projects to the industry.